TROPICAL METEOROLOGY

G. G. Tarakanov

MIR
PUBLISHERS
MOSCOW

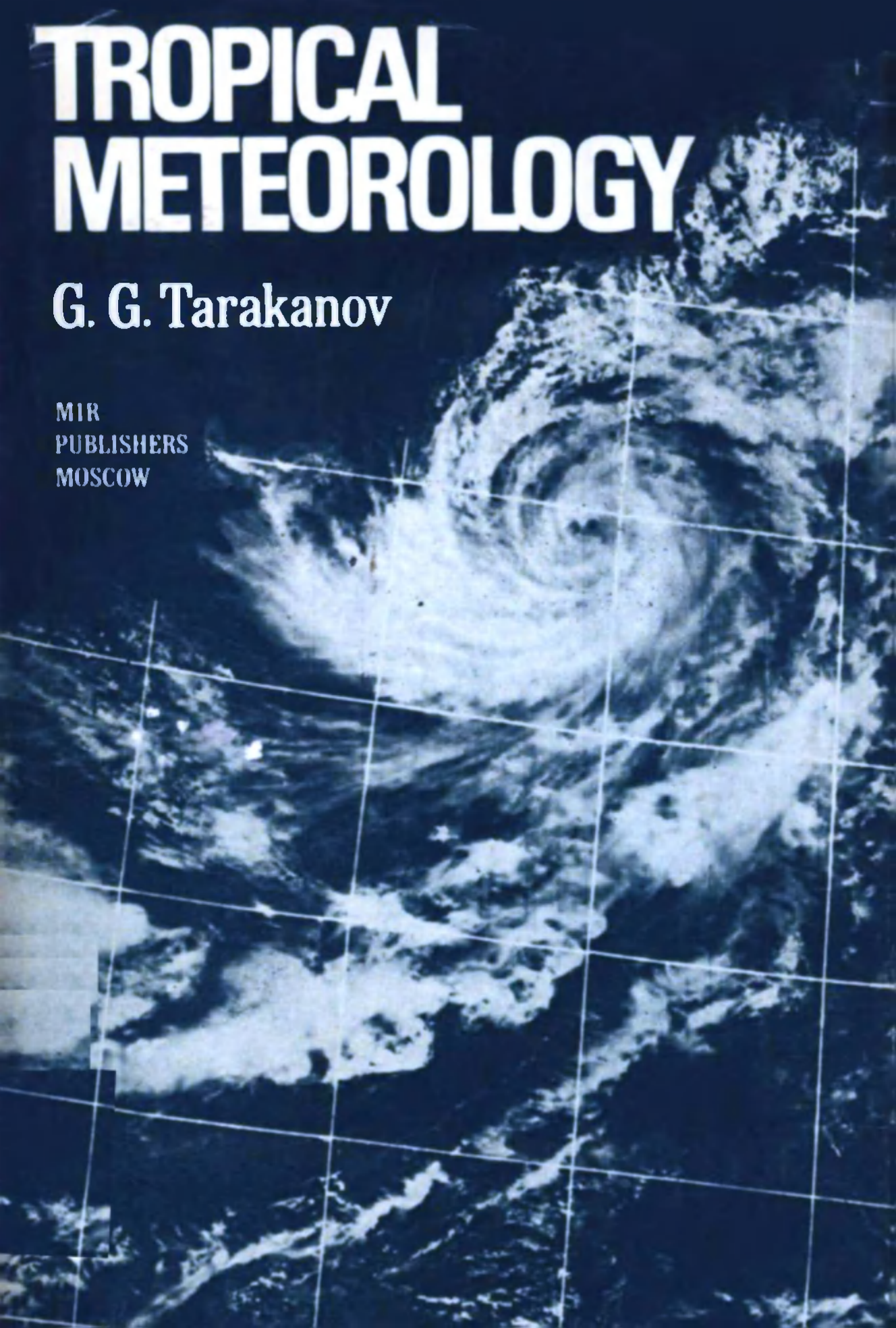

Г. Г. Тараканов

ТРОПИЧЕСКАЯ МЕТЕОРОЛОГИЯ

Ленинград
Гидрометеоиздат

TROPICAL METEOROLOGY

G. G. Tarakanov

Translated from Russian
by
Michael G. Edelev

Mir Publishers
Moscow

First published 1982
Revised from the 1980 Russian edition

На английском языке

© Гидрометеоиздат, 1980
© English translation, Mir Publishers, 1982

PREFACE

This text is written in accordance with the course in tropical meteorology as read at the Leningrad Hydrometeorologic Institute. It discusses the processes of the tropical atmosphere, basic weather elements, and general principles of weather analysis and forecasting in the tropics.

It is assumed that the reader has mastered the fundamentals of meteorology and has been through basic courses in dynamic meteorology, aerology and radio meteorology, synoptic meteorology, numerical forecasting and climatology. Therefore, to avoid parallels many aspects of mid-latitude meteorology are mentioned only briefly. Main emphasis is placed on the subjects characteristic of the tropical belt.

The bulk of literature produced in the 70s after an explosion of interest in the tropical atmosphere has necessitated a rigorous selection of material for the book, since the opinions of the researchers on some subjects have been far from unanimous, and this discrepancy has found its way into scaling estimates and forecasting techniques. The text includes mainly those results which are widely accepted by or are beyond doubt to the majority of tropical researchers. The techniques are generally of fundamental rather than local or minor importance.

The text is based on the classical and recent findings obtained in the field by a large group of Soviet scientists, among them R. V. Abramov, A. M. Borovikov, R. F. Burlutsky, G. N. Vitvitsky, E. M. Dobryshman, V. N. Ivanov, D. L. Laikhtman, L. S. Minina, A. N. Nevzorov, M. A. Petrosyants, V. M. Radikevich, N. A. Romanova, Yu. A. Romanov, V. S. Samoilenko, I. G. Sitnikov, A. I. Snitkovsky, and A. I. Falkovich, and their colleagues abroad M. A. Alyaka, H. Flohn, R. Frost, W. M. Gray, E. S. Jordan, C. L. Jor-

dan, P. Koteswaram, A. F. Krueger, J. S. Malkus, B. J. Mason, B. I. Miller, C. W. Newton, T. Nitta, E. Palmén, C. E. Palmer, C. S. Ramage, H. Riehl, M. Yanai, to mention only some of them.

At attempt has been made to introduce all the main areas of study involved in tropical meteorology while at the same time keeping the book within a reasonably small volume. The book is meant to be a working text and for that reason includes a number of review questions at the end of each chapter. A substantial bibliography (mostly in Russian) is included for the reader who wants to dig deeper into the subjects that have not been examined exhaustively.

I am greatly indebted to the faculty members of the Leningrad Hydrometeorologic Institute, B.M. Vorobyev, L.G. Kachurin, V. G. Morachevsky, B.D. Panin, and V.M. Radikevich, for the valuable comments and criticisms made during the preparation and editing of the manuscript.

G.G. Tarakanov

CONTENTS

Preface 5

Chapter 1. Introduction 9

1.1. Tropical Meteorology Defined. An Outline of the Tropical Atmosphere 9
1.2. Weather Observing System in the Tropical Region 13

Chapter 2. Variation of the Main Weather Elements 22

2.1. Temperature 22
2.2. Pressure 31
2.3. Wind 38
2.4. Pressure and Wind Fields 44
2.5. Cloudiness 55
2.6. Rainfall 60

Chapter 3. Convection 70

3.1. Types of Convection and the Initiating Conditions 70
3.2. An Entraining Jet Model of Cumulus Convection 77

Chapter 4. Tropical Synoptic Analysis 84

4.1. The Time Section 84
4.2. The Surface Chart 85
4.3. The Upper-air Chart 86
4.4. Fields of Divergence and Vorticity 00
4.5. Air Masses 102

Chapter 5. Circulation and Synoptic Systems of the Tropics 106

5.1. The General Circulation 106
5.2. The Equatorial Trough 109
5.3. The Trade Winds 116
5.4. Antitrades 118
5.5. Low-latitude Disturbances 119
5.6. Monsoons 132
5.7. Interaction Between Motions of Different Scales 142
5.8. Heat and Moisture Transport Mechanisms 145

Chapter 6. Tropical Cyclones 152

6.1. Formation of Tropical Cyclones 152
6.2. The Life Cycle of Storm 157
6.3. Structure of Tropical Cyclones 159
6.4. Relation Between Lowest Pressure and Highest Wind in Storms 167
6.5. Forecasting the Movement of Tropical Cyclones 175
6.6. Analysis and Prediction of Storm Intensity on Satellite Data 181
6.7. Impact of Tropical Storms 192

Bibliography 198

Index 201

Chapter 1 | INTRODUCTION

1.1 Tropical Meteorology Defined. An Outline of the Tropical Atmosphere

Tropical meteorology, as its name implies, deals with the structure of the tropical atmosphere and processes that occur in the tropics. Several opinions exist, however, on where the tropical region is to be confined. Therefore, before we start the discussion it would be appropriate to dwell on the area that will be our major concern.

Geographically, the tropical zone is known to lie between the Tropics of Cancer and Capricorn. Meteorologists often bound the region by the 30th parallels, which is far too arbitrary and cannot be assumed as a general definition. Besides, the atmosphere of the region is known not to exhibit strongly latitudinal behaviour. Another meaning takes the tropics to comprise the region between the latitudes of the subtropical highs considering their axes between easterlies and westerlies at the earth surface. This definition is, again, inaccurate since the pressure in the high pressure belts undergoes seasonal variations making the stated bounds evasive.

H. Riehl (1954) defined the tropics as 'that part of the world where most of the time the weather sequences differ distinctly from those of middle latitudes, the dividing line between easterlies and westerlies in the middle troposphere serves as a rough guide of the boundaries'. As the choice of this fluctuating line allows for seasonal variations the bounds so outlined cannot be fixed, too. They migrate with seasonal change shifting towards higher latitudes in the summer hemisphere and lower latitudes in the winter hemisphere.

A definition of tropical atmosphere, unavailable so far, would be on a more strong basis if it involved all the set of kinematic and thermodynamic properties that differ the tropical atmosphere from that of extratropical regions.

Energy budget. The tremendous amount of radiant energy

the tropics receives from the sun many times exceeds that it reflects back into space. The region thus acts as a heat accumulator. Polar regions, on the contrary, give off more heat than they absorb, working hence as "refrigerators". The resulted heat deficit at high latitudes is compensated by oceanic and air currents which transfer energy from low latitudes poleward. The atmosphere in this process behaves as a "heat engine" transporting excess heat toward the regions with heat deficit.

The mechanism involved in the heat transfer is extremely sophisticated. It is even more so because it includes conversion of energy. As a result, rather complex air motions develop with cyclones and anticyclones, strong and weak wind fields, clouds and precipitation. It is this air motion system, called the general circulation, that is responsible for the development of large-scale weather systems which together with small-scale local influences produce what is observed as a local weather.

In a study of atmospheric processes we will inevitably need to know the amount of excess heat in the tropics and the energy deficit at higher latitudes. We are also bound to understand why and how this excess heat is produced and what processes take part in exporting the energy to fill the deficit at the poles. The tropical atmosphere—its behaviour, heat budget, mechanisms of heat transfer to higher latitudes, etc.—is thus an indispensable link in the chain of causation that is responsible for the globe weather production. The more we know about the tropical atmosphere and its effect on higher latitudes the more reliable are prediction models of various time-range and the higher is the forecast skill.

Tropical meteorolgy is therefore an instrument to have an insight into the cause of atmospheric processes developed at various latitudes far off the tropical region. An immense role the region plays in the development of global atmospheric processes and the fact that the tropical atmosphere had been studied relatively poor prompted the Global Atmospheric Research Program (GARP)* to make the first large-scale

* The Global Atmospheric Research Program (GARP) is a joint undertaking of the World Meteorological Organisation and the International Council of Scientific Unions (ICSU) conceived in the 1960s and launched in the 1970s.—*Translator's note.*

field project in this international undertaking the GARP Atlantic Tropical Experiment (GATE).

The studies of tropical atmosphere are of great importance for navigation. Among the principal consumers of operational forecasts in the tropics are aircraft and ships for whom there exists a navigational guidance system helping them to find optimal and least hazardous courses.

Yet of immense importance is the prediction of severe tropical cyclones developed annually in the southwest Pacific, near the Philippine Islands, off the Australian coast, and in the Caribbean.

Some historic records. In May and November 1969 two medium intensity cyclones rushed onto the coastal land of India. They killed about a thousand people and caused losses of 300 million dollars.

In October 1942 a severe cyclone hit the westal seaboard of India. It took 15 thousand lives and killed 60 thousand cattle.

Memory is still alive in the Pakistani people of the severe storm raged in 1876. Driven by the powerful winds, the waters of the Gulf of Bengal surged over the coast in tides of unseen heights to kill 100 thousand people with about as much loss of life due to the epidemics followed the catastrophe.

However, the disaster happened at the west Pakistan coastline on the night of 12 to 13 November 1970 was even more serious. Papers called the cyclone raged in the night 'killer of the century'. In spite of warning, it took about 200 000 lives. In the midnight, the wind speed in the cyclone area was estimated at 65 m s^{-1}. This howling wind piled the waters up into huge (up to 9 m high) tides that swept the seaboard and offshore islands causing flash flooding of the coastal area.

Another tragic side of tropical weather is prolonged droughts periodically devastating some tropical regions. In 1969-1973 a catastrophic drought struck the Sahel, a region of 4 million square kilometers in west Africa criscrossed by the boundaries of half a dozen independent nations—Mauritania, Senegal, Upper Volta, Niger, and Chad. Twenty five million inhabitants of the area envisaged starvation death. Most heavily suffered population of the areas bounded on the

north by the Sahara. By the time the drought relieved in 1974 the herds of the Sahel had been reduced by starvation to one fifth of their former size, and the worst Saholian famine of the century had killed more than 100 000 people in spite of a massive international relief effort that saved thousands of others.

The atmosphere in the tropics and processes that take part in it differ distinctly from those of middle and high latitudes. The main distinctions are as follows.

1. In low latitudes the Coriolis parameter is small to completely vanish at the equator. Therefore, in the tropical region air movements can no longer be assumed geostrophic. Applying the geostrophic approximation in the equatorial zone may lead to entirely wrong results. On the high latitude margins of the tropical region the geostrophic relationships should be applied with extreme care since a small value of the Coriolis parameter may entail large errors. The nonlinear terms in the equation of motion are in this region equal in the order of magnitude to the pressure gradient.

2. Assuming the atmosphere is in hydrostatic equilibrium, the vertical momentum equation is transformed in the hydrostatic equation. For large-scale motions this assumption works rather well. For small and meso-scale motions, however, it is not valid in many circumstances. Neither could hydrostatic approximation be applied to intense convection. In the tropical region the above conditions are met all throughout the year. Hence, for small and meso-scale motion analysis the vertical equation of motion retains all the acceleration terms.

3. Owing to the intense convection the friction layer of the tropical atmosphere is of higher depth than that of higher latitudes. At 2 km altitude the viscosity terms in the equation of motion have been estimated to be of the same order as other terms, though lower than the pressure gradient term.

4. Large water content in the tropical atmosphere makes the role played by water phase transients more pronounced than in any other region of the earth.

5. With movements in the tropical atmosphere being ageostrophic, divergence and convergence processes exhibit themselves rather strongly. The formation of weather condi-

tions can most often be explained by a sign and value of the divergence. The only exclusion is, perhaps, tropical cyclones. Yet in their development, too, divergence is of major importance.

6. The atmosphere in the tropics (beyond the intertropical convergence zone and tropical cyclones) is distinctive for very weak variation of its weather quantities in the horizontal.

7. Some meteorological quantities of the tropical atmosphere vary in time with a larger periodicity than similar quantities do in higher latitudes.

8. Non-seldom are the conditions for meso-scale processes to develop into that of large scale.

Other representative features of the tropical atmosphere, which are to some extent derivatives of the enumerated above, will be discussed in more detail in the subsequent chapters of the book.

1.2 Weather Observing System in the Tropical Region

Any weather analysis and forecasting require information on the state of atmosphere. The quality and quantity of initial data is decisive for a reliable grid of an objective analysis to be produced and a skilled forecast to result. Of still more importance is the quality of initial data for research meteorologists.

Much of the data comes from a network of weather stations (meteorological and aerological). Discussing the functioning of a network we need an answer to three questions.

1. How dense should be the network?
2. How often should observations be sampled?
3. How accurate should be these observations?

Whether a network be in the tropics or anywhere a unanimous answer to the above questions cannot be given because of the other factors involved. Among them the requirements to the quality of collected data, the character and importance of the problem being solved, and economical possibilities of a service to whom the weather network belongs.

Density of weather station network. Historically the grid of weather stations in the tropics is far less dense than in

the middle and high latitudes. Besides, even land stations are spaced fairly unevenly. The closer to the equator the farther stations are spaced from each other. Huge expanses of ocean have no weather stations at all, not to mention those on sparse islands. This all results in lack of data, a serious problem of the tropical meteorology. The lack of tropical data makes the subjective and objective analysis of synoptic charts extremely difficult. In some regions the poor data coverage makes impossible any analysis, especially objective.

According to standards of the World Meteorological Organisation (WMO), meteorological stations should be distanced not far than 500 km when on land and 1000 km when at sea. For aerological stations this distance is, respectively, 1000 and 1500 km. The existing network of weather stations in the tropics does not meet the standards. Moreover it is placed irrationally—in some regions it is denser than needed and in the majority of area far behind the required density.

A question arises: what should be an optimal density of a grid? Vast distances between stations would result in a poor data coverage thus affecting forecast skill, making the weather reports unreliable. An increase in the number of stations would improve the quality of initial data, yet the cost of construction, supply and management of the stations, especially aerological, imparts the economy of the service.

Search for a rational weather station network is one of the major problems facing the tropical meteorology. The problem is compounded by a need to take into account the methods to be applied for arriving at a goal for which the network is oriented. Extension of objective analysis and weather prediction onto the tropical region requires, above all, the network which could supply adequate synoptic data. To test for a rational spacing, meteorologists often appeal to the so-called optimal interpolation, a method to estimate a distance between the stations, d, optimal from the viewpoint of root-mean-square (RMS) error of observations, ε, and RMS error of interpolation, $E_{\min}$.

A relationship between the three parameters for the 500-mb surface is illustrated in Fig. 1.1. The curves are plotted for the data of radio sounding in the tropics (0-30°N)

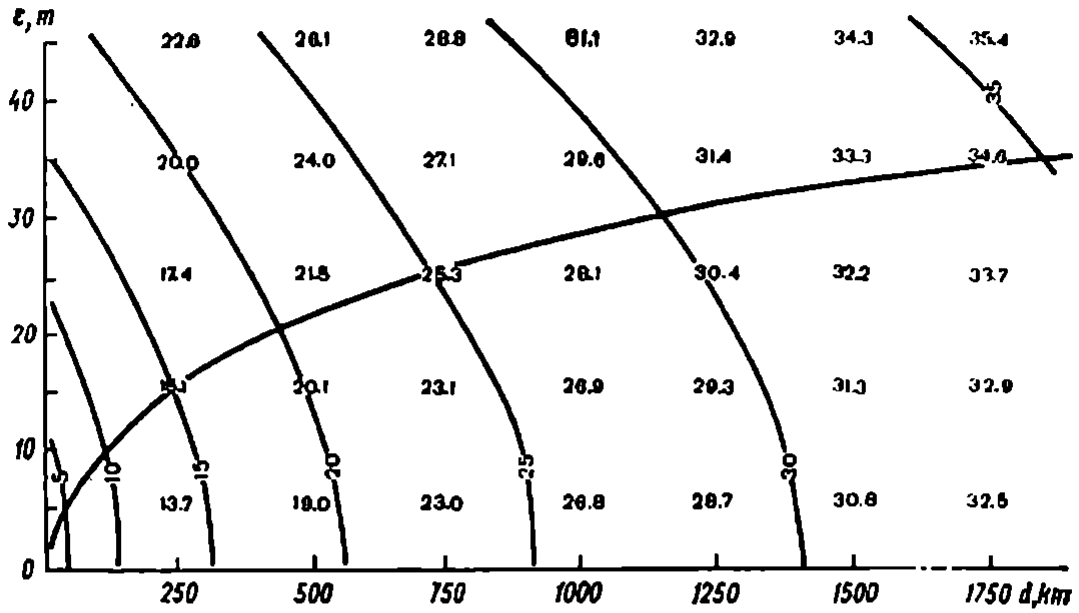

Fig. 1.1 Root-mean-square error in the interpolation of 500-mb surface height, E_{min}, as a function of observational RMS error, ε, and distance between stations, d

statistically averaged for a period of five years (1958-1963). The columns of figures in the field represent the values of E_{min}; thin lines, the isolines of E_{min}; heavy line, the condition of $E_{min} = \varepsilon$ serving to choose an optimal distance.

With reference to Fig. 1.1, we can estimate how an interpolation error depends on random observational errors and the distance between stations. It is seen that the less steep are the curves E_{min} = constant the more strong is the effect of the RMS error of measurements on the accuracy of interpolation.

Assume that we spaced aerological stations in accordance with the WMO standards at a distance of 1000 km of each other. Then referring to Fig. 1.1, the network may be deemed optimal if the geopotential height of the 500-mb surface would be measured accurate to $\varepsilon = \pm 28$ m. The respective accuracy of the Garp Atlantic Tropical Experiment (GATE) has been $\varepsilon = \pm 20$ m. Should we extend this accuracy on the entire network, an optimal distance between the stations should have been around 400 km. In the tropical region such a density of aerological stations cannot be reached by vari-

ous reasons, at least in the near future. Hence, with the existing density of the grid, increasing the accuracy of measurements cannot improve the quality of objective analysis.

In Fig. 1.2, a relationship between E_{min}, ε, and d is depicted for wind velocity at the 500-mb level (V_{500}). The curves are plotted with the same statistically handled data of upper wind radio sounding as in Fig. 1.1. Isolines E_{min} = constant for V_{500} illustrate that in this case lowering the observational error has a less pronounced effect on the accuracy of interpolation than has the density of the network so far as the stations are distanced closer than 1000 km. Another situation is in the areas where the grid is rather sparse (the stations distanced much wider than 1000 km). The improvement that could be gained with the same effort is almost negligible. That is, a sufficient increase in weather stations is required for an improvement in the interpolation accuracy to become sensible.

Frequency of weather observations. Frequency of observations is primarily decided by the purpose for which the collected data is intended. From practical considerations, sufficient information can be collected with 8-hourly synoptic observations. The thus obtained data retain its actuality margin and signals diurnal variations of weather elements with sufficient accuracy. For research purposes requiring the diurnal variation with more detail, such as a record of rainfall, intensity of rain and its amount between hours, development of clouds, storms and other weather phenomena between the principal synoptic hours, the observations should be more frequent. Moreover in the tropics there are some occasions when the observations need be made continuous as, for example, in tracking a tropical cyclone.

Continuous and frequent observations can, for instance, be provided by automatic stations. To collect the obtained information from these stations in time and transmit it to the data centers a third generation meteosatellite system has been devised. A retransmitting satellite of the system interrogates buoy-borne automatic stations at sea and automatic stations positioned in inaccessible terrain areas to transmit these synoptic observations first to the regional data centers and then to three World Meteorological Centers, located in Melbourne, Moscow and Washington. From the world con-

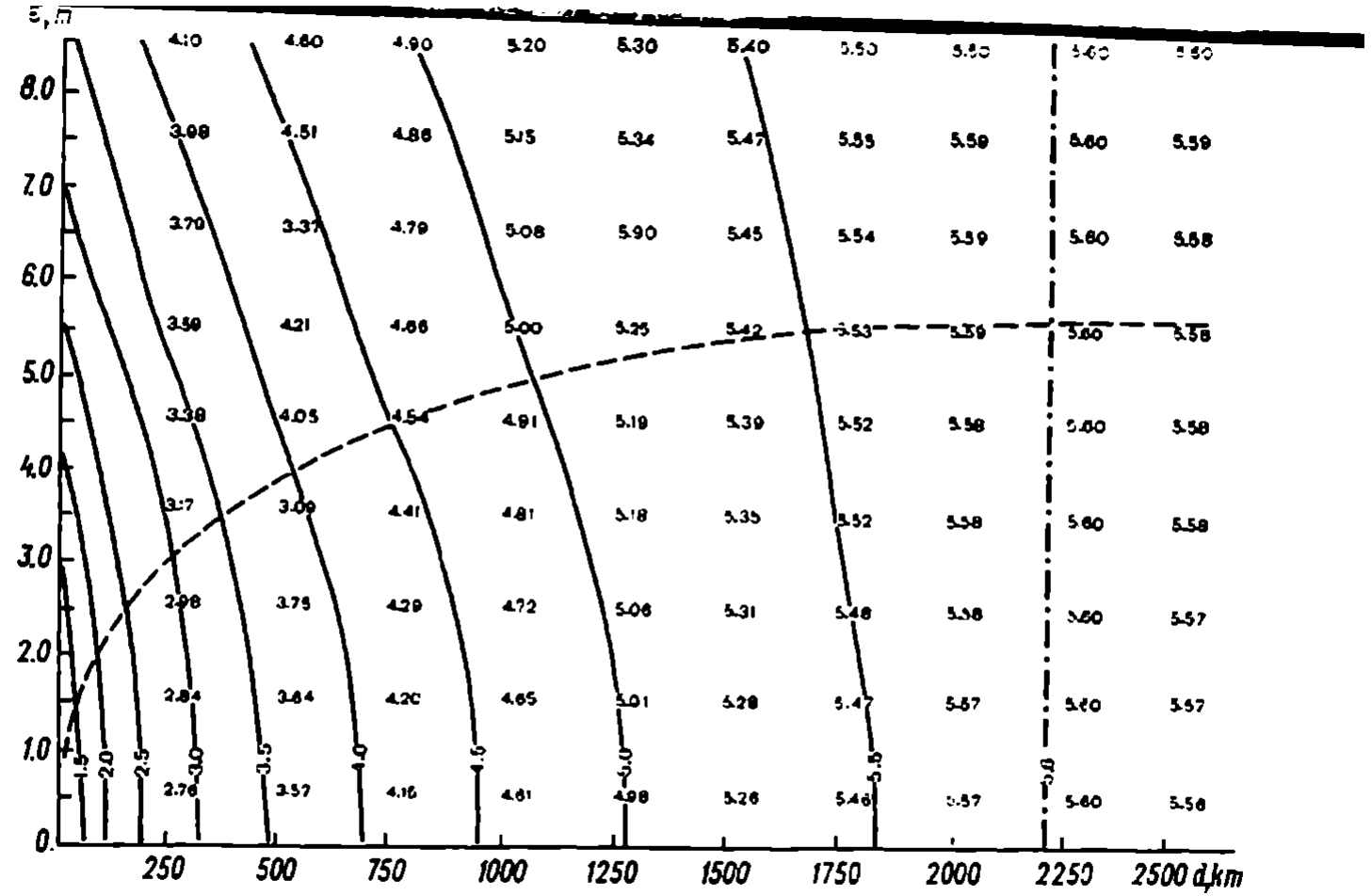

Fig. 1.2 Root-mean-square error in the interpolation of wind speed at 500 mb, E_{min}, as a function of observational RMS error, ε, and distance between stations, d

ters after appropriate processing data sets will go back down to the regional and national weather centers.

A similar experiment with observations collected from a fleet of free balloons drifted at various altitudes was conducted in Melbourne. An earth satellite was used to interrogate all the balloons and obtain their coordinates. The experiment supplied the data on the main weather elements and their distributions with height.

Accuracy of measurements. Prior to starting the GATE project, a policy statement had been adopted concerning fairly stringent requirements to the accuracy of measurement. At high altitudes, root-mean-square observational errors should not have been higher than $\varepsilon_v = \pm 2$ m s^{-1} for wind speed, $\varepsilon_T = \pm 1$ °C for temperature, and $\varepsilon_p = \pm 1$ mb for pressure; and at the surface, respectively, $\varepsilon_v = \pm 1$ m s^{-1}, $\varepsilon_T = \pm 0.5$°C, and $\varepsilon_p = \pm 0.1$ mb. The planned accuracy was actually achieved in the project proving itself superior in this aspect to daily tropical observations.

Satellite observations well support data of aerological and meteorological stations. The meteosatellites are inserted in either the geostationary or polar orbits, the former being preferable for the tropical watch. Orbiting so that it remains directly above a fixed point on the equator a geostationary satellite may be set to observe atmosphere at any preset time, that is, supply information on the state of the atmosphere at any synoptic or other hours. Photographic images taken in succession are well suited for comparison analysis as they depict one and the same area. Hence, meteorologists can trace by these images how the cloud cover is migrating to draw the information about the air currents at the level of the clouds.

Modern geostationary satellites supply images of high spatial resolution. It amounted to as high as 7 km in the infrared (IR) and 1 km in the visible-spectrum images during the GATE'74 expedition.

From satellite photos meteorologists can deduce dimensions of single clouds, cloud clusters, and vast cloud fields. From an image sequence they can infer the diurnal progression of the cloud clusters and the cloudiness day-to-day variation. Finally, satellites are far superior to the other facilities in locating various synoptic objects over the oceans

such as, for instance, the intertropical convergence zone and tropical hurricanes. At present various satellite-data-based methods are developed to trace these objects and forecast their evolution.

A good practice in working with satellite data recommends to compare the visible and IR images. For this purpose on the modern satellites of the type NOAA 4, NOAA 8 and some others information about the underlying surface and cloudiness is transmitted via the same TV channel by interlaced scanning of visible and IR images to observe the same pattern and compare physically different data on one photograph.

Various objects on satellite images are contrasted due to the inherent brightness. Brightness of a cloud, for example, is much higher than that of the underlying surface, therefore the former looks bright and the latter dark on a photograph. Brightness of a cloud in the infrared and visible spectra images depends, however, on entirely different and numerous reasons. For the visible image, they are the albedo of the cloud, its thickness, microphysical properties, and the phase state of water particles. In addition, it depends on how the sun beams enter into the cloud and from what angle the satellite camera sees it. The deep clouds normally reflect better and thus are better discernible than cirrus clouds which are transparent for visible photography. Brightness on the IR images is decided by the temperature of radiating surface. Cirrus clouds are cool and, hence, will be bright on an IR photograph.

For complete specification of the atmospheric state, coincident observations need to be made in both spectral regions. IR images are slightly inferior to their visible counterparts in resolution capacity. But the superiority of the infrared region is in that the pictures of the earth's atmosphere can be produced at any time whereas the views in the visible range may be obtained only in the day time, that is from the illuminated surface.

An important part of the weather information comes from radar stations. Their data provide for both operational analyses and research. The radars have high resolving power and can produce continuous observations. In that way they can fill the gap in the weather data from terrestrial

stations and satellites, which are discrete in time and space or provide a general picture with inadequate spatial resolution. In the absence of radar meteorologists have to interpolate the grid data over the grid spaces exploiting their knowledge of weather process regularities. With a radar they can continuously view an atmospheric object evaluating its state in time and space within the radar range. This capacity makes the radar an indispensable tool in studying or following cumulonimbus clouds, cloud clusters, and evaluation and tracking tropical cyclones. In the tropics, where dangerous phenomena form usually followed by the development of intense cloud systems, a need for a network of radar stations is felt more than elsewhere.

The radars of modern land stations operating on 2.7 and 3.05 GHz evaluate tropical cyclones within 400 km range and continuously follow their drift. Observing a dangerous trend, the radar service can issue a warning of close storm or hurricane to prevent or damp the potential losses. The radar is suitable for remote control, so it can be placed in remote areas. In Japan, for example, a typhoon tracking radar is placed on the Fuji mountain and remotely controlled from the office-building of the Japan Meteorological Agency in Tokyo.

Various radar techniques are employed to evaluate the precipitation regions masked from above by a continuous cloud cover. One of them is based on a difference in intensity of signals reflected from the rain and the land surface. The radar installation in this service operates in the bifrequency mode. Physically, the amplitude difference occurs because the effective scattering surface of the earth depends on the wavelength, λ, only slightly whereas that of the precipitation is proportional to λ^{-4}. Another way is to use a polarized beam and the correlation technique to exploit the difference in polarized (correlated) and random (uncorrelated) reflections.

Still another possibility is to put a radar set on board of a satellite. The satellite radars operating on cm- and mm-bands measure water amount in the atmosphere of the tropics, moisture content of clouds and rainfall, and vertical distribution of temperature and humidity in the atmosphere. A disadvantage of the radars is in their large weight,

dimensions, power requirements and relatively short life of the microwave generators. More practicable, therefore, would be to install instead of this active radar facility a thermo-microwave imager, say of the type successfully applied on board of the Soviet Kosmos-243 satellite.

Of especial promise for the satellite sounding are the active/passive radar sets materialized as radiometers. These devices can provide data on sea surface roughness at any weather conditions and, supported by the colour technique, on sea temperature.

The best effect could be obtained comparing the data of the surface radars and satellites. With multi-level cloudiness, the overhead views from the satellites providing no information on the depth in the vertical are hard to handle. The radar vertical cross-section can supply the lacked data leading to precise three-dimensional pattern of cloudiness.

Review Questions

1. What approaches exist to define the tropical region?
2. Where lies the scientific and practical importance of the tropical atmosphere studies?
3. Enumerate the main features of tropical atmosphere.
4. What should be the density of weather stations to meet the WMO standards?
5. Which distance between the weather stations may be assumed optimal and how can it be defined?
6. How often should the observations for operational analysis be sampled at weather stations?
7. Which accuracy is required in measuring the main weather elements at the surface and at high levels?
8. Discuss the role of satellite and radar sounding in the tropical weather observation system.

Chapter 2 VARIATION OF THE MAIN WEATHER ELEMENTS

2.1 Temperature

Temperature of the surface air layer in the tropics is mainly governed by the radiant energy budget, though some minor influence is felt from other factors. The budget is positive over the enormous sun energy income during the year, so air in the tropics is warm. Since the radiant flux varies periodically with the astronomical factors, the temperature follows it with the certain periodicity. Non-periodical variations are seldom and insignificant.

Since the isotherms by large run so nearly parallel to the latitude circles we can average temperatures around the globe to yield a pattern of the mean temperatures of latitudinal circles. Most striking in the temperature field pattern is that the line of temperature maxima coincides (or almost coincides) with the axis of the equatorial trough and follows it in the annual variation. In January the air is warmest near 5°S, exactly the latitude of the trough, and in July it is warmest at 20°N, slightly to the north. It is believed that this displacement results from the very high temperatures over the northern subtropical deserts. Besides, land masses are larger in the Northern than in the Southern Hemisphere, hence, the surface layer temperatures north of the equator are higher. Throughout the tropics the Northern Hemisphere is about 2 °C warmer than the Southern Hemisphere. This also increases the seasonal temperature range in the Northern Hemisphere: it amounts to 13 °C at 30°N and 7 °C at 30°S.

Mean annual temperatures are distributed symmetrically not with respect to the geographical equator but with respect to the "thermal, or heat, equator" situated at 5°N*.

* Often the thermal equator coincides with the equatorial trough. Then it is labelled the meteorological equator.

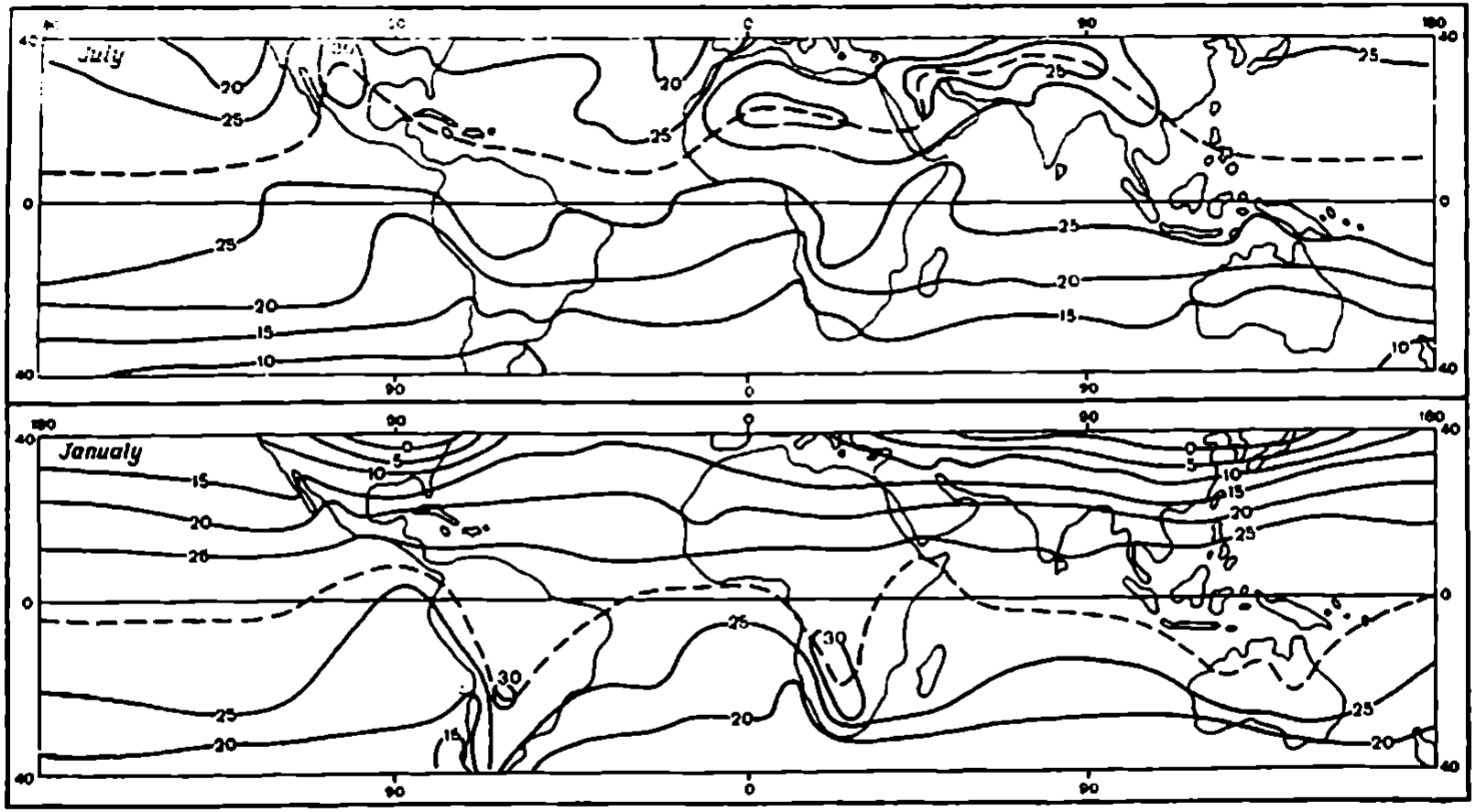

Fig. 2.1 Temperature (°C) at sea level in July and January (after Niewolt) and the thermal equator (dashed)

Annual temperature range approaches the vanishing point everywhere near the thermal equator.

The above location of the thermal equator at 5°N is largely conditional. It is only valid with latitudinal averaging of the mean annual temperature. At daily temperature charts the thermal equator is defined as a line connecting the maxima. By a similar procedure it can be traced on the maps of mean monthly temperature. On these graphs it does not coincide with any latitude, rather, it is a wandering curve which goes poleward over the land areas in the summer hemisphere and near the geographic equator over the oceans (Fig. 2.1).

The seasonal temperature range varies substantially with longitude as land changes for sea. Within a season, or a month, temperatures at different longitudes of the same latitude circle also differ markedly.

A revealing picture of longitudinal variations in mean temperature and its seasonal course is furnished by Fig. 2.2, where temperature is plotted against longitude at 15°S. Outstanding are the tremendous depressions of temperature just west of the South American and African continents, which are accentuated in winter. These depressions result not only from the equatorward transport of polar maritime air over the eastern parts of the oceans: the familiar upwelling of cold water along west coasts is also responsible.

Elsewhere Fig. 2.2 confirms the features of the temperature distributions just discussed: the small temperature range over the oceans compared with the continents—especially Africa and Australia, the difference being less pronounced in mid winter.

Annual variation of air temperature in various areas of the tropics depends on the physico-geographic and meteorologic factors. Conditionally, it is divided in two types—oceanic and continental.

The oceanic type of annual temperature variation is observed over a huge expanse of the oceans and offshore regions exposed to the trade winds. This variation is noted for its maximum in late summer and minimum in mid-winter. The annual temperature range decreases equatorward.

Typical oceanic temperature curves are observed, for example, at Havana and Honolulu, Both stations have their

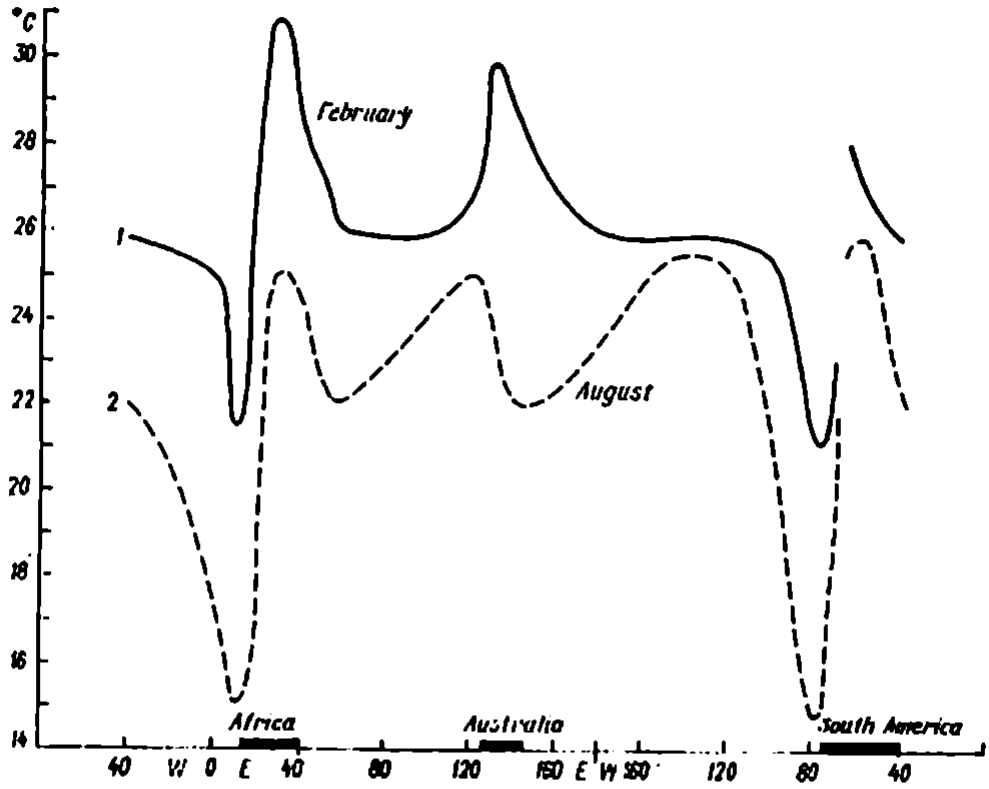

Fig. 2.2 Longitudinal profile of mean sea level temperature (°C) at 15°S (after Riehl)

hottest mean monthly temperature in August—28 and 27 °C, respectively, and lowest in January—22 and 21.5 °C. At Barbados Island (13°N) lying 11° closer to the equator than Havana the summer maximum is practically absent: mean temperature from May to October oscillates here near 30 °C, and a minimum of 25 °C is observed in March. At Fanning Island (4°N) that is almost at the meteorological equator, temperature is practically constant throughout the year. The mean temperature of the hottest month, October, is 27.5 °C, and the coldest, January, 27 °C.

On the geographical equator the annual temperature variation is practically also not observed. If the mean monthly temperature on the equator varied strictly with the sun, we should find two minima at the solstices and two maxima at the equinoxes. Cloudiness and rainfall, however, enter

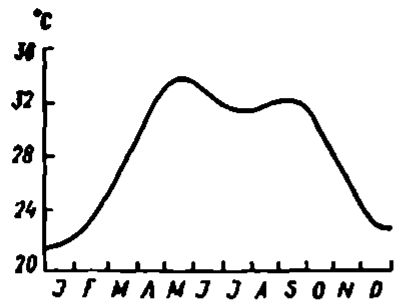

Fig 2.3 Seasonal course of mean monthly temperature at Khartoum (15°N, 32°E)

as factors of at least equal importance. In the rainy season, frequent daytime showers hold the maximum temperatures down, thus flattening the annual variation curve. The curve ascends a little at the autumn equinox only.

The continental type of annual temperature variation is observed over continental areas situated beyond the equatorial zone. This type of curve shows two maxima and two minima. The minima quite properly fall in the center of the respective winters. Then temperature rises sharply through the spring months and ascends the first maximum in the early summer. For the majority of the land areas this is the season of their greatest heat. Then temperatures drop under the influence of the increased cloud cover even though the precipitation may be quite small. This is the secondary minimum. At the end of the rainy season while the sun is still high in the sky the temperature rises again and the secondary maximum develops (Fig. 2.3).

The Khartoum curve can serve as an example for the type of temperature trace typical in continental countries. A minimum of 22 °C falls at mid-winter (January), a maximum of 34 °C at May-June. Then in July-August, due to the increased cloudiness and often rainfall temperature drops to 31 °C (a secondary minimum) and in September-October rises again amounting to 33 °C (a secondary maximum).

In equatorial regions of continental interior the annual temperature trace varies insignificantly. The mean monthly temperature at Addis Ababa, for instance, is close to 22 °C throughout all seasons. Temperature difference from month to month does not exceed a fraction of a degree increasing to a full 1 °C only in July.

From the mean isotherms for January and July (Fig. 2. 1) it is a simple matter to notice that near the equator, and over the oceans and even away from it, the horizontal temperature gradients are rather small. Polewards they in-

crease sharply, especially over the continents in winter time.

The main factor providing for the thermal homogeneity in the tropics consists in practically equal net radiant energy received by various regions. The secondary factor is in that the large part of the underlying surface consists of the oceans. They behave as a giant heat store. Air moving over the ocean receives from it both sensible and latent heat. Intruding a more cold continent the air would gradually give its heat off. A well developed heat transfer between the oceans and continents results in smoothing the temperature contrasts. The continental area in the tropics is relatively small for the really cold (subzero) air masses to be formed over it and prevent the smoothing action.

Data on the temperature distribution in various regions of the tropics are rather scarce. The GATE tropical Atlantic expeditions of 1972 and 1974 collected vertical temperature profiles mainly over the oceans. According to the available data we can single out three major types of temperature distribution: that in the trade wind belts, in the intertropical convergence zone, and over the continents (Fig. 2.4).

The trade wind belts differ by the most complicated structure of temperature field in the upper air (free atmosphere), curve *1*. In the lower layer extending up to 1 km, the temperature lapse rate is as often as not near the dry adiabatic. Further up, an ascending sonde will pass through one or several stable or inversion layers, that is layers with small or negative temperature lapse rate. As a rule, the inversion layers alternate with thin layers of positive lapse rate. The upper bound of such a separation layer (or layers) can be as high as 3 km. The temperature inversion layer of the region has come to be known as the trade wind inversion. Below the inversion layer the atmosphere is filled with water vapour; so the tropical troposphere of the region can be generally divided into a lower moist (0-3 km) and an upper dry layer.

Above the trade wind inversion, in a 3 to 6 km layer the lapse rate again becomes higher with increasing altitude to reach values of 0.8 °C/100 m and higher as reported by some GATE'72 soundings. Above 6-km altitude another inversion is observed (the secondary trade wind inversion) which, how-

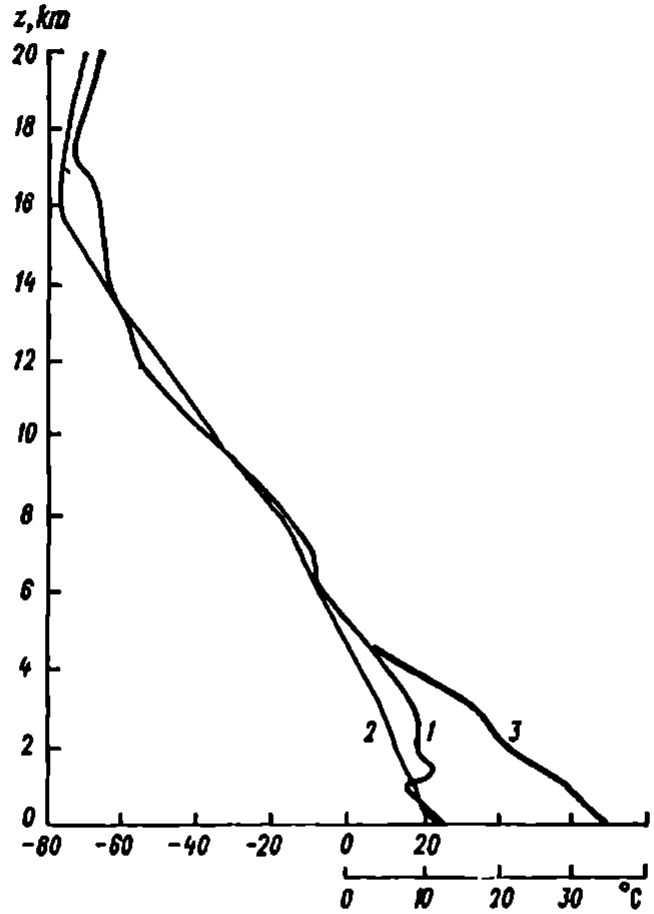

Fig. 2.4 Vertical temperature profiles:
1—in the trade wind belt (GATE'72 data); *2*—in the ITCZ (GATE'72 data); *3*—at Khartoum (after Riehl)

over, is much weaker than the main inversion below—often it is just a constant temperature layer with a depth of several hundred meters. Under this layer, which similarly may be called a secondary separation layer, moisture and dust blown off the African continent are concentrated. GATE observations have traced here the upper boundary of the aerosol layer. The upper boundary of the secondary inversion is situated at about 7-km altitude. The atmospheric stratum between the upper bounds of these inversions is termed the middle layer of the trade wind troposphere. The relative humidity in this layer is less than in the lower layer, yet under the secondary inversion it amounts to 60%.

Above the secondary inversion layer up to the tropopause at 15-17 km altitude, the temperature lapse rate is everywhere positive, being rather high (0.7-0.8 °C/100 m) up to 12-km height to sharply decrease afterwards. Some researchers, however, point out that in a thin layer under the tropopause the temperature lapse rate increases again to attain values not far from the dry adiabatic lapse rate.

In the intertropical convergence zone the vertical temperature profile has a different form (curve *2*). According to some soundings separation layers do exist in this region but not as a mean condition, and if observed, are rather shallow. In the lower layer (up to 600-700 m) the temperature lapse rate goes steeper than the moist adiabatic. Above that layer, the lapse rate decreases in value as temperature monotonously drops with height. The temperature lapse rate is notably higher in the upper part of the troposphere than in the lower. On the average, the lapse rate is about 0.6 °C/100 m.

Over the continents in the free atmosphere, inversions are absent and the temperature lapse rate is fairly high (curve *3*). In a lower 2-km layer, the lapse rate is 0.7-0.8 °C/100 m, then it lowers somewhat to rise again above 3-km level to 0.8 °C/100 m. In contrast to the trade wind belt, this region demonstrates an increase of humidity with height.

In the upper atmosphere, temperature varies insignificantly from season to season, the annual range decreasing with height (Table 2.1).

Diurnal temperature variation of surface air depends mainly on where the measuring station is located. Over the

Table 2.1 Mean seasonal air temperature (°C) at the daytime, from soundings at Khartoum (after Solot)

	Ground level	Height, km		
		2	3	5
November-April	31	19	12	—7
May-June	39	23	14	—6
July-August	33	20	12	—6
September-October	36	21	12	—7

oceans this variation is practically absent. The diurnal range here is only several tenths of a degree. For land surface air, the variation depends on whether the station is in the interior of a continent or at the shore, height above sea level, and cloudiness.

1. *Continentality.* At shore stations the diurnal temperature range is small. Moving deeply inside a continent, the range sharply widens and does so the more the farther from the ocean. Shores of large lakes and extensive areas of swamped or moist soil, however, introduce a disturbance to the pattern since here the diurnal temperature range is markedly smaller.

2. *Elevation over sea level.* This factor affects depending on the orography and physical conditions of the site. In vast mountainous countries the diurnal temperature range increases on the average with height as the incoming and outgoing radiation becomes with height more intense. This effect is especially pronounced in mountainous regions of dry climate where cloud cover does not reduce the incoming radiation. In valleys of mountain land, drainage winds come into play. They lower temperature in the night-time increasing thereby the diurnal temperature range. With isolated mountains, the effect of height on the diurnal temperature range is entirely different. Since in this case the exchange with free atmosphere is more intense and the influence of the surface is lessened, the diurnal temperature range will be narrow with height. At times this effect is strengthened by clouds formed under the influence of orography.

3. *Cloud cover.* Dense cloud cover markedly attenuates both the incoming and outgoing radiation thus reducing the diurnal temperature range. In the tropics, dense clouds are more often met at the equator. Therefore here is the narrowest diurnal difference. The farther poleward to the so-called dry tropics (15-25° latitude) the wider becomes the diurnal range to reach a maximum over massive deserts.

The diurnal temperature course at low latitudes drastically differs from that at middle latitudes. Contrast to the latter, at low latitudes the diurnal variation is almost invariable from day to day. Among the other factors that influence this behaviour are small annual variation in the duration of day and night time and far lesser occurrence of nonperiodical weather change.

2.2 Pressure

Gradual pressure drop from the subtropics to the equator is characteristic of the tropical region. The subtropical highs go round the globe both south and north of the equator. They migrate equatorward in winter and poleward in summer. In the Northern Hemisphere this seasonal displacement is more pronounced than in the Southern Hemisphere. Besides in the Southern Hemisphere the high pressure belt situates closer to the equator than in the Northern Hemisphere.

Between the high pressure belts in the equatorial region there is a low pressure area —so called equatorial depression or equatorial trough. In the annual mean, the trough is centered near 5°N, that is, it coincides with annual temperature maxima (see also Sec. 2.1). It does not remain on the same latitude during the year shifting southmost in January and northmost in July.

Latitudinal profiles of mean pressure for winter and summer seasons are presented in Fig. 2.5. It is readily seen that pressure is higher in the winter than in the summer hemisphere. From the mean pressure charts of Fig. 2.6 the pressure gradients become weaker as the distance to the equator is smaller and reach their minimum value near the equator. The lowest values amount to tenth fractions of a millibar per 100 km and in some situations they are zero very nearly. Obviously, it places stringent

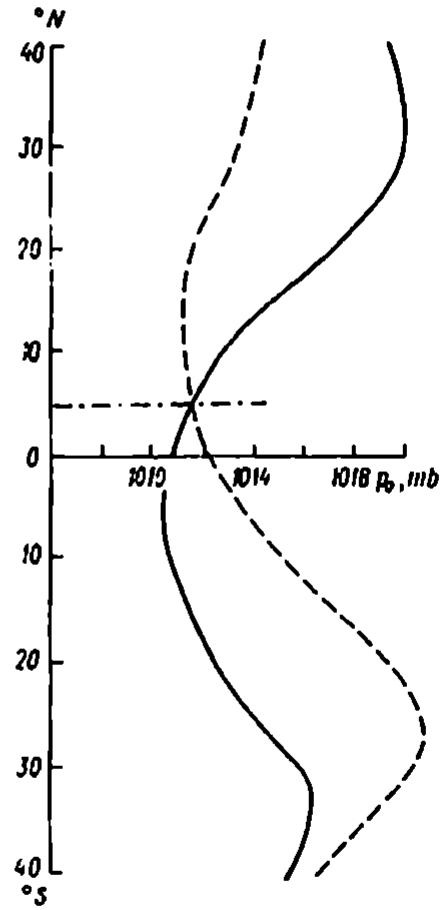

Fig. 2.5 Mean sea level pressure in January *(solid)* and July *(dashed)* (after Riehl), and the annually mean equatorial trough line *(dot-and-dashed)*

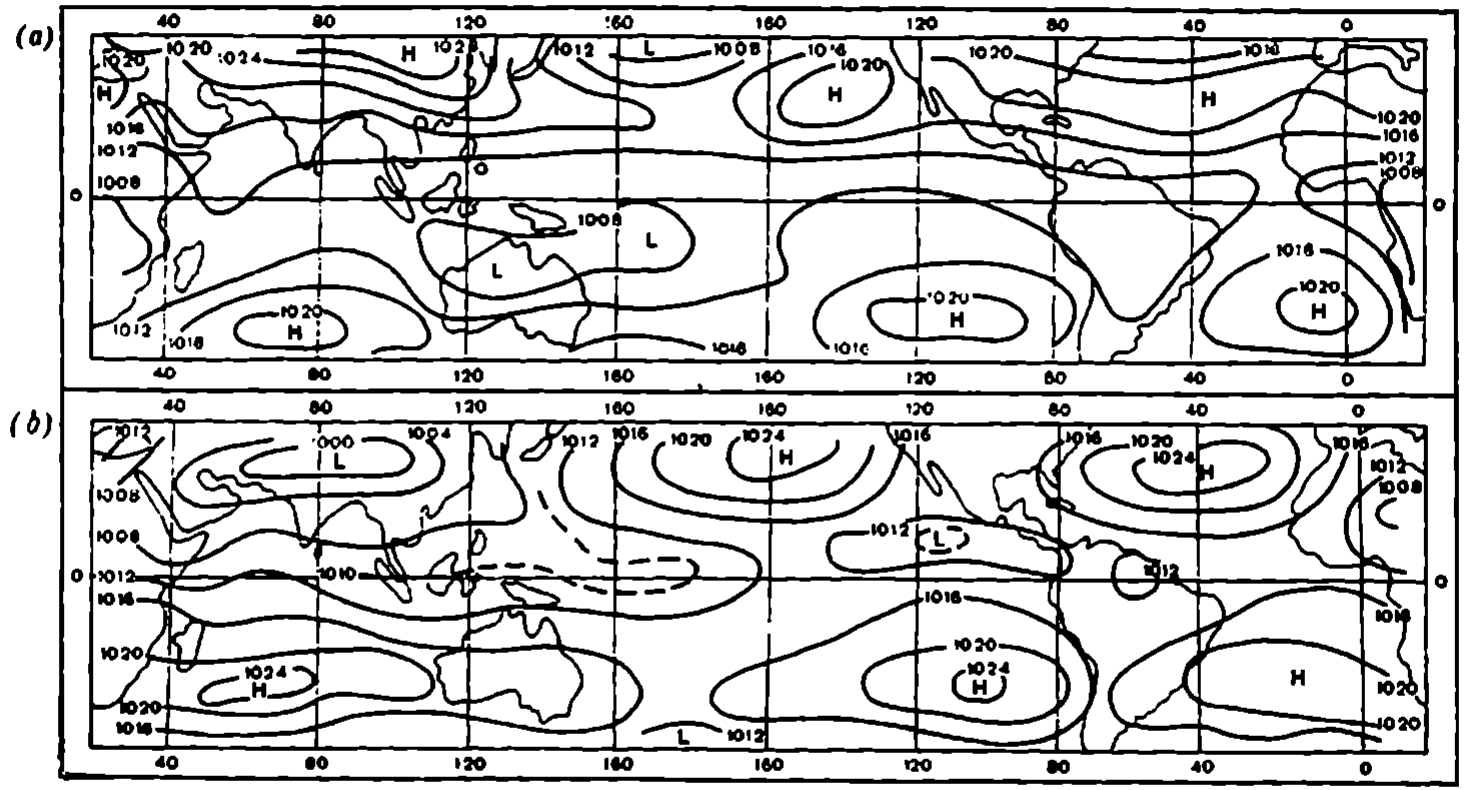

Fig.2.6 Mean pressure charts at sea level for January (*a*) and July (*b*)

requirements upon the accuracy of pressure measurements near the equator.

As in the middle latitudes, the pressure in the tropics does not remain constant through the year. Its variation sums up of both periodical and nonperiodical changes. The latter are most weakly expressed, their influence becomes more substantial at periods of greatest cyclonic activity in the tropics.

Periodical character of the pressure in the tropics is more pronounced than in the middle latitudes. However, throughout the tropics its magnitude varies in time and space. More elaborate analysis puts into a forefront the *semidiurnal*, *diurnal* and *five-day pressure oscillations*. So far, the origin of these waves has not found its rigorous physical interpretation.

At the ground, most powerful is the semidiurnal wave. The mean amplitude is 1-1.5 mb. The amplitude decreases with height to become not more than a half of a millibar at the troposphere's top, near the tropopause. The maxima of the wave come as a rule at about 10 A.M. and 10 P.M., the minima at about 4 A.M. and 4 P.M. local time. The diurnal pressure oscillation, on the contrary, has a very small amplitude at the surface (about 0.2 mb), but it rises in importance with altitude and at 5-km level amounts to one millibar, on the average.

In addition, GATE experiments have observed in the tropics the *3-day and 4-day pressure waves*, the latter being more clearly defined of the two. The wave front has an axis of symmetry making an angle of 30° with a longitudinal circle. The mean wavelength is 7000 km. The wave declines in amplitude nearing the equator. So between latitudes 15 and 10° it amounts to 0.8 mb and near the equator drops to within 0.3 mb.

Of major significance at the surface is the semidiurnal wave. It often distorts the pattern of pressure tendency which is used to report as an indicator of synoptic process development. As often as not the tendency is employed to decide how the synoptic objects move and evolve, how the synoptic situation changes as a whole, and whether the weather in the region has a tendency to change or hold. Coming into play, a semidiurnal pressure wave changes the synoptic pres-

sure field so pressure taken as it stands may lead to errors in synoptic scale forecast. Obviously, pressure tendency data should be corrected for this effect. This procedure requires the amplitude of the wave.

Let the observed tendency be denoted Δp_o and the true synoptic tendency Δp_t. If we want the synoptic tendency for a period subtending an ascending or a descending section of a semidiurnal wave, then the following expression is used

$$\Delta p_t = \Delta p_o \pm A/2$$

where the minus sign is applied to the ascending portion and the plus sign to the descending.

If the pressure gradient of the wave has one sign within one hour and another sign within two hours, then another formula is employed

$$\Delta p_t = \Delta p_o \pm A/6$$

Example 1. Let Δp_o be 2 mb/3 hr and $A = 1.2$ mb in the semidiurnal wave from 6 to 9 A.M., that is, in the period of pressure rise, then

$$\Delta p_t = 2 - 1.2/2 = 1.4 \text{ mb/3 hr}$$

Example 2. Let the initial data be the same as in Example 1 with the exception that Δp_o has been observed from 2 to 5 P.M., i.e., during the first two hours pressure in the wave descends and during the last hour ascends, then

$$\Delta p_t = 2 + 1.2/6 = 2.2 \text{ mb/3 hr}$$

The amplitude of the semidiurnal oscillation varies with time; therefore the above calculations can be but approximate. To improve the accuracy of tropic forecast, 24-hour pressure changes are often used instead of 3-hour pressure tendencies, as more representative.

It is believed that *pressure waves can exert some influence on the weather pattern in the tropics*, in particular on the cloud cover and precipitation. An investigation for this course was published in 1968 by Brier and Simpson who sought for a correlation of semidiurnal pressure wave with changes in cloudiness and rainfall at Djakarta and Wake Island (19°N, 166°E). They found that at Djakarta in some years the amplitude of the semidiurnal wave varied by 15% to

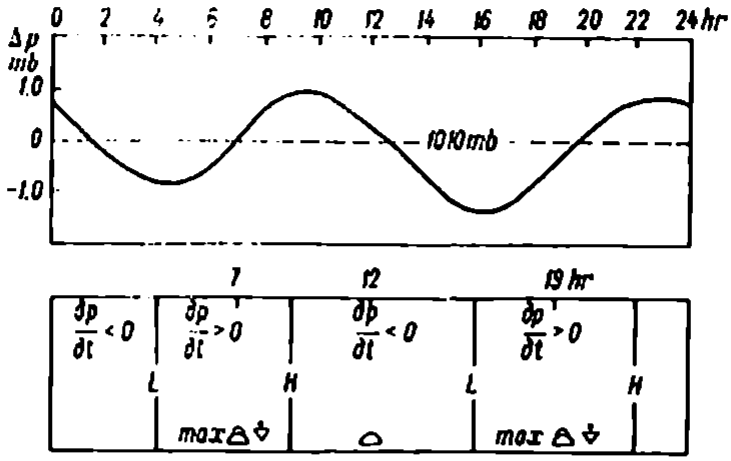

Fig. 2.7 Semidiurnal pressure wave and weather change at Djakarta (after Simpson and Brier)

20% from month to month and in some days even by 100%. About the same pattern was found at Wake. No change of phase for the wave was observed at either station during the year, neither does it change from year to year.

In papers that had been published prior to G.W. Brier and Y. Simpson's work, the semidiurnal pressure wave has been related to the cloudiness in the following way: at a period when pressure rises (from 4 to 10 A.M. or from 4 to 10 P.M.) clouds increase in number, then when pressure drops cloudiness parallels the change (Fig. 2.7). Assuming this statement as a hypothesis, Brier and Simpson suggested that if it is true, still more clouds are to be expected when pressure increase intensifies, when say ascending branches of other pressure waves superimpose, and respectively, still lesser cloudiness at the days when pressure rise slackens, say pressure increase in the semidiurnal wave coincides with pressure drop in other waves. The reverse might also be true, that is in periods when pressure drop intensifies a marked decrease in cloudiness is to be expected.

Return now to the observational data. Djakarta, situated at the northwest of the Java Island, is exposed to the southeast trades in southern winter (dry season) and to the equatorial trough, crossing the island, in summer (rainy season). The mean annual rainfall at Djakarta amounts to 1840 mm.

Surface pressure at Djakarta increases from 4 to 9 and from 4 to 10 P.M. and decreases from 10 P.M. to 4 A.M. and from 9 A.M. to 4 P.M. The mean annual amplitude of the semidiurnal wave is 1.38 mb though on some days it may be as high as 6 mb.

The Wake Island with an area of 35 km^2 is under the influence of the northeast trades all through the year. Its mean annual rainfall is 940 mm. Surface pressure increases from 5 to 10 A.M. and from 4 to 10 P.M. and decreases from 10 A.M. to 4 P.M. and from 10 P.M. to 5 A.M.; its mean annual amplitude amounts to 0.93 mb.

In the diurnal variation of cloudiness and rain at Djakarta there are three maxima—two major ones, that before daybreak and during sunset, and the secondary one after noon. At Wake Island there are only two main maxima—before daybreak and at sunset.

In the diurnal distribution of rain at Wake two maxima are recorded as a rule—the major one in the period from 3 to 6 A.M. and the secondary before daybreak, observed though relatively seldom.

The synchronous comparison of pressure and cloudiness change and of pressure and rainfall has not revealed an explicit correlation. Nor has it revealed any correlation of pressure change with the following change in clouds and rain. Therefore instead of this continuous comparison it has been decided to compare the cloudiness and rainfall on days with extremely large amplitude of semidiurnal wave with that on days when the amplitude is extremely small. The scope was narrowed even more to include into the comparison only those changes of cloudiness and rainfall which occur at periods of pressure increase or decrease, that is during 5 or 6 hours of 24.

At Djakarta the experiment has revealed higher increase in clouds between 4 and 9 A.M. on days with larger pressure rise than on days when pressure increased slowly. Thus, days of higher pressure rise are more potent for rain to fall and amount of precipitation to increase.

According to the assumed hypothesis (see Fig. 2.7) clouds are to diminish in parallel with pressure drop of the semidiurnal wave. However, large land area of Java as it is aids in cloud formation outweighing all the other effects. Moist

sea breeze and heated land counteract to produce intense convection and form clouds. Since clouds reduce incoming radiation the situations were studied with various initial cloudiness.

Cloud development was found to be suppressed markedly when pressure changed significantly and initial clouds were few. With total cloud cover this effect was less noticeable. So if a significant pressure decrease were recorded at 9 A.M. with a cloudiness of 10% to 30%, the cloudiness was not developed further. Cloudiness did increase if at the same conditions pressure decreased insignificantly (small amplitude of the semidiurnal wave). An outweighing influence of pressure drop was obvious in the days of continuous cloud cover at 9 A.M. On these dull days the less heated surface does not aid in breeze development, thus the conditions for clouds to develop are absent. In the circumstances, the net semidiurnal oscillation superimposes on the main disturbance which alone resulted in continuous cloud cover. The Djakarta observations demonstrated the effect of semidiurnal oscillation being more strong on the days with large pressure drop. So, on the days with small pressure drop the cloud cover initially continuous released to 70% (7 balls), with large descent to 50%.

At Wake Island cloudiness was found to increase with pressure, though slightly weaker. in the same manner as at Djakarta. Periods of pressure decline at Wake Island were not studied.

With the results of the above study at hand Brier and Simpson have concluded that cloud cover does increase with rise in pressure and decreases with its drop in the semidiurnal wave. The conclusion has been arrived at for two stations in different physico-geographic surroundings. Inductively, it may be extended onto other tropical locations.

It follows from the above, that *a relation between pressure rise and increase in cloud cover does exist, the respective quantitative estimates, however, have not been obtained so far.* For Djakarta and the Wake, cloud cover and rainfall increase by 15% to 20% when pressure ascends by 2 to 3 mb. The cloudiness and rainfall diurnal courses have maxima before daybreak and at sunset. Physical reasons for such a dependence have not been disclosed yet.

2.3 Wind

The wind field in the tropics has three major zones: (1) the trade wind belt of the Northern Hemisphere; (2) the trade-wind belt of the Southern Hemisphere: and (3) the equatorial trough region. At times the trough zone is called the transition region from the northern to the southern trades. In the southern winter it normally migrates northward to lie somewhere between 0 and 5°N, and in summer it displaces up to 15°N.

Characteristic of some regions in the tropics are monsoon currents. Above all it is the notorious Asiatic monsoon. In the area where it is active, southwest flows prevail in the northern summer and northeast flows in winter. Well defined are also African monsoons. In the northern summer the southern winds having a western component make wide incursions into the western African continent bringing rain over large territories. In winter these winds go only as far as the African coast around the Gulf of Guinea while the northeastern winds prevail farther north (Fig. 2.8).

The trades occupy the bulk of the tropics. Broadly speaking, they blow from ENE in the Northern Hemisphere and from ESE in the Southern Hemisphere. But the flow points a little more toward the equator in winter than in summer. So, the average wind direction in the Northern Hemisphere is around 50° in January and around 70° in July. In the Southern Hemisphere it is near 130° in July (wintertime) and near 110° in January (summertime)*.

On the geographical equator NE winds prevail in January and SE winds in July.

In the trade-wind region, winds increase in strength from summer to winter. Riehl has found that the greatest resultant wind speed of the trades in the Northern Hemisphere is 2.4 m s^{-1} in summer to increase to 4.3 m s^{-1} in winter, in the Southern Hemisphere the respective figures are 3.3 and 5.3 m s^{-1}.

In January the winds reach their main peaks at about 10°N and 20°S. Three adjoint minima are noted at the time: at 30°N and at 5 and 35°S. In July the main maximum shifts towards 15°S and the second maximum to 20°N. According-

* Measured clockwise from north on the 360° compass.

ly, the profile has three minima: at 35 and 10°N and at 30°S.

Therefore in winter of the respective hemisphere the region of peak wind velocities shifts 5 to 10° latitude equatorwards. The region of minimal wind speeds coincides at the time with the center line of the subtropical high pressure belts and with the equatorial trough line.

The trade winds are well known for their higher steadiness. A measure of steadiness, S, widely used in climatology, is ratio of mean wind vector modulus to its mean scalar velocity

$$S = |\mathbf{V}| / V$$

It is always unity, when the wind keeps blowing from the same direction, irrespective of fluctuations in wind speed, $|\mathbf{V}| = V$ and $S = 1$. If, on the contrary, all directions in wind field are equiprobable, then $|\mathbf{V}| = 0$ and $S = 0$, so that the wind is absolutely unstable.

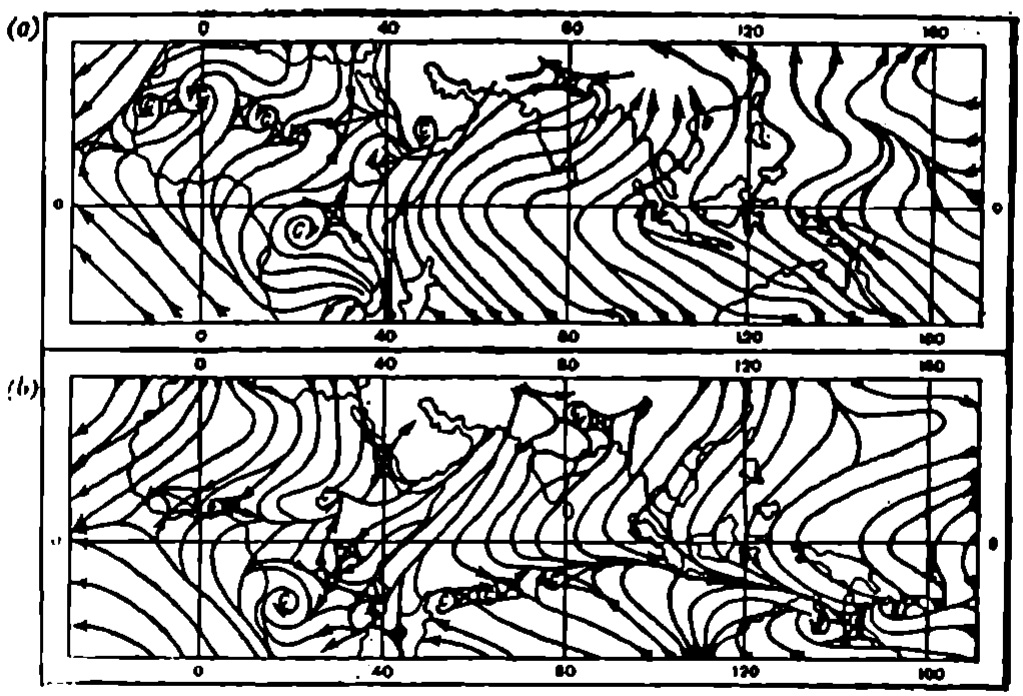

Fig. 2.8 Streamlines at sea level (Eastern Hemisphere) for July(*a*) and January (*b*)

For both trade wind regions the mean steadiness $S = 0.75$; for the trades in the northern Atlantic $S = 0.9$, for the subtropics it is equal to zero.

Over the equatorial trough the winds do not normally blow faster than 2 m s^{-1}. In January at the trough line the winds blow mainly westward. South of the trough a south component appears which increases with the distance southward from the trough line, while the north component is observed northward. At about 10° latitude from the equatorial trough the meridional component has a maximum of 1.5 m s^{-1}. The maximum steadiness within the trough region in January lies near 0.7.

At the trough line in July the westerlies prevail whose southern component is rather weak (about 0.5 m s^{-1}). Similar to January, farther south the south component increases, and farther north the stream moves first strongly eastward then the north component gains in importance. They are strongest at about 10° latitude from the equatorial trough. The steadiness at the trough line is 0.5, however, it rises sharply to both the north and south. Within the trough, steadiness nowhere exceeds 0.8.

The wind data collected during the GATE missions have brought evidence that the wind field of the southern trade wind belt varies with height differently in various locations. However, a general pattern of this change can be evaluated. So, within 1.5 to 3 km from the earth's surface the prevailing winds are the south-easterlies having the average speed of 5-8 m s^{-1}. The highest speed in this region may be 11-12 m s^{-1}. Closer to the equator, the wind becomes weaker and the air layer from the trades more shallow. On some days even westerlies of 1-2 m s^{-1} may be observed near the equatorial trough (8-10° latitude from its center line) in the trade-wind region at about 1.5 km altitude, holding as long as one or two days.

Not infrequently the 1.5-2 km layer of westerlies comes to stay above the field of the SE trades. The westerlies may curtail after a few hours, though they may last as long as a few days. Closer to the equatorial trough these periods gain in duration and the westerlies layer descends. Otherwise, the weak easterlies prevail in the region.

Still higher overlies the thick stratum of easterlies having

a small south component. In some periods this layer protrudes up to a height of 12-13 km with a wind speed of 30 m s^{-1} at 12-km layer. In other periods the base layer of easterlies descends down to 9 km. The south meridional component of wind speed in the stratum varies broadly in the vertical and in time.

Above the layer of the easterlies (up to 21 km in the vertical) the westerlies of 20 m s^{-1} dominate the region. This field has two features: the first is the shallow layer of easterlies found at times near the tropopause, the second is the notable unsteadiness in the position of westerlies bottom. Each 15-16 days this boundary sharply ascends to a height of 16-17 km and then gradually descends to the initial position afterwards (Fig. 2.9).

Over the northern trade wind belt, a similar variation with altitude is observed with the only difference that the

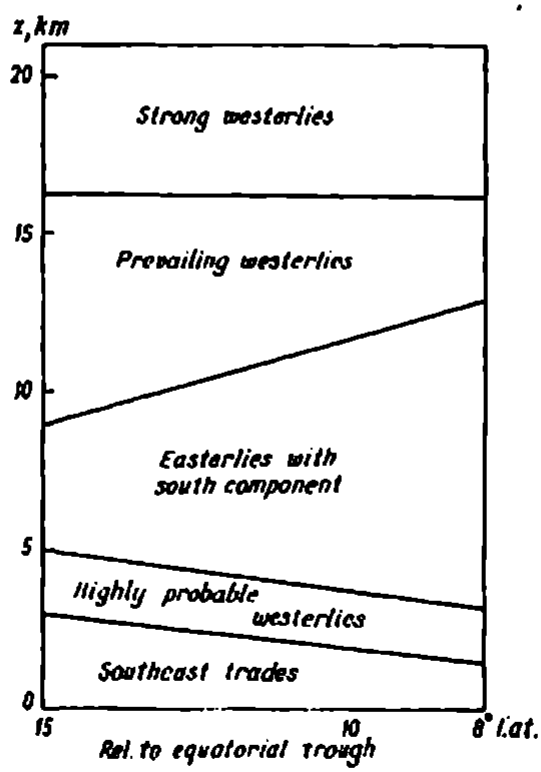

Fig. 2.9 Schematic vertical wind profile in the SE trades at 8-15° latitude relative to the equatorial trough

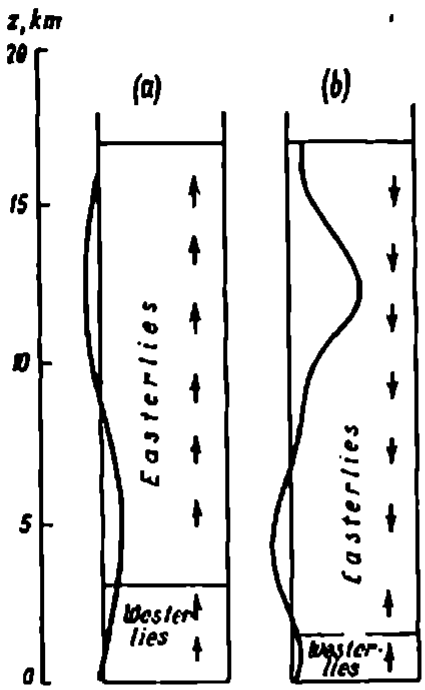

Fig 2.10 Schematic wind profile in the ITCZ plotted as the march of meridional component in relative units (heavy lines) for (a) well-developed ITCZ; (b) diffuse ITCZ; direction of vertical movement is indicated by arrows; and path of meridional component, by curves

north component takes place of its southerly counterpart of the Southern Hemisphere.

The GATE data have also supplied a pattern of air mass motions over the intertropical convergence zone (ITCZ). Figure 2.10 shows the flow distributions over both the developed and diffuse ITCZ. In the region of the well developed ITCZ up to 3-km altitude the winds are mainly westerlies with a maximum for the west component of 3 m s^{-1} at about 1.5 km altitude. In the bottom layer (up to 0.6 km) a meridional component is absent. Aloft, the south component is traced amounting to 1-1.5 m s^{-1}. From 3 to 17 km in the vertical extent, the prevailing flows are easterlies with a maximum of the east component at the 12-km level. It can reach here a value of 15-16 m s^{-1}. The meridional component remains southerly at the bottom part of this layer. It peaks at about 7 km altitude to subdue higher up and reverse its direction for northerly at 8-9 km. The north component has its maximum of 1-2 m s^{-1} at 12-13 km then weakens and the flow becomes easterly at 16-17 km height. All throughout the depth from 0 to 17 km height there have been recorded updroughts lifting at 1-2 cm s^{-1} on the average.

Winds with the west component are also observed in the diffuse ITCZ, in the layer from the ground to 1.5 km. It may be as high as 1-2 m s^{-1}, while the south component in the layer has values below 1 m s^{-1}. Winds with the east component are traced from the 1.5 km level up to the tropopause. The strongest eastern component is observed at 12 km.

It amounts to 13 m s^{-1}. Above 1.5 km altitude the south component subdues and at 3 km already the north component appears. Its maximum of 1.5 m s^{-1} lies between 3 and 4 km. At 6 km altitude the meridional component is absent and aloft the south meridional component again appears to reach its maximum at the 12 km level.

Updroughts in the diffused ITCZ are observed up to 3 km altitude in their highest. Farther up a thin layer is to be found where vertical movements are absent, and above it air movements are directed downward.

Still in 1945 R.D. Fletcher noted a relatively frequent appearance of westerlies in the equatorial region, which could not go into the traditional framework of the tropical circulation. The so-called *equatorial region of westerlies* looks anomalous when compared with the above distribution of wind and pressure. Early the equatorial westerlies were believed random phenomena or even a product of erroneous measurements. When the observational data became more abundant the region of westerlies proved a reality.

In the eastern part of the globe the equatorial region of westerlies migrates seasonally along the equator. It can be found over Africa and the Indian Ocean, Indonesia and the Northern Australia. At times it extends over the western Pacific. In the western hemisphere it is pronounced less strongly. From the charts prepared by Flohn one may assume that the westerlies can be recorded at the seaboard of Columbia and in the equatorial areas of South America.

The equatorial region of westerlies varies in width from one year to the next. In the years of prevailing westerlies their width holds unchanged near the equator even in the winter hemisphere making wide incursions into the summer hemisphere. The total width can be in such seasons as wide as 32° in the Northern Hemisphere (India-Pakistan area) and 20° in the Southern Hemisphere (Northern Australia and South Africa). In autumn and winter the equatorial region of westerlies places uniformly on either side of the equator. It is 8-14° latitude wide. In a narrow nearequatorial belt of the eastern hemisphere the westerlies blow in all seasons. The average width of the equatorial westerlies is about 6° the low troposphere, 8-10° at the seaboard of the Bay of Guinea, in the western Africa and in the eastern

Indian Ocean, yet it narrows to 4° latitude in the western parts of the Indian Ocean and Pacific.

The continuous belt of the westerlies can be found on the mean many-year weather charts only. Daily observations show that winds vary markedly in this belt. Daily synoptic charts trace the equatorial westerlies only at separate areas.

2.4 Pressure and Wind Fields

The horizontal Coriolis force is very small in the tropics and equals nil at the equator. Therefore the quasi-geostrophic balance may no longer be true here, which poses a most serious problem before tropical weather analysts and forecasters. Many scale analysis models and simplifications used to advantage in the middle latitudes appear unfit in the tropics.

Weather forecasting is essentially extrapolation of weather data in space and time. To provide the extrapolation wind-pressure relationships are required without which the procedure would be not only difficult but often even impossible. In some part of the tropics this role may undertake the geostrophic relationships though a certain degree of care should be exercised in their application. So far no unanimous opi-

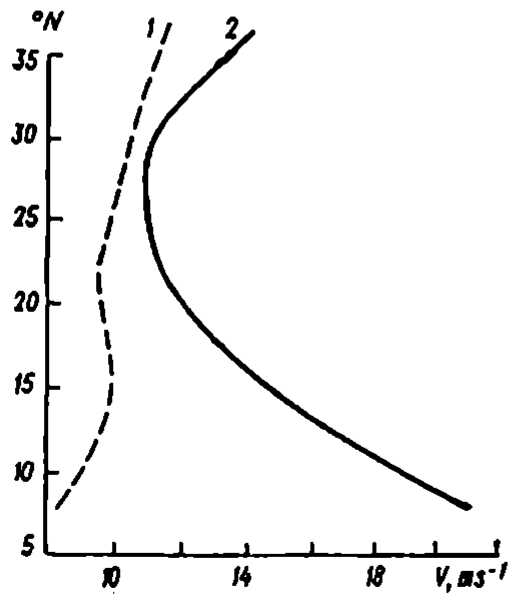

Fig. 2.11 Mean latitudinal profile of (*1*) actual and (*2*) geostrophic wind (after Jordan)

nion exists as to what latitude should be taken such a limiting one where the quasi-geostrophic approximation could be still applicable.

Figure 2.11 presents the mean latitudinal distributions of geostrophic and actual winds at the top of the friction layer. It is readily seen that north of 20°N the geostrophic wind deviates from the actual insignificantly but the deviation sharply increases equatorward. At 10° latitude the mean difference amounts to 9 m s^{-1} that is outweighs the value of observed wind itself. Notably, the actual wind is everywhere weaker than its geostrophical approximation.

The distribution of geostrophic and resulted wind in the east nearequatorial Atlantic in July-August is illustrated in Fig. 2.12. As the distance toward the equator becomes smaller the geostrophic wind turns farther off the actual wind direction, which is notably close to the pressure gradient direction and in some areas (4.5°N) even totally coincides with it. In July-August the equatorial trough ascends highly northward. The related convergence zone can be readily followed. It places between 5 and 18°N. Simultaneously, the secondary convergence zone may be traced between 2 and 6°N.

In many circumstances better results are provided with the cyclostrophic wind. In comparatively small cyclones—and they are indeed less in the tropics than in the temperature zone—the centrifugal force is in exact balance with the horizontal pressure gradient. The cyclostrophic balance approximation is much superior to the geostrophic when applied to the tropical cyclones. The actual wind in the cyclones blows at 50-60 m s^{-1}, the cyclostrophic approximation gives rise to 70-75 m s^{-1} whereas the geostrophic relationships supply 200-250 m s^{-1}.

The cyclostrophic balance can exist only when the curvature of the air stream is cyclonic because with an anticyclonic curvature the centrifugal force and pressure gradient act in the same direction. This fact, in particular, has given rise to a hypothesis that anticyclones cannot exist in the equatorial region. Observations, however, have not proved it.

At the top of the tropical friction layer, air stream is directed so that it crosses the isobars. Moreover, even above this level wind makes an angle with the isobars (isohypses).

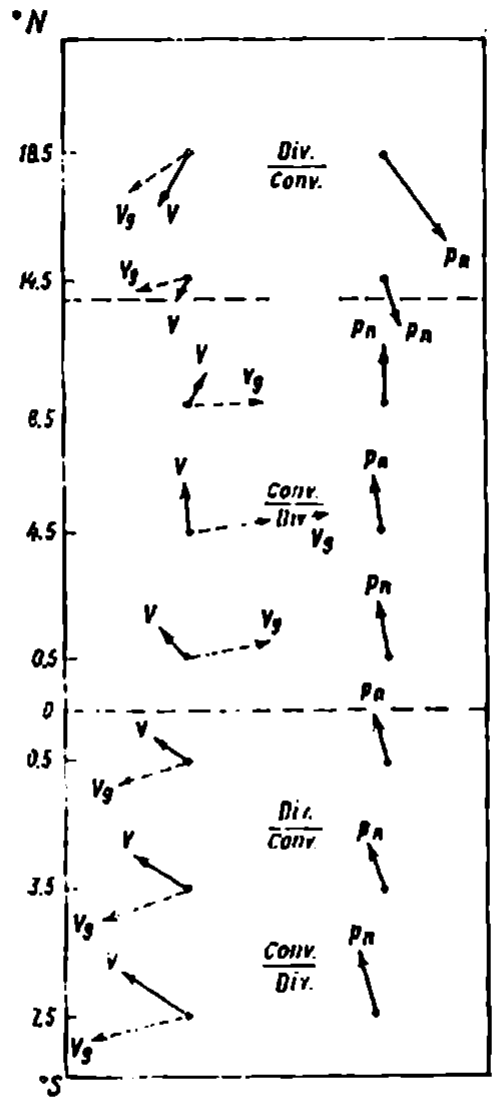

Fig. 2.12 Distribution of pressure gradient, p_n, geostrophic wind, V_g, resultant wind (computed on 1911 trough 1970 data), V, and divergence areas in the eastern equatorial Atlantic (after Lamb and Hastenrath) Scale: 1 m s^{-1} ~ 5 mm; 10^{-2} m s^{-2} ~ 3 mm

Reasoning from those observations it has been suggested that small pressure gradients (geopotentials), commonly observed in the tropics, balance the turbulent friction force which does not disintegrate at 1 km altitude but does exist much higher. However, the scale analysis on the GATE'72 and '74 data has rejected the suggestion as baseless. The fric-

tion force has been proved about two orders of magnitude lower than the geopotential gradient.

Proceeding from the above argument a conclusion may be that wind in the tropics cannot be computed from the pressure field at all. However, a need in such computations persists, as well as in the reverse operation that is in computing geopotential gradients from the wind observations. The last procedure is of especial importance for numerical forecasting. Many attempts are known to have been made in relating the wind and pressure fields. In what follows we shall discuss several ways to approach this objective.

Grimes (1951) has suggested the following form of the horizontal momentum equations

$$\begin{aligned} \frac{\partial u}{\partial t} - \eta v &= -\frac{1}{\rho}\frac{\partial P}{\partial x} \\ \frac{\partial v}{\partial t} + \eta u &= -\frac{1}{\rho}\frac{\partial P}{\partial y} \end{aligned} \tag{2.4.1}$$

where $P = p + V^2/2$ is the dynamic pressure (p = atmospheric pressure and $V^2 = u^2 + v^2$), η is the absolute vorticity, u and v the horizontal components of wind speed.

Assuming $\partial u/\partial t = \partial v/\partial t = 0$ yields

$$u = -\frac{1}{\rho\eta}\frac{\partial P}{\partial y}, \quad v = \frac{1}{\rho\eta}\frac{\partial P}{\partial x} \tag{2.4.2}$$

The equations (2.4.2) are similar to the geostrophic relations but the role of the Coriolis parameter is played by the absolute vorticity, and the pressure variable is the dynamic pressure rather than atmospheric. The obtained relationships represent the connection of the wind and pressure fields in the general form. Hence they should describe a steady motion even where the Coriolis parameter becomes small and the deflecting force cannot exactly balance the pressure gradient. Providing for the relative vorticity makes this balance possible. The air motion field obeys the same laws as does the geostrophic wind of mid-latitudes. However, absolute vorticity should not be treated as a constant quantity. In the high latitudes of the Northern Hemisphere it is positive whereas in the high latitudes of the Southern Hemisphere it assumes negative values. Hence, somewhere

in the equatorial zone a boundary, or a narrow transition zone, should exist between these polar values.

In the tropics absolute vorticity is zero very nearly so that in the narrow transition zone the formulas (2.4.2) have the same shortcoming as the geostrophical relationships. The isoline $\eta = 0$ has been labelled the *kinematic equator*. It runs parallel to the geographic equator and migrates within the nearequatorial region from 5°N to 5°S. It means that absolute vorticity changes its value as well as sign at least within this area. When η changes its sign then according to (2.4.2) the motion should reverse its direction, that is obey a course it would have in the other hemisphere. If an analysed area is in the Northern Hemisphere the direction of flow reverses when the anticyclonic vorticity outbalances the Coriolis parameter, rendering the absolute vorticity negative. This situation is not infrequently observed in the nothern part of the central Africa. The developed winds have the local name "antiflows".

The relations (2.4.2) describe motions of tropical air, but they pose several problems in practical computations of wind from the pressure field, firstly, because the pressure gradients, being very small, are deduced with large errors; secondly, because both sides of (2.4.2) contain the sought parameter—wind ($P = p + V^2/2$, $\eta = l + \partial v/\partial x - \partial u/\partial y + f$, $f = 2\Omega \sin \varphi$) and, finally, because at the kinematic equator, where the absolute vorticity tends to zero, the equations (2.4.2) become void of sense.

A scale analysis made for the terms of motion equations with the data of GATE'72 and '74 expeditions has shown that the nonlinear terms are of the same order of magnitude as the other terms in the tropics. Air particles have some inertia and "store momentum", as it were. Based upon this examination, for a steady-state motion in free atmosphere the horizontal equations of motion can be written

$$\begin{aligned} u\frac{\partial u}{\partial x} + v\frac{\partial u}{\partial y} &= g\frac{\partial h}{\partial x} + fv \\ u\frac{\partial v}{\partial x} + v\frac{\partial v}{\partial y} &= g\frac{\partial h}{\partial y} - fu \end{aligned} \qquad (2.4.3)$$

or otherwise

$$u = -\left(g\frac{\partial h}{\partial y} + v\frac{\partial v}{\partial y}\right)\Big/\left(f + \frac{\partial v}{\partial x}\right)$$
$$v = \left(g\frac{\partial h}{\partial x} + u\frac{\partial u}{\partial x}\right)\Big/\left(f - \frac{\partial u}{\partial y}\right) \qquad (2.4.4)$$

It is seen that the wind speed is defined not only by the local geopotential gradient but also by the inertial properties of the stream. The sought wind is seen to be on both sides of (2.4.4) so its computation would be rather difficult.

The equations (2.4.3) can be used to compute the geopotential gradient from the wind field. For the tropics, especially in the equatorial region, this procedure is of value, since computing the geopotential gradient from the pressure field may lead to errors both in the gradient value and in its sign. This situation occurs because the accuracy in the geopotential evaluation is comparable with the values of geopotential gradients.

With wind field data available the geopotential gradients can be obtained from the following relationship, deduced from (2.4.3):

$$\frac{\partial h}{\partial x} = -\frac{1}{g}\left(u\frac{\partial u}{\partial x} + v\frac{\partial u}{\partial y} - fv\right)$$
$$\frac{\partial h}{\partial y} = -\frac{1}{g}\left(u\frac{\partial v}{\partial x} + v\frac{\partial v}{\partial y} + fu\right) \qquad (2.4.5)$$

Objective analysis, numerical forecast, and modelling of atmospheric processes require the wind (velocity) and pressure (mass) fields should be matched. This balancing is best effected with complete equations of motion by a technique suggested and developed by Marchuk, Miyakoda and Moyer, Nitta and Hovermale. The technique, that has been called the dynamic balancing, is carried out by multiple integration of the complete equations first one time-step forward, then backward by the schemes that provide selective suppression of small-scale disturbances. One of the techniques of time differentiating employed in numerical integration is the Euler-backward scheme, often called the Matsuno scheme.

The dynamic balancing is essentially as follows. On integrating the prognostic equations forward the mass and veloc-

ity fields are modified and mutually adjusted. The gravity waves that occur in the process of adjustment are suppressed by a selected numerical integration scheme. Integrating backward, the scheme returns to the initial time point. As a result, the large-scale features of the fields remain practically unchanged whereas small-scale disturbances are largely damped out.

Multiple repetition of the cycle of forward and backward integration—the procedure that is often labelled pseudoprognosis—gives rise to a certain balance of the fields. These balanced fields are used in further computations. The iterative procedure used in adjusting the fields converges when the fields become balanced.

The dynamic balancing is in fact one of the approaches to the problem of mutual adjustment of fields which has been extensively treated in the works of Kibel and Obukhov.

The integration procedure may be arranged so that in the process of adjustment all the fields would change. This type of computation is termed a free adjustment. In another approach the pseudoprognosis may be made so that one of the fields remains unchanged (restored).

Of particular interest is the dynamic balancing while the pressure (geopotential) field is restored thereby modelling adjustment of wind to pressure field. This version of dynamic balancing may be used to compute the wind field from the pressure field in the tropics.

Consider now the dynamic balancing with complete equations as applied to the barotropic and baroclinic models.

To effect adjustment in the framework of the baroclinic model we employ the following set of equations:

$$\begin{aligned}
&\frac{\partial u}{\partial t} + u\frac{\partial u}{\partial x} + v\frac{\partial u}{\partial y} = -\frac{\partial \Phi}{\partial x} + fv \\
&\frac{\partial v}{\partial t} + u\frac{\partial v}{\partial x} + v\frac{\partial v}{\partial y} = -\frac{\partial \Phi}{\partial y} - fu \qquad (2.4.6) \\
&\frac{\partial \Phi}{\partial t} + u\frac{\partial \Phi}{\partial x} + v\frac{\partial \Phi}{\partial y} = -\Phi\left(\frac{\partial u}{\partial x} + \frac{\partial v}{\partial y}\right)
\end{aligned}$$

where Φ is the geopotential, the other designations are merely conventional.

Adjustment with the baroclinic model we shall discuss on

the basis of the quasi-hydrostatic system of complete equations in a sigma system of coordinates (x, y, σ)*, which does not allow for friction and adiabatic heating effects.

$$\frac{\partial u}{\partial t} + u\frac{\partial u}{\partial x} + v\frac{\partial u}{\partial y} + \dot{\sigma}\frac{\partial u}{\partial \sigma} = -\frac{\partial \Phi}{\partial x} + fv$$

$$\frac{\partial v}{\partial t} + u\frac{\partial v}{\partial x} + v\frac{\partial v}{\partial y} + \dot{\sigma}\frac{\partial v}{\partial \sigma} = -\frac{\partial \Phi}{\partial y} - fu$$

$$T = \frac{\sigma}{R}\frac{\partial \Phi}{\partial \sigma} \qquad (2.4.7)$$

$$\frac{\partial u}{\partial x} + \frac{\partial v}{\partial y} + \frac{\partial \dot{\sigma}}{\partial \sigma} = 0$$

$$\frac{\partial T}{\partial t} + u\frac{\partial T}{\partial x} + v\frac{\partial T}{\partial y} - \frac{RT}{g}(\Gamma_a - \Gamma)\frac{\dot{\sigma}}{\sigma} = 0$$

It is assumed that the initial and boundary conditions required to obtain the solutions of (2.4.6) and (2.4.7) are given. As the initial values for u and v one may use the respective components of zonal wind or geostrophic wind computed for the area under investigation via the conventional geostrophic relationships applied at the nearest latitude where the geostrophic approximation is valid.

The values of $\dot{\sigma}$ required to integrate the system of equations are computed with the continuity equation in the manner usually employed for the baroclinic and nongeostrophic prognostic models.

Rewrite the equations of (2.4.6) and (2.4.7) containing the time derivatives in a compact form

$$\partial z/\partial t = F \qquad (2.4.8)$$

where for (2.4.6)

$$z = \begin{vmatrix} u \\ v \\ \Phi \end{vmatrix}, \quad F = \begin{vmatrix} -u\frac{\partial u}{\partial x} - v\frac{\partial u}{\partial y} - \frac{\partial \Phi}{\partial x} + fv \\ -u\frac{\partial v}{\partial x} - v\frac{\partial v}{\partial y} - \frac{\partial \Phi}{\partial y} - fu \\ -u\frac{\partial \Phi}{\partial x} - v\frac{\partial \Phi}{\partial y} - \Phi\left(\frac{\partial u}{\partial x} + \frac{\partial v}{\partial y}\right) \end{vmatrix}$$

* $\sigma = p/p_s$, where p_s (labelled also π elsewhere) is surface pressure.

and for (2.4.7)

$$z = \begin{vmatrix} u \\ v \\ T \end{vmatrix}, \quad F = \begin{vmatrix} -u\frac{\partial u}{\partial x} - v\frac{\partial u}{\partial y} - \dot{\sigma}\frac{\partial u}{\partial \sigma} - \frac{\partial \Phi}{\partial x} + fv \\ -u\frac{\partial v}{\partial x} - v\frac{\partial v}{\partial y} - \dot{\sigma}\frac{\partial v}{\partial \sigma} - \frac{\partial \Phi}{\partial y} - fu \\ -u\frac{\partial T}{\partial x} - v\frac{\partial T}{\partial y} + R\frac{T}{g}(\Gamma_d - \Gamma)\frac{\dot{\sigma}}{\sigma} \end{vmatrix}$$

The time-differentiating scheme needed for dynamic balancing iterations will be facilitated through the Euler-backward scheme as follows

$$\begin{aligned} z^*_{n+1} &= z^{(\nu)}_n + F^{(\nu)}_n \Delta t \\ z^{(\nu)}_{n+1} &= z^{(\nu)}_n + F^*_{n+1} \Delta t \end{aligned} \tag{2.4.9}$$

$$\begin{aligned} z^*_n &= z^{(\nu)}_{n+1} - F^{(\nu)}_{n+1} \Delta t \\ z^{(\nu+1)}_n &= z^{(\nu)}_{n+1} - F^*_n \Delta t \end{aligned} \tag{2.4.10}$$

where the subscripts n and $n + 1$ denote the time points; Δt is the time step; z^*_{n+1}, z^*_n, z_{n+1}, z_n the initial and final values of z at the moments n and $n + 1$; F_n, F^*_{n+1}, F_{n+1}, F^*_n the values of function F calculated with z_n, z^*_{n+1}, z_{n+1}, and z^*_n, respectively; the superscripts ν and $\nu + 1$ are the numbers of the iteration cycles.

As is readily seen, the formulas (2.4.9) are employed to integrate forward by one step and (2.4.10) to integrate by one step backward. The total iteration cycle of two steps forward and two steps backward integration returns the process to the time base.

Notice that in the dynamic balancing within the framework of the baroclinic model, each iteration cycle computes vertical speed and geopotential by the diagnostic equations (the hydrostatic and continuity equations) and boundary conditions for $\dot{\sigma}$ with respect to σ (at $\sigma = 0$, $\sigma = 1$, and $\dot{\sigma} = 0$) in much the same manner as it is made with the prognostic baroclinic model at each time step.

The iteration procedure is repeated several cycles ($\nu = 1, 2, 3, \ldots$) until the fields practically cease varying from one cycle to the next. This is an indicator of the iterations being converged and an adjustment being effected.

The resulted fields are assumed to be balanced. When we compute a wind field from a given (observed) pressure, or geopotential field, the achieved balance means that we obtained the sought wind field and no further computation is needed.

Numerical experiments performed with the equations (2.4.6) and (2.4.7) have demonstrated that the iterative process converges if the Euler-backward scheme is used with certain values of time step. Then the number of iterations depends on the imbalance of the initial fields and on what type of adjustment is utilized—free or with restoring one of the fields. So, in the framework of the nonlinear barotropic model, if the geopotential is restored after each four-step cycle for the initial one and the geostrophic wind is inputted as the initial wind then the fields can be balanced in 40 or 60 cycles.

Another approach, due to D. Laikhtman, may be employed to quantify the relationships between averaged wind and pressure fields. To illustrate, we assume that a pressure field is given by climatic pressure maps and the wind field is sought.

With reference to the pressure maps we make further assumptions with respect to pressure:

a. The minimum pressure lies on the equator, i.e. $(\partial p/\partial y)_{\varphi=0} = 0$.

b. The latitudinal component of pressure gradient is far less than its meridional component north and south of the equator, i.e. for $\varphi \neq 0$

$$\frac{1}{\rho}\frac{\partial p}{\partial x} \ll \frac{1}{\rho}\frac{\partial p}{\partial y}$$

so that in further computations we may set

$$\frac{1}{\rho}\frac{\partial p}{\partial x} = 0$$

c. The pressure field is symmetrically spaced about the equator.

In conformity with climatic data, we think the wind varies only slightly along latitudinal circle, that is

$$\frac{\partial u}{\partial x} = \frac{\partial v}{\partial x} = 0$$

Let the x coordinate be directed eastward, y coordinate northward, and the origin be at the equator. With all the above assumption in mind, for a single layer (planar) stationary problem the set of equations may be written as

$$v\frac{du}{dy} = fv + K_x\frac{d^2u}{dy^2} \tag{2.4.11}$$

$$v\frac{dv}{dy} = -\frac{1}{\rho}\frac{dp}{dy} - fu + K_y\frac{d^2v}{dy^2} \tag{2.4.12}$$

where K_x and K_y are the horizontal eddy exchange coefficients.

Let us expand the wind and pressure gradient components and the Coriolis parameter of the above equations in power series of y:

$$u = u_0 + u_2y^2 + u_4y^4 + \ldots \tag{2.4.13}$$

$$v = v_1y + v_3y^3 + v_5y^5 + \ldots \tag{2.4.14}$$

$$-\frac{1}{\rho}\frac{dp}{dy} = p_1y + p_3y^3 + \ldots \tag{2.4.15}$$

$$f = \beta y + \beta_1y^3 + \ldots \tag{2.4.16}$$

In the series (2.4.15) and (2.4.16) the coefficients of y are known values (pressure, say, is inferred from the climatic maps) and in the rest two series they are unknown. The value of K_y is known to be 5×10^6 m^2 s^{-1} in low latitudes. From (2.4.13) and (2.4.14) we have

$$du/dy = 2u_2y + 4u_4y^3 + \ldots, \tag{2.4.17}$$

$$d^2u/dy^2 = 2u_2 + 12u_4y^3 + \ldots$$

$$dv/dy = v_1 + 3v_3y^2 + 5v_5y^4 + \ldots \tag{2.4.18}$$

$$d^2v/dy^2 = 6v_3y + 20v_5y^3 + \ldots$$

Having substituted (2.4.13)-(2.4.18) into (2.4.11) and (2.4.12) and equated the coefficients of equal powers (y^0, y^1, y^2) in y, subject to the boundary conditions which suggest that at $y = y_1$ the flow is quasi-geostrophic, we get a set of equations to define the unknown coefficients. A solution of this system, say, for y_1 corresponding to $\varphi = 5°$,

to u and v gives the following expressions

$$u = -2.64 + 1.45 \times 10^{-24} y^4 + \ldots \quad (2.4.19)$$

$$v = -3.81 \times 10^{-6} y + 1.22 \times 10^{-7} y^3 + \ldots \quad (2.4.20)$$

where y is in metres.

These formulas were used to derive the wind components in the nearequatorial zone from the mean pressure field. The computed values correspond by and large to zonal winds observed in the region (2-3 m s^{-1}).

2.5 Cloudiness

The prevailing form of cloud in the tropics is cumulus. All the types of the cumulus cloud are here much more frequent than in the middle latitudes. The most frequent type of cloud is cumulus humilis. It often has a rough tattered appearance caused by turbulence; then it is frequently called fractocumulus or stratocumulus. The diurnal march of cumulus clouds has a daytime maximum and nighttime minimum. It should be noted, however, that where the effect of the semidiurnal pressure wave is undistorted by other factors involved in cloud formation the cloudiness march may have two maxima and two minima. On the ascending branch of pressure wave cloudiness increases, on the descending branch it decreases. Daytime heating and the semidiurnal pressure oscillations influence cloud formation processes so that the diurnal march of cloudiness appears to be rather complicated. There are three maxima—in the morning, at noon, and before sunset, and three minima—a major one (at night) and two secondary, before and after noon (see Sec. 2.2).

In the trade-wind region over the oceans the prevailing cloud types in all seasons are cumulus humilis and cumulus mediocris. They are usually sided by stratocumuli and altocumuli. All the cumulus clouds in the trades differ in a markedly uniform appearance with clear-cut bases and tops due to the homogeneous conditions in which they have been formed. These coulds are often called trade cumulus clouds.

When a cumulus builds to considerable height a cumulus congestus cloud forms whose top reaches the bottom of the

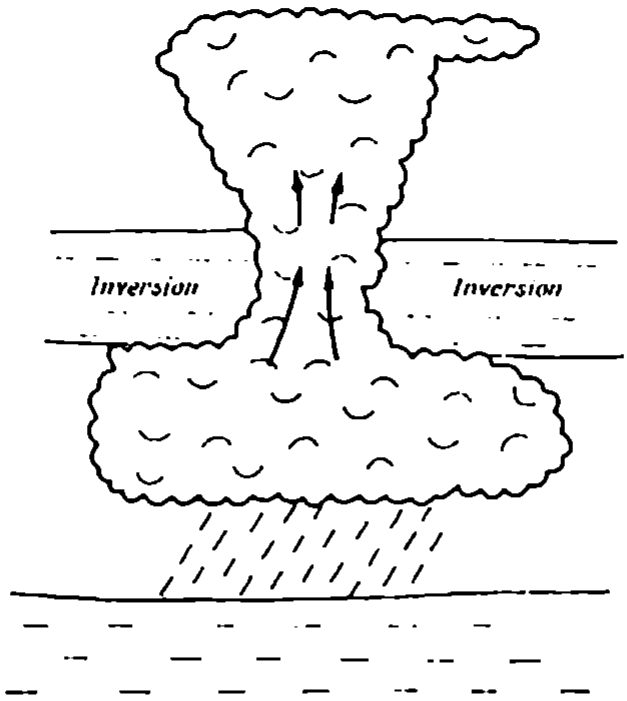

Fig. 2.13 Chimney cloud build up (after Riehl)

inversion layer. If this layer is shallow and the process of cloud convection is rather strong then the clouds form long "necks" protruding from the tops of the lower cloud mass above the inversion or stable layer. The clouds have much greater vertical than horizontal extent (Fig. 2.13) and became known, due to Riehl, as the chimney clouds.

A vast variety of cloud types, including altostratus-nimbostratus systems, is observed in the intertropical convergence zone. However, prevailing again are cumulus clouds—cumulus humilis, cumulus mediocris, cumulus congestus, and cumulonimbus.

Observations during the tropical experiments of 1972 and 1974 have demonstrated that clouds of vertical development have never come isolated. As a rule, they join into clusters (banks) of cumulus congesti or cumulonimbi with a common base. The tops of the merged clouds are very close to each other, so often they can be found also joint together. The clusters are from several tens of kilometers to 300 km long and in some cases they are even longer. The width of the

banks is 10 to 15 km. They are normally oriented along the wind, being distanced 100 to 150 km apart.

As in the middle latitudes, cumulonimbus clouds with crystal tops form when convectively uplifted air builds up above the freezing level. The height of individual cumulonimbi varies to rather high levels of 18 or 19 km.

An interesting phenomenon is the lateral spreading of cumulonimbi tops, anvils, which must occur due to sharp braking of the uplifting air near the tropopause. Cirrus clouds that form in this spreading have markedly larger dimensions (area) than the parent banks of cumulonimbi. So, a sheet of cirrus clouds thus formed may be 400 to 500 km long and about 200 km wide. This phenomenon is of importance in interpreting satellite imagery where clusters of cumulonimbi may be covered by cirrus fields of larger area than underlying cumulonimbi.

Tropical experiments have revealed another interesting feature of cloud formation process in the eastern part of the central Atlantic. Here clouds develop in two convection layers, as it were, in the bottom layer from 0.5 to 3.5 km and in the top layer spreading from an altitude of 3.5 km upwards. The bottom layer gives birth to cumulus humilis, cumulus mediocris, and cumulus congestus clouds. Warm cumulonimbi, similar to cumulus congesti in appearance, are also met in this layer. Showers will fall from these clouds. The second layer is the area where various types of altocumulus (most frequently altocumulus castellatus, or towers) form along with clouds of vertical development which vary in size up to cumulonimbi, and whose tops mostly flow at 11 or 12 km height. The chimney clouds are essentially classic cumulonimbi with well developed anvils. They will precipitate with heavy showers. Clouds from the bottom and top layer may merge, often forming large cumulonimbi. Their base is at 500-700 m, and top reaches 11-12 km height.

Figure 2.14 gives a schematic illustration on how such a cloud forms. A cloud bank is shown extending from the north to the south for more than 150 km. From the north the cluster looks as a single cloud 25-30 km in width, but from the east and west it is a complex cloud structure having several anvils whose tops lie at 9 km altitude. Well seen in the northern part is the main "tower" whose base is at

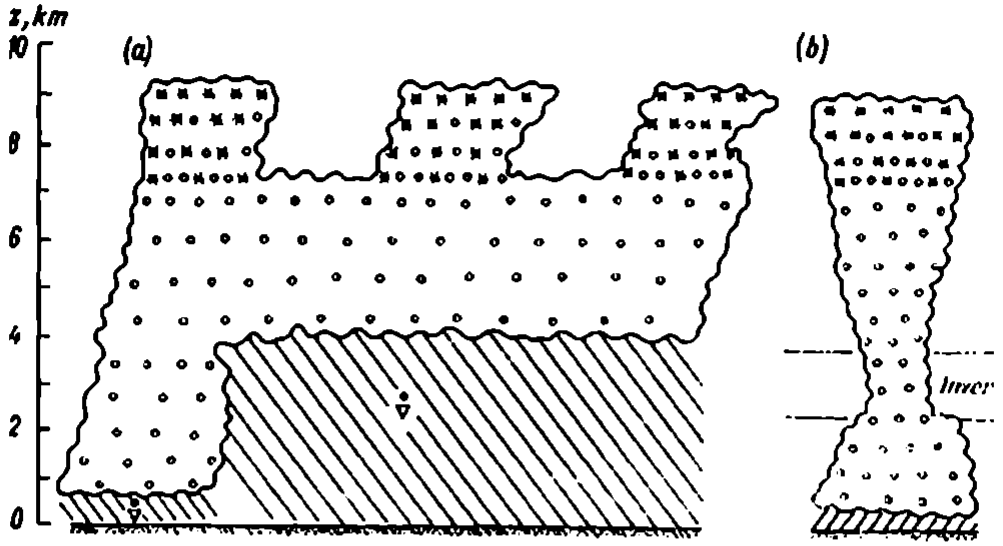

Fig. 2.14 Schematic cloud cluster as observed (*a*) eastward and (*b*) northward from an aircraft on Aug. 16, 1972, at 10°N and 24.5°W (after A. M. Borovikov and A. N. Nevzorov)

500-700 m. At 4 km height the tower merges with the bottom of the top-layer clouds. Wind slightly shifts the anvils southward. Heavy shower downpours from the cloud.

Though cumulus of vertical development prevail in the tropics numerous other types of clouds may be observed here. Undulatus clouds are fairly abundant, cirrus clouds are often met, and in the ITCZ the observer may trace stratified clouds (nimbostrati, altostrati, and cirrostrati). In general, cloudiness pronouncedly differs in the interior, at the boundary, and beyond the ITCZ (see Table 2.2).

Difference in frequency of cloudiness is also of significance. GATE'72 has reported that the ITCZ has never experienced the absolutely clear skies. A continuous cloud cover persists 40% of time, a cloudiness of 1 or 2 balls holds for 5% of time, and 30% to 80% of skies are covered with clouds for 15% of time. For the rest time cloudiness is close to continuous.

According to the same observations, at the edge of the ITCZ there are no days with cloudless skies, too, but continuous cloudiness here is only for 18% of time, 1 to 2 balls cloud cover holds for 30% of time, and that of 3 to 8 balls for another 30% of time. All the rest time cloudiness is almost continuous.

Table 2.2 Frequency of cloud types (in per cent from observational days) in the tropical Atlantic, July-August 1972 (after Samoilenko and Solntseva)

Cloud type	ITCZ		
	inside	margin	outside
Cu hum., Cu fr.	67.8	87.3	97.1
Cu med.	34.0	48.6	51.1
Cu cong.	22.2	28.2	19.0
Cu calv.	40.5	32.8	7.3
Cu cap.	1.7	2.3	—
Sc cug.	48.8	20.2	8.0
Sc tr.	2.7	3.8	—
Sc op.	4.2	4.8	3.6
St fr.	16.4	3.8	—
Ac cug.	30.4	30.5	10.2
Ac tr.	22.6	24.3	30.7
Ac und.	3.7	8.8	17.5
Ac lent.	3.0	3.2	—
Ac floc.	1.4	0.3	—
Ac dupl.	2.4	3.8	0.7
Ac op.	9.0	5.1	1.5
As tr.	2.4	2.6	—
As op.	4.4	3.8	—
Ns, As prec.	23.5	9.3	—
Ci spic.	15.4	10.7	7.3
Ci fil., Ci int.	6.1	19.4	16.8
Ci unc., Ci rad., Ci floc.	4.8	7.1	13.1

In other parts of the tropics continuous cloud canopy is rare. About half of the time the cloudiness is below 5 balls, and the inferior clouds also cover not more than 50% of the skies. Not infrequently the skies have no clouds at all.

As will be recalled, the nonperiodical weather changes in the tropics are largely governed by the convergence of wind. Wind plays significant role in the formation of clouds, too. GATE'72 has reported that well developed convergence of surface wind has preceded any congestion of cumulonimbi and onset of long rainy periods. The strong convergence has

retained even after the onset of rains. Decrease in convergence was followed by relaxation in the amount of precipitation and even by cessation of rain on coming to divergence. With these data at hand, V.S. Samoilenko and N.I. Solntseva have compiled Table 2.3. Convergence has

Table 2.3 Convergence and weather

Convergence (-10^{-5} s^{-1})	Clouds		Precipitation, mm
	type	horizontal extension, km	
<0 (div)	Decay and evaporation	<1	Relief. Downpouring lanes, or <0.1
0—0.5	Cu hum., Cu med., Cu cong.		
0.5—1.0	Separate cells Cb (Cu hum., Cu med., Cu cong., Sc. cug.)	1—10	0.1—1
1.0—3.0	Widespread Cb with squalls (Cu med., Cu cong., Sc cug., Ac cug.)	10—50	1—10
3.5—5.0	Close banks of Cb—Ns (Cu fr., St fr., Sc cug.)	50—200	10—50
Tropical low	Frontal system of Cb-Ns (Ci spic., Cs, etc.)	>200	$\geqslant 50$

been computed for an area of 70 000 km² that corresponds to a square of graticule with a side of 2.5° in equatorial latitudes. The authors of the table believe that the typical values of convergence of the wind field in the noarequatorial latitudes may be anywhere within 0 to 10^{-5} s^{-1}, which well agree with the value of convergence averaged for several years.

2.6 Rainfall

High temperature and humidity of the tropical atmosphere provide for a significant water content in tropical clouds. The clouds are so rich in water that even a small one may produce a heavy shower. Short duration, but heavy showers from single cumulonimbus clouds are

a rather frequent phenomenon in the tropics. Shower-type precipitation may also fall from cloud banks and cloud congestions that may consist of different size clouds (cumulus mediocris, cumulonimbi, etc.). Precipitation in the tropics is mainly of shower type. Most lengthy precipitations are those from cloud systems related to the ITCZ and tropical cyclones.

Precipitation in the ITCZ may be of shower type or continuous lengthy (several hours) or short (2-3 minutes), very heavy or negligible. Widespread precipitation of ITCZ falls from nimbostratus or, more seldom, altostratus clouds which are characteristic of tropical troughs. Cumulonimbi clustered into extended banks produce shower rains.

The observations performed during the GATE'72 experiment indicated that slight and moderate rains are the more frequent occasion than heavy ones. Nevertheless, seldom but heavy rains along with the moderate make up for three quarters of the total rainfall (see Table 2.4).

Table 2.4 Frequency (in per cent from the total) of rain types, from GATE'72 observations (after Samoilenko and Solntseva)

Rain	Frequency	
	count	per cent
Shower		
light and very light	23	29.1
moderate	20	25.3
heavy	6	7.6
very heavy	9	11.4
Widespread		
light and very light	13	16.4
temperate	6	7.6
heavy	1	1.3
very heavy	1	1.3
Total	79	100

The table demonstrates that 73.4% of all rains are of shower type, and the slight and moderate rains of both shower and steady type far outnumber the heavy rains.

In the tropics, rains most frequently fall from warm clouds consisting of non-supercooled droplets whereas extratropical rains downpour predominantly from mixed clouds. The closer to the equator the more frequent are rains from warm (droplet) clouds, although rains from mixed clouds predominate.

Formation of warm cumulonimbi is a phenomenon inherent in the tropical region. B. Mason collected the results by various researchers who had studied clouds and rainfall in the tropics to deduce that in the eastern Africa, for example, showers not infrequently are from cumulonimbi whose tops are at least 0.5 to 1 km lower than the 0°C-isotherm. He quotes also significant rainfall at the Bahama Islands from the clouds of poor vertical development with the tops not above 2000 m while the zero isotherm being at 5000 m.

The pilots flying on the route Trinidad-Barbados-Granada evidence that on 75% of all days with rain the clouds cannot reach the zero isotherm altitude while Barbados experiences about 180 and Trinidad about 240 such days annually.

Weather reconnaissance airplanes based at Puerto-Rico have studied 687 cumuliform clouds in the region. None of the clouds reached the zero isotherm level between 4500 and 5000 m. A cloud did not precipitate if its top was at or below 2300 m; however, if the top build to about 3000 m then 20% of such clouds precipitated, and with the top at about 4000 m rain was produced almost from 50%.

At the Hawaiian Islands in the trades season rain falls from the clouds whose vertical extent is at least 1700 m. The lowest temperature whenever measured at the tops of such clouds was 7 °C. The rainfall intensity may be as high as 10 mm per hour. It should be noted that the shower from warm clouds is everywhere rather intense though, as a rule, of short duration.

Consider the mechanism by which rain is formed in warm clouds. In short, it may be visualized as follows. Updrafts cool the uplifting air and make the water vapour to condense. The cloud starts rising in shape and the droplets increase in dimensions until they become rain drops. Then owing to condensation in the supersaturated bulk of the cloud and coalescence of large drops they become heavy enough to fall as precipitation.

The conditions for uplifts to develop are created in the tropics practically every day. First of all, it is the thermal convection which is supported by the convergence of winds in the boundary layer. However, when winds diverge in the lower layers the convective streams become suppressed and the convection cell cannot develop in full. Orography may also add in forming the uplifts.

As uplifting air is cooled adiabatically and its temperature nears the dew point, the amount of water vapour it can hold increases, so that rising air becomes saturated. For condensation to occur air either must be at high supersaturation—several times that of pure water vapour—or must contain impurities, called condensation nuclei. The above supersaturation is highly unnatural. Hence, only the second way is feasible—to condense on condensation nuclei, which are always abundant in the atmosphere.

Nuclei may be hygroscopic, i.e. with an affinity for water, such as sea salt, which holds water even at low relative humidities to become finally small water droplets; or they may be solid insoluble particles on which water condenses at high relative humidities. The size of these nuclei ranges from about 10^{-8} to 10^{-4} cm. With these particles present, the atmosphere attains less than 1 supersaturation during condensation.

The number of particles over various regions is also different. Over cities the number averages about 150 000 cm^{-3}, over open country it drops about three times to amount to 50 000 cm^{-3}, while over oceans and mountain tops it decreases further two order of magnitude to be 1000 cm^{-3}.

Not all particles, certainly, become condensation nuclei. As will be recalled, a droplet begins with a cloud condensation nucleus (CCN) that is a particle which has a potential to obtain a cloud droplet. For the majority of clouds the CCN count varies from 30 to 1000 cm^{-3}. Comparing the figures of aerosole particles with that of CCN it is readily seen that only a small part of the former become activated, that is take part in droplets formation.

The most important stage in formation of precipitation is the process of growth in which cloud droplets grow to raindrop size. Water vapour condensing on activated nuclei make the droplets grow fast to 20-30 μm, but further rate

of growth is slowing down. Even if the supersaturation were extraordinarily high, the time required for cloud droplets to grow to small raindrops by condensation is about a day, whereas rain is known to fall in the tropics less than an hour after cloud formation. Hence, another physical process must be responsible for precipitation growth.

The most important growth process of cloud drops is the collision and coalescence of different drop sizes due to differences in fall velocity. Large droplets collide and coalesce with small ones. The coalescence depends on the difference in fall velocities (large drops fall faster), on the electric charge of droplets (charge ratio q_1/q_2 defines the coalescence efficiency for drops with radii r_1 and r_2), and on the moisture content of the cloud. (Moisture content in the tropics is known to be fairly high, so all other conditions being equal, the coalescent growth proceeds here more intensely than in moderate latitudes.) Prevailing importance among the above factors for the coalescence has the difference in fall velocity bringing the gravitational coalescence into the forefront.

As will be recalled, the radius of a drop grows by coalescense as

$$dr/dt = e\delta\,\Delta v/4\rho_w$$

where ρ_w is the density of the water, δ the moisture content of the cloud, Δv the difference in fall velocities, $e = f(r_1, r_2, q_1, q_2)$ the capture coefficient being the product of the coalescence efficiency, depending on q_1/q_2, and the collection efficiency, depending on r_1/r_2.

The initial size of droplets plays a significant role on the way toward precipitation. A small droplet requires long time to grow. If, for example, we assume that no evaporation takes place and a cloud contains 1 g/m^3 of liquid water and a relatively high collection efficiency of 75 per cent, a 20-μm drop requires about 20 minutes to grow to 40 μm by coalescence.

The 40-μm droplet is not a raindrop yet, it takes still more time for the droplet to acquire precipitation size. In other words, a precipitation would take markedly larger time to form than is normally observed. It would be only natural to suggest that droplets of 40-50 μm in diameter exist near the cloud base. This postulation is not void of

sense at all. Still in 1952 Woodcock reported that he had found giant salt nuclei up to 20 μm in diameter in the tropical region over the oceans. Having carried into the cloud, they can easily grow by direct condensation to diameters of 40-50 μm. Being uplifted at a speed of 2 m s^{-1} these drops can grow to 100 μm at an altitude of 2 to 2.5 km above the cloud base and then enlarge at high rate by accretion. In about 600 m of updraft the drop grows to a critical size with $r_{cr} = 3200$ μm upon which it breaks into a number of smaller ones which again grow to break in turn upon acquiring the critical size. If the initial number of drops was n_0, it rises upon first cycle to n_1 (with $n_1 \gg n_0$) to n_2 (with $n_2 \gg n_1$) upon second cycle, and so on. This process is termed the Langmuir chain reaction, due to Langmuir who proposed in 1947 the theory of rain producing from warm clouds. According to the theory, when a cloud accumulates a large number of grown droplets with a radius larger than 40 μm, the updraft can no longer support the water in the cloud and it starts an intense downpour bringing about a complete disappearance of the cloud.

A critical condition for the chain process of drops growing and breaking to realize consists in that the droplets should accumulate in the cloud above the level of highest updraft velocities, w. In the circumstances, many drops even of large size ($r \approx 1000$ μm) will fall slower than uplift, that is $|v| < |w_{max}|$. A shower will only be produced if an area where droplets accumulate forms above this level. Falling through this layer, droplets grow by accretion and condensation to enlarge at the cloud base to $r < r_{cr}$. Therefore, for the chain process to be effective and produce rain showers from clouds consisting solely of liquid water, still another condition must be fulfilled, namely, the cloud layer extending from the cloud base to the level where $w = w_{max}$ must be 2.0 to 3.5 km thick, assuming a uniform water content of the cloud of 1.0 to 1.2 g m^{-3}.

In the mixed clouds, rain develops on the same mechanism as in middle latitudes. Tropical rainfall figures are in general higher than in middle or higher latitudes. The precipitation south of 30°N makes up for 2/3 of the hemisphere's rainfall; in the Southern Hemisphere the corresponding latitudes have slightly lesser rainfall though outweighing

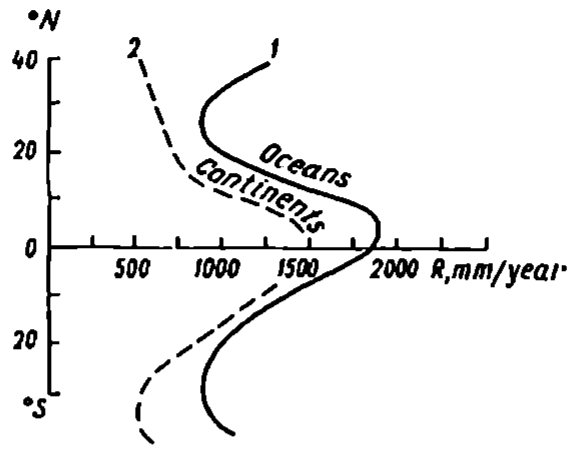

Fig. 2.15 Zonal distribution of annual rainfall over (*1*) oceans and (*2*) continents (after Palmer)

that in the other part of the hemisphere. Somewhat higher rainfall in the northern tropics (see Fig. 2.15) may be explained by the placement of the equatorial trough which north of the equator most of the year.

Tropical regions are outstanding in that the annual rainfall varies widely in time and space. At some locations, as, say, at the Fanning Island, the annual rainfall may vary from 3 mm in one year to 500 mm in the next. The area where rainfall is a maximum lies at the equatorial trough, while minimal rainfall is along the subtropical high-pressure belts. This course of rainfall is valid both over the continents and over the oceans (see Fig. 2.15). The tropics may be conventionally divided into three zones having their characteristic precipitation regimes.

(1) The region of the equatorial trough where precipitation occurs throughout the year.

(2) The trade wind region where rains occur in summer and are seldom in winter.

(3) Regions adjacent to the subtropical highs, where precipitation is sparse throughout the year.

In each region, the amount of precipitation may drastically vary from year to year. The mean distribution of the annual rainfall is presented in Fig. 2.16. It is seen that the area of maximum rainfall embraces the globe near the equator. Sufficient rainfall takes place in the western quarters of

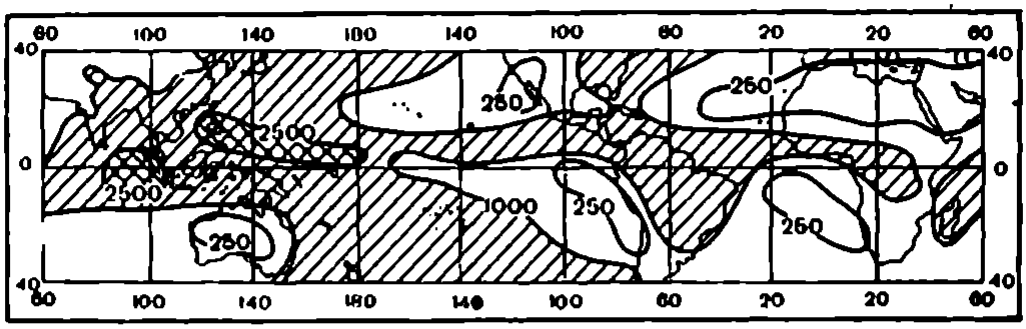

Fig. 2.16 Annual rainfall in the tropics; hatched areas get more than 1000 mm of rain a year

the oceans. The arid area extends from Iran and Afghanistan through the Arabian desert and Sahara into the eastern Atlantic. The arid zone of the Northern Hemisphere also embraces Mexico and the South-West of the United States. In the Southern Hemisphere, the most arid areas are to be found over Australia, South Africa and America with the adjoining eastern parts of the oceans.

Of particular interest is the seasonal march of rainfall in the tropics. The latitudinal profiles of rainfall averaged over seasons and longitudes (Fig. 2.17*a*) indicate that the warm season in this hemisphere collects more rain than the

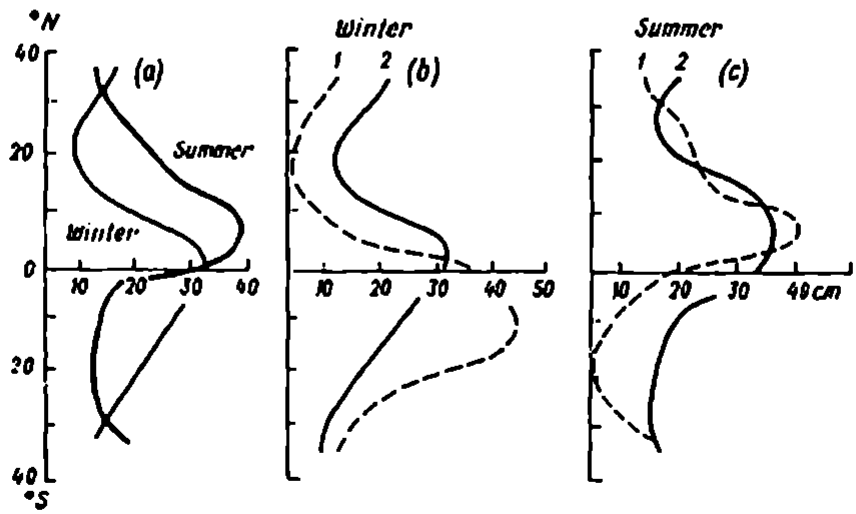

Fig. 2.17 Latitudinal profiles of seasonal rainfall over (*1*) land and (*2*) ocean (after Palmer)

colder season. Viewing the oceanic and continental seasonal profiles separately, Fig. 2.17*b* and *c*, the migration of precipitation area, related to the displacement of the equatorial trough, is markedly pronounced over the continents. The maximum rainfall over oceans remains in the Northern Hemisphere in all seasons, being more abundant to the north in June-August than in December-February.

The regions of the trades adjacent with the equatorial trough experience one maximum in the annual rainfall. North of the equator it is in August, and south of the equator in March accordingly as the trough displaces more northward or southward. Near the equator where the trough crosses any latitudinal circle twice a year, the annual course of rainfall has two maxima. At any longitude where the trough oscillates more or less symmetrically about the equator, heavy rains near the equator occur from March to May and from October to November. It should be noted that the displacement of the trough is not equal at different longitudes and varies from year to year. Besides, various disturbances of the main current in the tropical atmosphere and the interaction of the tropical circulation cell with the processes of higher latitudes have an appreciable effect on the weather regime in general and on the rainfall regime in particular. This all brings about a perceptible change in the seasonal rainfall, as observed in various years in various regions, the change being more smooth where rainfall is abundant and pronounced where it is scarce.

Review Questions

1. What is the thermal equator? Where is it located? Does the location undergo seasonal variations?
2. What types of annual temperature variation exist in the tropics and what differs them from each other?
3. What does the diurnal temperature variation depend on in the tropics?
4. How does the horizontal temperature gradient vary with latitude in the tropical region?
5. How does temperature vary with altitude in various areas of the tropical region?

6. How is pressure distributed in the tropics? What are its horizontal pressure gradients?
7. What are pressure waves? Enumerate the pressure oscillations you know.
8. What is the time to observe pressure minima and maxima in the semidiurnal pressure wave? What is the mean amplitude of the wave?
9. What relation exists between the semidiurnal pressure wave and weather?
10. What winds blow in the trades of the Northern and Southern Hemisphere? Characterize their steadiness.
11. What is the equatorial region of westerlies? Where is it placed?
12. How does the zonal wind differ from the geostrophic at various latitudes of the tropical zone?
13. Characterize the wind regime in the well-developed and diffused intertropical convergence zone.
14. How are the vertical motions distributed in the well-developed and diffused ITCZ?
15. Put down the formulas that relate pressure and wind in the tropics. In what way do they differ from the corresponding expressions for the middle and higher latitudes? Why are these formulas so hard to apply?
16. What is the kinematic equator? Where is it placed?
17. What are the procedures involved in adjustment of wind and geopotential fields?
18. Which types of cloud dominate over the tropics?
19. What are cloud clusters? What are their dimensions?
20. Discuss cloudiness in the ITCZ.
21. What is the two-layer mechanism of cloud development?
22. How does the convergence of wind influence the formation of clouds and precipitation in the tropics?
23. Which types of cloud precipitate in the tropics?
24. What type of precipitation prevails in the tropics?
25. What mechanism is involved in the formation of rain in warm clouds?

Chapter 3 | CONVECTION

3.1 Types of Convection and the Initiating Conditions

The tropical atmosphere overlies the warm underlying surface which favours heating of its lower layers and producing high temperature lapse rates. Most part of the tropics is known to consist of oceans, therefore the conditions to render sea-surface air wet can be present over vast area. The average temperature lapse rate for the lower half of the tropical troposphere is 0.55 °C/100 m; in the 500-m boundary layer it is close to the dry adiabatic. Owing to high temperature the mean moist-adiabatic temperature lapse rate in the tropics amounts to 0.45 °C/100 m. On the whole, therefore, the tropical atmosphere is conditionally unstable.

Unstable balance of atmosphere plays the leading part in initiating convection. In the tropics, convection is produced by a mechanism which is almost identical to that in the middle latitudes. Tropical wind convergence, however, is a bit more important than its mid-latitude counterpart as sometimes it triggers, and drives a convection. A basic condition, obviously, is high humidity of the air. Orography also makes its contribution. All the four factors—unstable balance, wind convergence, high humidity, and orography—influence convection in one way or another, the major one remaining unstable stratification of the atmosphere. Indeed, no factor can initiate convection in a stably stratified atmosphere.

When present in combination with one or another of the mentioned factors, or with all of them, instability of various intensity gives rise to different types of convection. One of them is *cumulus convection* which results in shallow cumulus clouds frequently observed in the trades. A different type is *deep*, or *penetrating*, *convection* which promotes

formation of deep cumulonimbus clouds. This convection has drawn its name from the fact that it penetrates deeply above the top of conditionally unstable atmosphere. A third type in this classification is *suppressed convection* which is a progenitor of a small number of cumulus humilis. Most typical for this convection is an atmospheric situation with orderly ascending motions in the boundary 1.5 to 2 km layer and descending motions above. Similar situations occur at times in the ITCZ (see Chap. 2), though they may be observed in other synoptic systems as well (see Chap. 5).

Let us discuss the motion of an air parcel embedded in an atmospheric environment obeying the hydrostatic equation

$$-\frac{1}{\rho}\frac{\partial p}{\partial z} - g = 0 \tag{3.1.1}$$

where ρ is the density of air, $\partial p/\partial z$ the vertical pressure gradient, g the acceleration of free fall.

Suppose that the hydrostatic balance inside the parcel is offset so that it obtains a vertical acceleration dw/dt. Then the vertical equation of motion can be written as

$$\frac{dw}{dt} = -\frac{1}{\rho'}\frac{\partial p'}{\partial z} - g \tag{3.1.2}$$

where ρ' is the density and $\partial p'/\partial z$ the pressure gradient along the vertical across the particle.

If we now assume, as is a custom in the parcel method, that the rising particles immediately adjust to the pressure of their surroundings so that $\partial p/\partial z = \partial p'/\partial z$, then we can eliminate the pressure gradient between (3.1.1) and (3.1.2) to obtain

$$\frac{dw}{dt} = \frac{\rho - \rho'}{\rho} g$$

Substituting ρ and ρ' from the equation of state for air and assuming it being quasi-static ($p = p'$) yields

$$\frac{dw}{dt} = \frac{T' - T}{T} g \tag{3.1.3}$$

where T is the temperature. This is the well known buoyancy formula. Parcels which are warmer than their surroundings will accelerate upward. Parcels which are cooler will ac-

celerate downward and return to and beyond their starting place.

If a parcel rises following the dry adiabat, its temperature will be

$$T' = T'_0 - \Gamma_d \Delta z$$

where Δz is the height increment, Γ_d the dry adiabatic lapse rate, and T'_0 the temperature of the parcel at the initial level. Suppose that the geometric (environmental) lapse rate of the surroundings near the T_0 level is $\Gamma \neq \Gamma_d$, then for the surroundings

$$T = T_0 - \Gamma \Delta z$$

Substituting T and T' into (3.1.3) we get

$$\frac{dw}{dt} = g \frac{T'_0 - T + (\Gamma - \Gamma_d)\Delta z}{T} \qquad (3.1.4)$$

Over land where tropical air is rather hot, at least in surface layers, it acquires an unstable stratification ($\Gamma > \Gamma_d$). Overheated air parcels ($T'_0 > T_0$) experience, in accordance with (3.1.4), a positive buoyancy and accelerate upward in what is at times called "termals".

Over oceans, at the initial level we often have $T_0 = T'_0$ which yields

$$\frac{dw}{dt} = g \frac{\Gamma - \Gamma_d}{T} \Delta z$$

When a parcel moves in the vertical through an environment with $\Gamma < \Gamma_d$ a restoring force appears which for a parcel of unit mass advanced a unit displacement is

$$F = -g \frac{\Gamma_d - \Gamma}{T}$$

The minus sign implies that the force is downward if the parcel ascends and vice versa.

In vertical movement of a saturated parcel its temperature varies moist-adiabatically. Making the same type of argument,

$$F_s = -g \frac{\Gamma_s - \Gamma}{T}$$

If $\Gamma_s < \Gamma$ which is true at least for the lower half of the tropical troposphere, then $F_s > 0$. It means that parcels

become buoyant if the atmosphere is conditionally unstable.

As will be recalled, any convection in the atmosphere implies the existence of ascending and, compensating them, descending motions. Denote for some level z the area of ascending motion as A_+ and that of descending as A_-; also denote the typical displacement in updraft l_+ and in downdraft l_-. Owing to continuity of mass

$$l_+A_+ = l_-A_-$$

so that the ascending air mass be compensated for the descending.

The work done by descending displacements is

$$W_- = Fl_-^2A_-$$

by the ascending

$$W_+ = F_s l_+^2 A_+$$

and their ratio

$$\frac{W_+}{W_-} = \frac{F_s l_+^2 A_+}{F l_-^2 A_-} = \frac{F_s A_-}{F A_+} \tag{3.1.5}$$

. If energy is released in the process so that $W_+/W_- > 1$, then

$$\frac{A_+}{A_-} < \frac{F_s}{F} = \frac{\Gamma - \Gamma_s}{\Gamma_d - \Gamma} \approx \frac{1}{5} \tag{3.1.6}$$

Hence, the area of uplifting air mass must be at most 1/5 as large as the area of descent.

From (3.1.5) it is readily seen that the more narrow is the cross-section area of an upstream, that is the smaller the scale of the disturbance, the larger is the amount of energy that can be released in the updraft and the stronger the disturbance can be excited by the conditional instability. In other words, the conditional instability of the type can produce small scale disturbances (cumulus scale convection cells) and taken alone is unable to form even small depressions or cloud clusters, which involve larger scale disturbances. This is ordinary conditional instability, otherwise termed conditional instability of the first kind.

The different conditions may occur in the moist-liably stratified areas of the tropical atmosphere. When convergence due to frictional inflow exists over a considerably large area in the planetary boundary layer, it may produce

large-scale fields of updraft currents. These currents drive the convection of even larger scale producing cloud clusters and fields. First, a sort of separating layer occurs above the cloud. Mixing with the surrounding air (see Sec. 3.2) cools the air surrounding the cloud. However, owing to latent heat release, in-cloud temperatures remain higher than the environmental, accelerating the upward mass flow in the cloud into substantial velocities. The cloud air penetrates into the separating layer, evaporating droplets of the cloud lower its temperature and the layer finally decays, creating conditions for the further enhancement of the convection. This process is repeated at the following level extending into more higher layers. The rising cloud may protrude toward substantial heights not infrequently reaching the tropopause. The entire process develops into deep (penetrating) convection. It is this type of convection that is responsible for formation of cumulonimbi and cloud clusters. When the cooperative interaction between the cumulus convection and a large-scale perturbation leads to unstable growth of the large-scale system (which may be of the order of 100-200 km) the process is referred to as *conditional instability of the second kind*, or CISK.

The lower half of the tropical troposphere is conditionally unstable almost everywhere, but convection sets in not always even where the conditions of CISK are present. It implies that the conditional instability proper is not sufficient for a convection to occur. Because of energy transfer upwards convection may cease rather quickly. Being warmed by latent heat of condensation the upper layer becomes less steep in the temperature lapse rate. Therefore, a source of "overheated" saturated parcels is required to support convection. This source, as in middle latitudes, can be provided by a *convectively unstable layer* (CUL). Where this layer exists it serves a progenitor of a convection whose kind depends upon the onsetting atmospheric conditions. Ordinary convection gives rise to cumulus convection cells. If it is conditional instability of the second kind, then deep convection sets in. If under any instability downward streams are observed above 1.5-2 km, then the process can develop only to suppressed convection. The reason for that lies in that the downdrafts form strong layers of separation which prevent

convection from penetrating further upwards. In the circumstances, neither CISK nor the presence of a convectively unstable layer can provide any material development of convection.

Convectively unstable layer is normally situated at the earth's surface. It varies in depth from tens of metres to 1 or 2 km. Conveniently, it is at times divided into a lower part, adjacent to the earth's surface, and one or several upper layers. Convection may be initiated in the lower and in the upper part as well.

The adiabatic model of convection includes the following quantities.

(1) The depth of convectively unstable layer, H_{CUL}.

(2) The height of lifting condensation level, $\overline{h}_{lc}$.

(3) The height of free convection level, $\overline{h}_c$.

(4) The energy of instability which is defined in terms of the mean temperature difference between ascending particle and environment, $\overline{\Delta T}$, and the terminal velocity of convective upflow, w (in m s^{-1}).

(5) Humidity of air, which is determined in terms of the dew point deficit at the earth's surface $(T - T_d)_0 = \Delta T_{d0}$ and by the sum of dew point deficits at various levels of free atmosphere, $\Sigma_{850}^{500}(T - T_d) = \Sigma \Delta T_d$.

Analysis of convection in the tropics by the adiabatic model is essentially the same as for the middle latitudes and is to be found in a course on basic meteorology. However, the parameters of convection in the tropics somewhat differ from that in mid latitudes.

Table 3.1 summarizes the mean values of convection parameters that have been obtained by various authors from soundings over the tropical Atlantic during the GATE'72 and '74 expeditions. The corresponding parameter values are given for comparison with the convection over land areas in the middle latitudes.

From this table we may infer the following conclusions.
1. The dew point deficit in the lower layer of the tropical troposphere is smaller than at middle latitudes, and as a consequence the lifting condensation level situates lower.
2. The depth of convectively unstable layer during showers and thunderstorms is larger in middle latitudes than in the tropics.

Table 3.1 Mean values of convection parameters in the tropics

Convection processes *	H_{CUL}, mb	$\bar{h}_{lc}$, km	$\bar{h}_c$, km	$\overline{\Delta h}$, km	ΔT, K (w, m/s)	ΔT_{de}, K	ΣT_d, K
Cumulus convection, ML	10	1.2	1.9	0.7	—	12	31
Cumulus convection, TW	20	0.6	1.8	1.2	—	5	33
Deep convection, cumulonimbi, showers, thunderstorms, T	23	0.5	13.1	12.6	3.3 (10)	3	14
Showers, ML	50	1.2	4.4	3.2	1.7 (7)	7	15
Thunderstorms, showers, ML	50	1.3	7.9	6.6	2.5 (9)	7	16

* T = tropical region. TW = trade wind belt. ML = middle latitudes.

3. The height of free convection level and the strength of cumulus clouds ($\overline{\Delta h} = \overline{h}_c - \overline{h}_{lc}$) in the showers and thunderstorms of the tropics is markedly higher than in middle latitudes.
4. The energy of instability in the development of deep convection in the tropics is about 1.3 times as high as that in the development of thunderstorms and about 2 times as that during showers in middle latitudes.

Upon analysis of individual observations one may extract from the wealth of conditions governing the parameters of convection the following which are the most frequent. In mid-latitude summer, fine weather is observed over land with the atmosphere stably stratified and substantially dry both at the ground and aloft. In the tropical Atlantic, fine weather may be observed when the air is conditionally unstable toward high altitudes and substantially humid at sea surface. The convection may propagate as high as 10 to 12 km, that is, elevate higher than on the days with thunderstroms and showers in middle latitudes. It means that the conditions for the development of convection exist over the Atlantic permanently, but clouds cannot form because the air aloft is relatively dry. In all the cases with $\Sigma_{400}^{800} \Delta T_d \geq 25$ K separate cumuliformis are observed whose strength is markedly shallower than $\Delta h = h_0 - h_{lc}$. Observations indicate that the tops of the clouds on the rainless days are at the level of dew point deficits of 6-7 K. These deficits are normally observed at the top of inversion layer in the trades. Under these conditions cloud tops become diffusive.

3.2 An Entraining Jet Model of Cumulus Convection

The parameters of convection we have discussed in the previous section are based on the classical approach to convection analysis which treats convection adiabatically, that is assuming that the air undergoing a convection uplift does not exchange heat and moisture with the environment. In turn, the environment is assumed not to change upon convection onset. The environment retains its stratification and distribution of humidity with height. The ascending air changes its state adiabatically without any in-

teraction with the environment. With this assumption the ascending air will follow the path that is solely defined by the original state of the air, that is, by its temperature and humidity at the surface, rather than the environmental stratification.

Observations indicate that the adiabatic model describes the actual process very approximately since the assumption of the ascending air being isolated from the environment contradicts the reality. The ascending air parcel is interacting with the surroundings on its rise and undergoes continuous mixing. This brings about a cooling of the parcel as the air mixed in is cooler and a fraction of cloud drops evaporates from the parcel while it ascends. The process of penetration of outside air in the developing cloud has become known as *entrainment*. Entrainment substantially changes the temperature lapse rate and water content of a cloud thus changing the very character of the cloud. So, for example, even with an appropriate instability the development of a cloud in a low-humidity atmosphere terminates on the stage of cumulus humilis. On the other side, favourable conditions for the development of shower-prone cumuli can be created with a moderate instability but the relative humidity must be at least 75% up to the 500 mb level.

Models involving entrainment describe the real convection processes generally better both in the middle latitudes and in the tropics. In what follows we shall consider one of the models.

It is essentially based on the theory of free turbulent jet in a drifting current. In contrast to the well known adiabatic models, this model accounts for mixing of cloud (jet) with environmental air. The respective vertical flows, temperature field and other parameters are computed with due allowance for variable mass of the moving parcels.

The basic parameter in the theory of free turbulent flows is the mass rate of flow, m, numerically equal to the amount of air with density ρ' passing the section of flow s' in unit time

$$m = \rho' s' w \qquad (3.2.1)$$

where w is the vertical velocity; the primed quantities henceforth will designate those of the cloud (jet).

The momentum of mass rate will be, accordingly,

$$mw = \rho' s' w^2 \tag{3.2.2}$$

To write the momentum equation we should equate its change in time to the sum of all acting forces. For a developed jet, the friction force, viscous drag of cloud motion and other forces are considerably less than the buoyancy force, so that

$$\frac{\mathrm{d}(mw)}{\mathrm{d}t} = \frac{\mathrm{d}}{\mathrm{d}t}(\rho' s' w^2) = \rho' s' w g \frac{\rho' - \rho}{\rho'} \tag{3.2.3}$$

here, ρ = density of air outside the cloud (jet).

Solving (3.2.3) for $\mathrm{d}w/\mathrm{d}t$ we get

$$\frac{\mathrm{d}w}{\mathrm{d}t} = g\frac{\rho - \rho'}{\rho'} - \frac{1}{\rho' s'}\frac{\mathrm{d}}{\mathrm{d}t}(\rho' s' w) \tag{3.2.4}$$

Multiplying (3.2.4) by $1/w$ and recalling that $w = \mathrm{d}z/\mathrm{d}t$ yields

$$\frac{\mathrm{d}w}{\mathrm{d}z} = \frac{g}{w}\frac{\rho' - \rho}{\rho'} - \frac{1}{\rho' s' w}\frac{\mathrm{d}}{\mathrm{d}t}(\rho' s' w) \tag{3.2.5}$$

Experiments have revealed that entrainment, i.e. relative change of mass rate in time, is proportional to T'/RT, thus

$$\frac{1}{\rho' s' w}\frac{\mathrm{d}}{\mathrm{d}t}(\rho' s' w) = \frac{c}{R}\frac{T'}{T} w, \tag{3.2.6}$$

where R is the radius of the cloud (jet), T the air temperature, c the entrainment constant (a dimensionless quantity assumed to be equal to 0.2).

Subject to (3.2.6) the equation (3.2.5) becomes

$$\frac{\mathrm{d}w}{\mathrm{d}z} = \frac{g}{w}\left(\frac{T_0' - T_v}{T_v} - \delta' + \delta\right) - \frac{cT'}{RT} w \tag{3.2.7}$$

where T_v is the virtual temperature, δ' the amount of both liquid and solid water, δ the moisture content outside the flow.

Proceeding in a similar fashion we may obtain the equations for temperature T' and relative humidity q.

$$\frac{dT'}{dz} = \frac{L_c}{c_p}\frac{d\delta'_w}{dz} + \frac{L_c + L_l}{c_p}\frac{d\delta'_i}{dz} - \frac{g}{c_p}\frac{T'}{T} - (T' - T)\frac{cT'}{RT} \tag{3.2.8}$$

$$\frac{dq'}{dz} = -\left\{\frac{Mp}{m_v e'_s} q\left(\frac{L_c}{kT'^2}\frac{dT'}{dz} + \frac{Mg}{kN_A T}\right) + \frac{1}{e'_s}(q'e'_s - qe'_s)\frac{cT'}{RT}\right\} \tag{3.2.9}$$

Here, L_c is the specific latent heat of condensation, L_l the specific melting heat of ice, c_p the specific heat of dry air at constant pressure, k the Boltzmann constant, N_A the Avogadro number, M the molecular mass of air, m_v the molecular mass of water vapour, e_s the saturation vapour pressure, δ'_w the amount of water, and δ'_i the amount of ice.

If these equations are added by the equations for the radius of the jet R

$$\frac{2}{R}\frac{dR}{dz} = \frac{cT'}{RT} - \frac{dw}{w\,dz} + \frac{dT'}{T'\,dz} + \frac{Mg}{kN_A T} \tag{3.2.10}$$

and the total water content of the cloud

$$\frac{d\delta'}{dz} = -\frac{m_v e'_s}{Mp}\left[\frac{dq'}{dz} + q'\left(\frac{L_c}{kT'^2}\frac{dT}{dz} + \frac{Mg_i}{kN_A T}\right)\right] - \left[\frac{m_v}{Mp}(q'e'_s - qe_s) + \delta'\right]\frac{cT'}{RT} \tag{3.2.11}$$

then we arrive at the set of five simultaneous equations (3.2.7) through (3.2.11) in five unknowns: w, T', q', R, and $\delta' = \delta'_w + \delta'_i$. Yet these equations do not complete the model. Since the cloud is deformed by a lateral wind the set has to be supplemented with a relationship for the horizontal wind component of the cloud, v.

Figure 3.1 displays a routine computational pattern of cumulus cloud convection parameters with the simultaneous set of (3.2.7)-(3.2.11). It is seen that the cloud develops much higher above the level $T = T'$. The neck in mid-troposphere is a shallow inversion layer which the cloud has protruded to build up to 10 km height. As we have discussed in

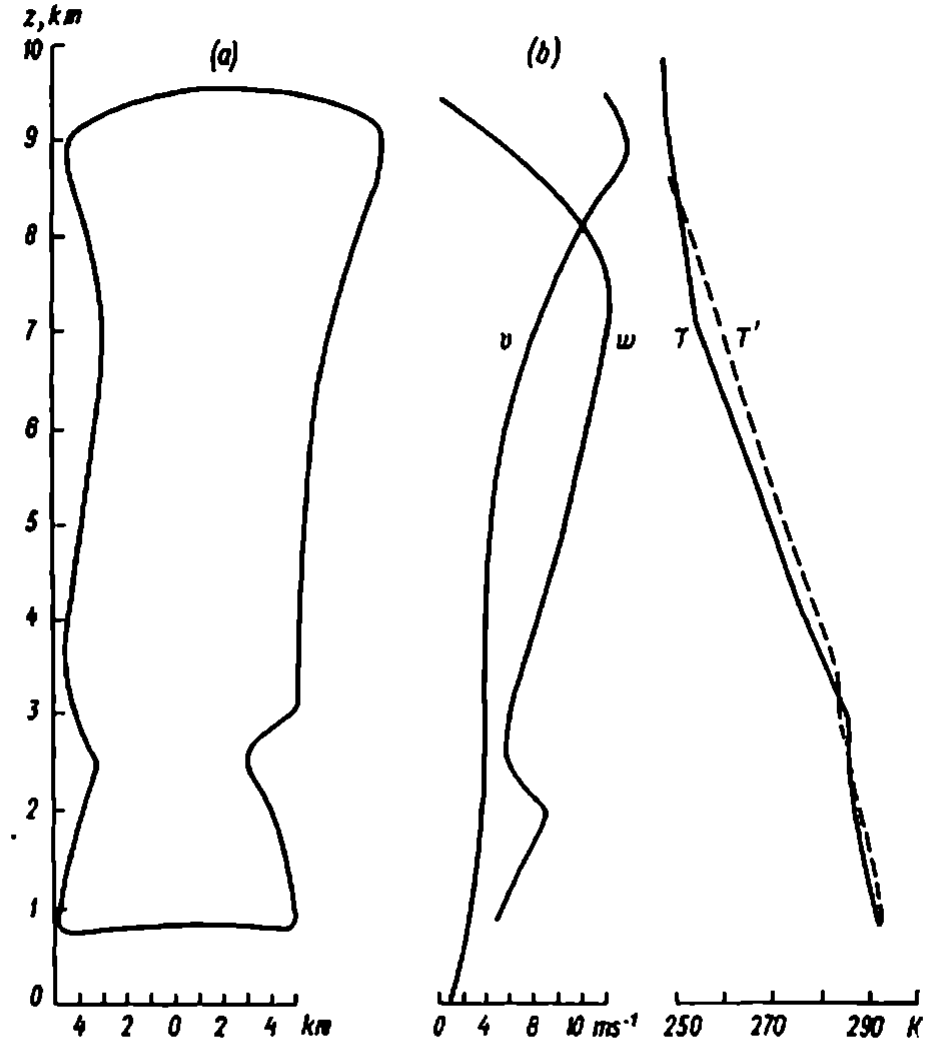

Fig. 3.1 (a) Cumulonimbus cloud simulated with a jet entrainment model for distributions of temperature, humidity, and wind typically met over the tropical ocean and an initial updraft $w_0 = 5$ m s^{-1}; (*b* Vertical profiles of:

vertical convection, w, (computed); wind velocity, v, (observed); environmental temperature, T, (observed); cloud temperature, T', (computed)

Sec. 2.5, the penetration of an inversion layer by a cloud can often be observed in the tropical atmosphere. If we perform the above computation with the same initial data set as in Fig. 3.1 but for one alteration $w_0 = 1$ m s^{-1}, the result will be that of Fig. 3.2, that is, this time the cloud is unable

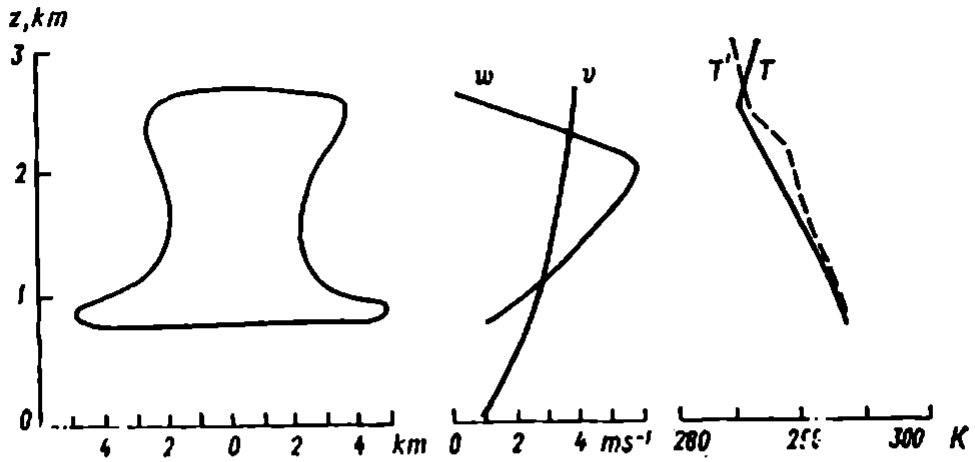

Fig. 3.2 Cloud shape simulated with a jet entrainment model on the data of Fig. 3.1 but for $w_0 = 1$ m s^{-1} (legend those of Fig. 3.1)

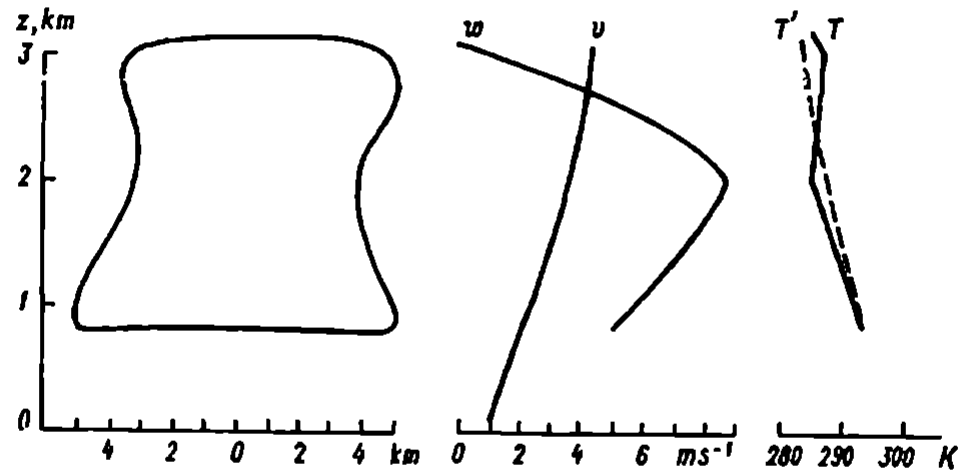

Fig 3.3 Same as Fig. 3.1 but for an inversion depth twofold increased

to overturn the inversion layer. Processing again with the data of Fig. 3.1 but with a twice stronger inversion layer, the cloud cannot ascend above the inversion layer even with $w_0 = 5$ m s^{-1}, topping at 3 km level (Fig. 3.3).

With various initial data sets reflecting the real state of the tropical atmosphere, the model is capable of simulating practically all the variety of cloud types met in the tropics. For example, strong inversion layers are most frequent over the eastern portions of the tropical oceans making here

clouds with flat tops more frequent than at the western parts of the oceans where the inversions are weaker and can easily be protruded by clouds which then develop high aloft. Strong cumulonimbi, therefore, are more often observed over the western parts of the oceans, producing heavy rains here more frequently (see also Sec. 2.6). The simulation of the cloud shapes well confirms the observed pattern.

Review Questions

1. Which factors are beneficial for convection in the tropics?
2. How can ordinary conditional instability be defined?
3. What is conditional instability of the second kind (CISK)?
4. Enumerate the convection forms in the tropics.
5. What is the role of the convectively unstable layer in development of convection?
6. Enumerate the parameters of convection involved in the adiabatic model.
7. Where lie the shortcomings of the adiabatic model?
8. What is entrainment? What effects can it cause?
9. What is the basic idea of the entraining jet model of cumulus convection?
10. Derive the velocity lapse rate equations for the entraining jet model.
11. Describe the equations that make up the simultaneous set of the model.
12. What must be the conditions for a cloud to protrude above an inversion layer?

Chapter 4 | TROPICAL SYNOPTIC ANALYSIS

Tropical meteorology has not produced any innovations in synoptic representations of data. Surface and upper level constant pressure charts are plotted and analyzed as in the middle latitudes. Since the station density over most parts of the tropics is very low the use of time sections at key stations is frequently practiced along with calculation of vorticity and wind divergence, and local signs of weather changes.

4.1 The Time Section

An analyst's success may largely depend on keeping good time sections. Such sections show the complete picture of the state of the weather at one location for some particular length of time. They provide a means for observing time of passage, structure, intensity and approximate horizontal dimensions of disturbances. In correlating the different elements of a time section the analyst can fully employ all his synoptic and theoretical knowledge. He is also enabled to detect errors and unrepresentative observations with greatest certainty and forecast weather over a radius up to 700-800 km.

The vertical coordinate of time sections can be height, pressure or geopotential. Time is plotted from left to right on the section when the station is located in the trades, where systems predominantly move from the east. It is plotted from right to left for the westerlies. If disturbances move at a fairly steady rate, the time section then becomes equivalent to a space cross section.

The following elements are suggested for plotting:
(1) all upper winds;

(2) 24-hour surface-pressure changes as often as available;
(3) 3- or 6-hour surface reports;
(4) 24-hour changes of the height of upper isobaric surfaces;
(5) pressures, temperatures, and humidities of upper air.

The analysis consists of entering
(1) trough lines and shear lines (orange);
(2) height of the 5 g/kg moisture surface in the rainy season (green);
(3) base and top of trade inversion (purple);
(4) tropopauses (purple);
(5) isolines of 24-hour height changes of upper isobaric surfaces (black).

4.2 The Surface Chart

Surface maps in the tropics are plotted on data of standard observations at weather stations. The data are entered with internationally standardized rules, symbols, and graphics. In chart analysis, besides isobars, the ITCZ is found and plotted and, if needed, also the stream lines and 24-hour isallobars.

Analysis of conventional surface charts has remained the standard practice of forecast services. Isobars are drawn at 3-mb intervals; 2-mb and even 1-mb intervals are more appropriate equatorward of latitudes 20°.

Isobaric field in tropical zones is less informative as compared with that of higher latitudes. Superposition of the semidiurnal pressure wave on the synoptic pressure pattern produces appreciable deformations. So the troughs that overlap the semidiurnal oscillation minimum have their center lines and the adjoining ridges to appear deeper, while the troughs that coincide with the maximum of the wave look shallower and the ridges stronger than natural. In addition, the overlaying wave induces in the initially undisturbed field the ridges and troughs that displace rapidly with the wave, that is at the speed many times that of common synoptic objects in circulation cells. The wave maxima and minima alternate at a meridian every six hours so that the sign of the deformations changes with each 6-hour map.

The ITCZ is traced employing similar procedures as for fronts on the temperate zone maps. The first approximation

is that the ITCZ essentially coincides with the equatorial trough line, then a consideration is given to the distributions of wind, cloudiness and precipitation, characteristic of the convergence zone (see also Secs. 2.2, 2.3, and 5.2). Satellite imagery of cloudiness may prove of great value. Obviously, the tracing of the ITCZ on weather maps calls for a certain analytical maturity.

4.3 The Upper-air Chart

The tropical troposphere is usually divided into a lower and an upper portion with different flow configurations. Waves of small amplitude moving in a broad basic current often characterize one layer, while vortices of large dimension predominate in the other. A more representative layer for low-latitude analysis is 850 mb; for high-latitude analysis, 200 mb. Choice of the levels, certainly, depends on region and season.

Near the boundary between the two tropospheric layers the wind often shifts rapidly; the height of the boundary fluctuates in space and time and cannot be located in advance. The analyst who works with charts located in the layer of strong vertical shear is at a serious disadvantage as he has to analyze all the available levels.

Since the slopes of isobaric surfaces in the tropics are very small it is never possible to make a reliable analysis from pressure-height data alone. Since wind and contour directions can deviate appreciably and the spacing between two stations is often very great, streamline analysis is often more satisfactory. Its object is to represent the fields of wind direction and wind speed, and therefore the fields of vorticity and divergence, which are so important in all synoptic work.

The degree to which *these objectives are attainable depends entirely on quantity and quality of the observations.* There exist several ways to approach a streamline field.

1. When stations are widely spaced, many analysts extrapolate trough lines, shear lines and centers from the time sections and past maps and then sketch streamlines that approximately outline the field of wind direction. A fairly approximate analysis results.

2. When a dense network of wind reports is available, the analyst can resort to more sophisticated methods. Streamlines can be drawn with spacing inversely proportional to the wind speed. This however is a cumbersome task requiring much time.

3. More practicable methods have been developed by Bjerknes and Sandström. The fields of wind direction and wind speed are drawn separately. As before, the field of wind direction is represented by streamlines fitted so that the lines everywhere are tangent to the wind. Very often it is difficult to arrive at an accurate streamline analysis by freehand drawing. For this reason it has been recommended that *isogons*, lines connecting points with equal wind direction, be drawn prior to streamlines. Construction of an isogon field is difficult and requires much practice. Isogons need not be continuous lines like isobars. For instance, at the center of a vortex the wind is zero; all wind directions are found a short distance away. Isogons for all directions therefore emanate from a vortex center.

The isogon technique requires concentrated attention to detail; therefore it should be carried out in limited areas only, say, in the areas of the greatest analytical interest. After completion of the isogons we can draw a number of short lines (arrows) on each isogon parallel to the wind direction. In practice this is quickly done with an isogon board. Many new "winds" are created by this technique to aid in the drawing of streamlines.

Lines connecting points with equal wind speed are called *isotachs* or sometimes *isovels*. They are usually drawn after the streamlines. The gradient of wind speed in the area must dictate the isotach interval to be used. For the low levels of the tropics isolines of 5-knot interval (2.5 m s^{-1}) are recommended. In the high troposphere, where the wind speed gradient is much stronger, 10- or even 20-knot intervals (5 or 10 m s^{-1}) may be most suitable. In jet stream zones the isotachs tend to be parallel to the streamlines, and the centers of high wind speed are ellipses with a long major and short minor axis. Isotachs are drawn with the same rules that apply to isobars.

Most often the weather charts reveal the following special streamline configurations of wind field.

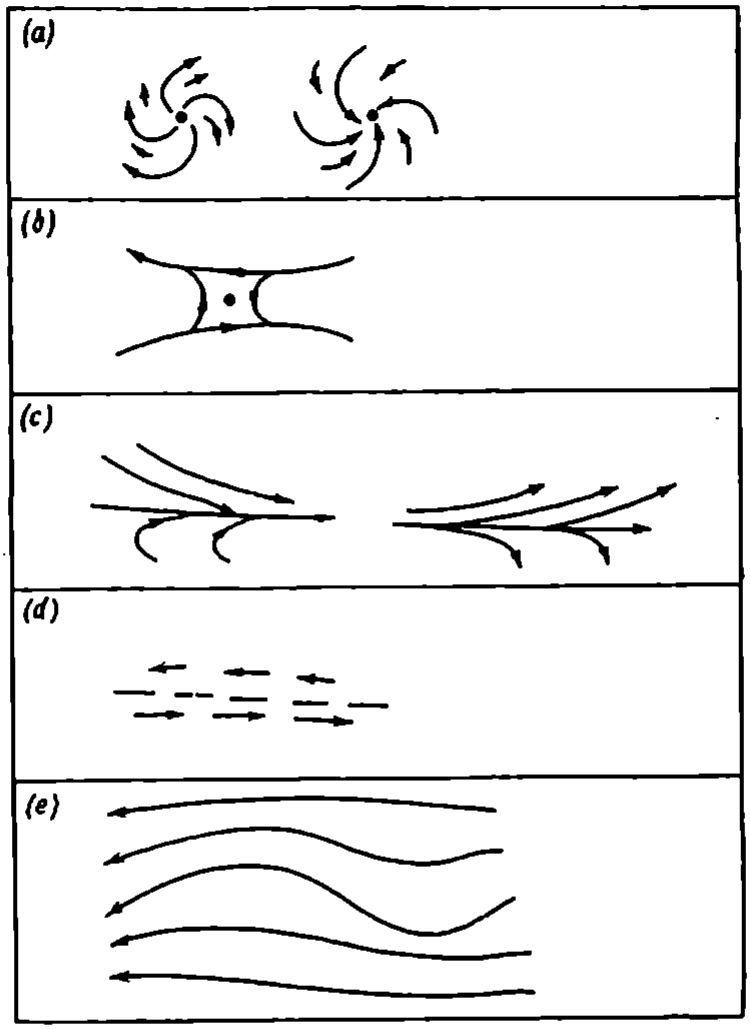

Fig. 4.1 Special characteristics of wind fields:
(a) points of divergence and convergence; (b) col or saddle point with adjacent neutral streamlines; (c) lines of convergence and divergence, asymptotes; (d) line discontinuities of the wind; and (e) wavelike disturbance in a wind field

1. Points of convergence or divergence (Fig. 4.1*a*). At these points the wind speed is zero and therefore the direction indeterminate. They are called "singular" points. In a field of pure divergence, the streamlines emanate from a center or converge toward it as straight lines. If rotation is added, the streamlines spiral inward or outward, either clockwise or counterclockwise, similar to anticyclonic or cyclonic systems of the temperate zone.

2. Neutral points, also called *cols* or *saddle points* (Fig. 4.1*b*). At a neutral point the air is calm so that neutral points are also singular points. The streamlines in the vicinity of this point characterize the air circulation in a deformed stream field. Similar systems may be found in the middle latitudes as well.

3. Lines or curves of streamline convergence and divergence (Fig. 4.1*c*). Palmer calls these lines *asymptotes*. This name is widely used by analysts dealing with tropical wind fields. The asymptotes can be defined as the streamlines from which diverge or toward which converge the adjacent streamlines. The first are called the divergence or positive asymptotes and the second the convergence or negative asymptotes. Theoretically the neighbouring lines should not touch the asymptote, yet in practice they merge with it because of small scale of synoptic charts. Evaluation of asymptotes is an important stage in a wind field analysis. They are helpful in defining the general configuration of a streamline field. It should be kept in mind, however, that a divergence, or convergence, cannot be decided by the asymptotes alone. Rather, the distribution of wind velocity magnitude should be taken into account (see Sec. 4.4), too. Asymptotes coincide with the center lines of troughs and ridges.

4. Line discontinuities of the wind. They are simple yet important streamline systems for the tropical analyst (Fig. 4.1*d*). With ample data available their tracing is rather simple, but may become tedious when data is sparse.

5. Waves in the streamline field designating the presence of a disturbance in the wind field. They appear normally in wide zonal flows, propagating mainly only over a portion of it (Fig. 4.1*e*).

Irrespectively of the drawing procedure chosen, the analyst should locate the special features at the outset of the analysis and mark them. The sketching of streamlines should then start in the simplest portions of the map and proceed from there to the more complicated areas. Enough lines should be drawn to depict the whole field, but not too many. At the end it is convenient to mark troughs, ridges, streamline convergence and divergence lines, and wind discontinuities. To precisely identify the lines of ridges and troughs the anal-

yst should evaluate the points of maximum curvature. For comparison, he should also mark the former position of the higher order characteristics.

4.4 Fields of Divergence and Vorticity

Fields of streamlines and isotachs permit complete evaluation of the field of velocity divergence. In the natural coordinate system

$$\mathrm{div}_2 V = D = \frac{\partial V}{\partial s} + V\frac{\partial \beta}{\partial n}$$

where s is the coordinate in the direction of flow, β the angular direction of the wind, and n the coordinate along a normal to the flow direction.

The field of velocity divergence is seen to be produced by (a) variations of wind speed along the streamlines and (b) coming together or going apart of the streamlines.

When the wind speed increases downstream in a field of parallel streamlines, we have divergence; when it decreases, convergence.

When the streamlines go apart in an area with uniform wind speed along the streamlines, we have divergence; when they come together, convergence.

In an actual wind field the velocity seldom remains constant following the flow and the streamlines never parallel for long. Usually both above factors of the divergence act in combination, with the streamlines converging or diverging and the speed varying along the flow. Streamline fanning alone need by no means denote divergence.

When the wind speed increases downstream and the streamlines fan out, we have divergence: otherwise its presence is subject to the condition

$$\left|\frac{\partial V}{\partial s}\right| < V\frac{\partial \beta}{\partial n}$$

When the wind speed decreases downstream and the streamlines approach each other, we have convergence in accord-

ance with the condition

$$\frac{\partial V}{\partial n} < \left| V \frac{\partial \beta}{\partial n} \right|$$

It should be kept in mind that when the wind speed decreases downstream and the streamlines spread out and when the wind speed increases downstream and the streamlines come together, the divergence become a small residual of two large opposing terms. In general it cannot be measured, as only a minor error in evaluating either component, or both, can alter the sign of the small residual. In middle and high latitudes, such patterns of flow are most frequent, i.e. the geostrophic wind is a fair approximation.

In the tropics, the geostrophic control is much weaker, and direct evaluation of the divergence field, or at least its sign, has a better chance of success. It is a good rule for the analyst to locate the areas where both components of the divergence act in the same sense. They are the active regions. Elsewhere in the tropics little development is likely, as the flow tends to be "balanced".

In general for the tropics the value of divergence is scaled to be of the order 10^{-5} s^{-1}. It is a good practice to compute divergence for some area, A, encompassed by a contour, L, rather than a single point. Then the average divergence for this area is

$$D = \frac{L}{A} \bar{V}_n \qquad (4.4.1)$$

where

$$\bar{V}_n = \sum_{i=1}^{m} V_{n,i} / m$$

is the mean projection of wind velocity vector on the outer normal to the contour L, and m is the number of sampling points on the contour.

Falkovich estimated the divergence computed with the equation (4.4.1) to be a divergence of disturbances having a characteristic scale of 2 or 3 times the diameter of the area A enclosed by the contour L. Therefore to estimate the divergence of synoptic scale disturbances (characteristic length of 1000-1500 km) L must be chosen such that the diameter of computing area be about 500 km.

Streamline-isotach analysis permits also computation and construction of vorticity fields. Contrary to the middle lati-

tudes, where vorticity can be deduced from the field of geopotential or pressure, this procedure can no longer be adhered to in the tropics. In low latitudes, vorticity can be obtained only from wind data.

Similar to computations of divergence fields, vorticity is recommended to be evaluated for some area, A, within an enclosing contour, L. Then the average value of vorticity ζ is computed with the formula

$$\zeta = \frac{L}{A} \bar{V}_L \tag{4.4.2}$$

where

$$\bar{V}_L = \frac{1}{m} \sum_{i=1}^{m} V_{L,i}$$

is the mean projection of wind velocity vector on a line tangent to the contour L. By convention the positive direction of the tangent line is counterclockwise in the Northern Hemisphere and clockwise in the Southern Hemisphere.

Weather forecasting of late in the tropics has divergence in ever frequent use as a synoptic factor. To illustrate we discuss one of the procedures.

Assuming a constant density, the continuity equation provides the following relation between divergence and vertical motion

$$w - w_0 = -\int_0^z D \, dz \tag{4.4.3}$$

where w_0 is the vertical velocity at the bottom of a layer Δz, w the vertical velocity at the top of the layer, $D = \mathrm{div}_2 = \partial u/\partial x + \partial v/\partial y$ the two-dimensional horizontal divergence, and z the vertical coordinate.

When the bottom of the layer under consideration is at the ground level where vertical motion is zero, then

$$w = -\int_0^z D \, dz$$

or averaging the divergence for the layer from 0 to z

$$w = -\bar{D}z \tag{4.4.4}$$

The vertical movement accordingly will have the same sign throughout the layer and the speed will increase from the surface to the top. When $D > 0$ the equation (4.4.4) yields downward movement, and when $D < 0$ upward movement.

The average value of divergence may not always lead to correct estimation of vertical movements, since more rigorously they are not independent of the divergence variability with height.

Let us divide the layer under discussion in two sublayers, the lower Δz_l and upper Δz_u. Then the equation (4.4.3) rewrites

$$w = -\int_0^z D\,dz = -\int_0^{z_1} D\,dz - \int_{z_1}^{z_2} D\,dz = -D_l\,\Delta z_l - D_u\,\Delta z_u$$

where D_l is the average divergence in the lower layer, and D_u is the average divergence in the top layer.

The ascending motion will be observed when

$$-D_l\,\Delta z_l - D_u\,\Delta z_u > 0$$

This inequality will be satisfied if

(1) $D_l < 0$ and $D_u < 0$, that is, convergence takes place in both layers;

(2) $D_l < 0$, $D_u > 0$, but $\Delta z_l\,|D_l| > \Delta z_u D_u$, i.e. the air converges in the lower and diverges in the upper layer, and the product of the absolute value of convergence and the lower layer thickness must be higher than that of divergence times the upper layer. Assuming the layers are of equal thickness, the magnitude of the lower layer convergence must be larger than the upper layer divergence, or otherwise if the convergence and divergence are equal in magnitude, the upper layer must be more shallow.

(3) $D_l > 0$, $D_u < 0$, but $\Delta z_l D_l > \Delta z_u\,|D_u|$, i.e. with divergence in the bottom layer and convergence in the top layer. The product of the divergence by the lower layer depth must be lower than the absolute value of the convergence multiplied by the upper layer depth. With both depths equal, the divergence must be lower than convergence; otherwise, when the convergence equals the divergence the lower layer must be thinner.

Descending motions ($w < 0$) will be observed when

$$-D_l \Delta z_l - D_u \Delta z_u < 0$$

This inequality is satisfied when the following conditions are met.

(1) $D_l > 0$ and $D_u > 0$, i.e. divergence takes place in both layers;

(2) $D_l < 0$, $D_u > 0$, but $\Delta z_l \mid D_l \mid < \Delta z_u D_u$, that is the air in the lower layer converges and in the upper layer diverges, yet the product of the absolute value of convergence and the lower layer depth must be less than that of the divergence and the upper layer depth. Both layers equal in depth, the convergence in the lower layer must be less than the divergence in the upper layer in magnitude. The divergence and convergence being equal in magnitude, the convergent layer must be more shallow than the divergent.

(3) $D_l > 0$, $D_u < 0$, but $\Delta z_l D_l > \Delta z_u \mid D_u \mid$, i.e. the upper layer is convergent, the lower layer divergent, and the product of the lower layer into its divergence must be larger in value than the product of the absolute value of the convergence into the upper layer. Should both layers be equal in depth, the divergence must be larger than convergence; should the divergence and convergence balance in magnitude, the lower layer must have larger depth than the upper.

The value of divergence at the initial moment not always proves to be a representative indicator of changing, or stabilizing, weather. The efforts to employ divergence at the zero time for further forecasting by synoptic methods failed to produce the wanted objective. This is due to the fact that divergence is variable in nature. Its further value depends on certain factors, major of which being the values of divergence and vorticity at the level of origin. Subsequent values of vorticity can also exert their influence on the changing weather. Therefore, weather variability, or stability, is governed by a combined action of divergence and vorticity. Several countries in the tropics have succeeded in obtaining fairly reliable relations between the weather conditions and combinations of divergence and vorticity.

Let us recourse to the vorticity equation in the form

$$\dot{\zeta} = -(\zeta + f) D_3 - \beta v \qquad (4.4.5)$$

where $\beta = \partial f/\partial y$ is the Rossby number.

Now we write the divergence equation in the form

$$\dot{D} = f\zeta - D^2 + 2J(u, v) - \beta u - \alpha\nabla^2 p \qquad (4.4.6)$$

where

$$J(u, v) = \frac{\partial u}{\partial x}\frac{\partial v}{\partial y} - \frac{\partial u}{\partial y}\frac{\partial v}{\partial x}$$

is the Jacobian $D(u, v)/D(x, y)$, and $\alpha = 1/\rho$.

The equations (4.4.5) and (4.4.6) are very hard to compute divergence and its change. The computation obviously becomes simpler if a way is found towards neglecting some of the terms on the right hand sides of the equations.

A. Krueger has estimated the terms of (4.4.5) and (4.4.6) for the tropical region. The average value of both vorticity and divergence is 3×10^{-5} s^{-1} at normal conditions for layers of about 1.5 km deep. The quantity $\nabla^2 p$ is much harder to scale. According to Krueger, it is around 5×10^{-10} s^{-1}, and the terms $f\zeta$ and D^2 around 10^{-9} s^{-2}. The quantity $J(u, v)$ depends totally on the structure of the flow. In potential, i.e. non-oddiug, both linear and curvilinear, flow, the quantity $J(u, v)$ must be zero very nearly. However it gains significantly when a disturbance is introduced in the flow. In the tropics the disturbed flows are more frequent than the linear and ordered ones. When $J(u, v)$ is of a material value, the terms $-D^2$ and $2J(u, v)$ may be shown to cancel out, i.e. $-D^2 + 2J(u, v) = 0$. For the mean wind speed and time intervals of 6 to 12 hours, the estimation shows the terms βu and βv may be neglected. For larger time intervals, however, this may no longer be done. In the nearequatorial regions with $\varphi < 7°$ the terms $f\zeta$ and $J(u, v)$ are negligibly small. For the tropical areas away from the equator ($\varphi > 7°$), the terms $\nabla^2 p$ and $J(u, v)$ may be neglected or, letting $-D^2 + 2J(u, v)$ be equal to zero, the quantity $\nabla^2 p$ alone. In view of above, for a disordered flow the equations (4.4.3) and (4.4.4) from latitude 7° away may be written in a simplified form

$$\dot{\zeta} = -(\zeta + f)D \qquad (4.4.7)$$

$$\dot{D} = f\zeta \qquad (4.4.8)$$

From latitude 7° equatorward we may write only the equation for orderly motions

$$\dot{D} + D^2 = -\alpha \nabla^2 p \qquad (4.4.9)$$

For latitudes equal to 7° and further poleward the complete equations may be simplified as follows

$$\dot{\zeta} = -(\zeta + f) D \qquad (4.4.10)$$

$$\dot{D} = f\zeta - D^2 \qquad (4.4.11)$$

In accordance with the equations (4.4.9) nearequatorial divergence varies independently of vorticity.

For the extraequatorial regions with $\varphi \geqslant 7°$, variation of divergence depends on the initial values of the divergence, D_0, and vorticity, ζ_0. To find the divergence as a function of time we need to solve a simultaneous set of equations (4.4.7), (4.4.8), (4.4.10), and (4.4.11).

In the equatorial latitudes of $\varphi < 7°$ with $\nabla^2 p = 0$

$$D(t) = \frac{D_0}{1 + D_0 t} \qquad (4.4.12)$$

or $\nabla^2 p > 0$

$$D(t) = \frac{D_0 \sqrt{\alpha \nabla^2 p} - \alpha \nabla^2 p \tan\left(\sqrt{\alpha \nabla^2 p}\right) t}{\sqrt{\alpha \nabla^2 p} + D_0 \tan\left(\sqrt{\alpha \nabla^2 p}\right) t} \qquad (4.4.13)$$

for $\nabla^2 p < 0$

$$D(t) = \frac{D_0 \sqrt{-\alpha \nabla^2 p} - \alpha \nabla^2 p \tanh\left(\sqrt{-\alpha \nabla^2 p}\right) t}{\sqrt{-\alpha \nabla^2 p} + D_0 \tanh\left(\sqrt{-\alpha \nabla^2 p}\right) t} \qquad (4.4.14)$$

If a divergence is given by its initial field and the Laplacian of pressure is deemed constant within a considered interval of time ($\nabla^2 p = \text{const}$), then the divergence may be computed over this interval toward the subsequent time point. If in some area

$$D_0 \geqslant 0 \quad \text{and} \quad \nabla^2 p > 0$$

at the initial moment, then in a reasonably large time t the equation (4.4.13) predicts a convergence zone which as a rule becomes an area of thunderstorm activity.

Hence, in the equatorial region at $J(u, v) = 0$ a vast area of unstable weather can develop. The thunderstorm

activity here progresses in narrow strips which become known as *lines of disturbance*. The lines of disturbance give rise to squalls, hence another name for them is *squall lines*. Synoptic maps, unfortunately, are unsuitable to follow movement of disturbance lines. A most striking feature of the lines is in that they form, suddenly disappear and reappear within an area of relatively large positive Laplacian of pressure, $\nabla^2 p$, that is within the area of disturbance.

Radar surveillance materially facilitates tracking of squall lines and their study. With radar sets, the researcher can track the motion and evolution of the objects to enter the collected data on a map and assess their structure in more detail. So it has become known that the squall lines exist longer than separate cumulonimbi producing them. The clouds may exist on a squall line as long as 40 minutes to an hour (in some cases somewhat longer) whereas the squall lines may live for several hours. Within the structure some clouds decay, others carry on existing; in place of disappeared clouds new convective cells occur to produce new clouds and thus to support the life cycle of the line.

Squall lines are most often met over West Africa and India. Mechanisms by which they form are nearly identical for both areas. In West Africa, they evolve in moist southeast draft of the low troposphere, while aloft, in the mid- and upper troposphere, easterly currents transfer relatively dry air. This signifies a well defined vertical wind shear in the troposphere. Since easterly currents prevail the system of cumulonimbus clouds travels from east to west. The ascending moist air that intrudes the bottom layer of a cloud in its forepart (Fig. 4.2) is immediately uplifted by the easterly flows and pushed ahead of the main cloud column. The easterly currents of the middle troposphere trying to catch up with the disturbance have to descend. On their downward motion they penetrate the precipitation area where rain falls out from both the main cloud column and an extended part of the cumulonimbus cloud adjoining from the rear. Evaporation in the rain brings about a profound cooling of the descending undercloud currents with the result that a circulation begins in the squall line, which strongly resembles the circulation at cold fronts (see Fig. 4.2). However, disturbance lines

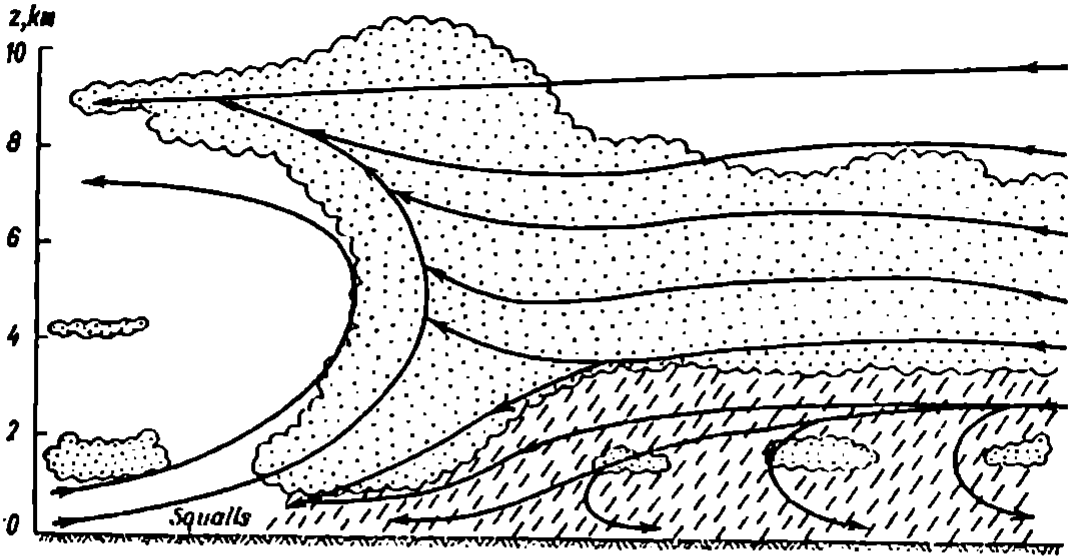

Fig. 4.2 Schematic cross-section through a line of squalls, representing a typical distribution of streamlines (after Hamilton and Archbold)

do not divide air masses of different properties and cannot therefore be taken as fronts.

The areas of disturbance to be related with squall lines form as a rule in the afternoon when the conditions are set in that favour development of convection. Some convections are known to have occurred by night. But normally the areas of disturbance disappear by night. A variety of orographic inhomogeneities (surface relief, uplands, valleys, hill chains, etc.) often adds in squall lines development in disturbance areas. Water surface and some land regions having stably stratified layers above favour on the contrary to squall lines destruction.

The life cycle of the disturbance area in a uniform-speed current amounts to 6 to 12 hours.

In the nearequatorial areas with disordered motion for which $J(u, v) \neq 0$ the equation (4.4.14) can no longer be representative. In the circumstances the disturbance lines are essentially motionless to stay at the same latitude for a long time. An example of the pattern can be delivered by the region of West Africa. Hence, in the areas with disordered motions of air an extreme care should be exercised

in extending the above conclusions on the development of and processes in disturbance lines.

For the extraequatorial tropics of latitudes 7° to 20°, the general solutions of (4.4.7) and (4.4.8) will be of the form

$$D(t) = D_0 + f\zeta_0 t - f(\zeta_0 + f) D_0 \frac{t^2}{2} + (\zeta_0 + f)(D_0^2 + f\zeta_0) \frac{t^3}{13} - \ldots + \ldots \quad (4.4.15)$$

$$\zeta(t) = \zeta_0 - (\zeta_0 + f)\left[D_0 t - (D_0^2 - f\zeta_0) \frac{t^2}{2} + D_0 (D_0^2 - f^2 - 4f\zeta_0) \frac{t^3}{13} - \ldots + \ldots \right] \quad (4.4.16)$$

Within latitudes 7° and 20°, these series will converge for 6-hour intervals. If we truncate the series on the term of t^3 then an error of about 2% results for both D and ζ. Truncation with the t^2 term yields an error of 10%. If the 10 per cent error is agreeable, the series with only the first three terms retained will be

$$D(t) = D_0 + f\zeta_0 t - f(\zeta_0 + f) D_0 t^2/2 \quad (4.4.17)$$

$$\zeta(t) = \zeta_0 - (\zeta_0 + f)[D_0 t - (D_0^2 - f\zeta_0) t^2/2] \quad (4.4.18)$$

From (4.4.17) a future divergence is to depend on the initial values of divergence and relative vorticity (D_0 and ζ_0) and absolute vorticity ($\zeta_0 + f$).

When the initial field is nondivergent ($D_0 = 0$), (4.4.17) yields

$$D(t) = f\zeta_0 t$$

that is at $\zeta_0 > 0$ a divergence occurs and at $\zeta_0 < 0$ a convergence. From the above scaling, the quantity $f\zeta_0$ is of order 10^{-9} s^{-2}. Hence, already in 3 hours ($t = 10\,800 \approx 10^4$ s) the divergence will be of order 10^{-5} s^{-1}.

For an initially divergent field having a zero vorticity ($D_0 \neq 0$, $\zeta_0 = 0$) we have

$$D(t) = D_0 - f^2 D_0 t^2/2$$

that is the divergence will diminish with time, approaching zero asymptotically. However, it will belittle in intensity very slowly.

It is a simple matter to see that the expected vorticity also depends on the initial values of vorticity and divergence (ζ_0 and D_0). Let at first assume that we have a zero vorticity field, $\zeta_0 = 0$, then

$$\zeta(t) = -fD_0t + D_0^2ft^2/2$$

Since the first term of the expression is by an order of magnitude larger than the last, at $f > 0$ and $D_0 > 0$ the vorticity will be negative, and at $D_0 < 0$ positive, i.e. $\zeta(t) > 0$. It implies that the field of initially positive divergence will give rise to the anticyclonic vortex, whereas the field of negative initial divergence will support the cyclonic vortex.

Now assume that a field under discussion is nondivergent ($D_0 = 0$) then

$$\zeta(t) = \zeta_0 - (\zeta_0 + f)\, f\zeta_0t^2/2$$

It is readily seen that in an initially nondivergent field the cyclonic vortex will slowly die out. The anticyclonic vortex also will recede at $|\zeta_0| < f$ but develop stronger at $|\zeta_0| > f$.

In the real atmosphere the wind field always, or almost always is divergent and has a property of vorticity. The computations are thus bound to be conducted with the complete expressions. For convenience, the calculations may be effected beforehand and the results entered into a table.

To illustrate, assume that we seek divergence for a location at 17° latitude in 6 hours beyond the time zero. At the time $D_0 = 10^{-5}$ s^{-1} and $\zeta_0 = -2 \times 10^{-5}$ s^{-1}.

The Coriolis parameter at 17° latitude

$$f = 2\Omega \sin 17° = 4.4 \times 10^{-5} \text{ s}^{-1}$$

The projection period in seconds is $t = 6$ hours $= 21\,600$ s $\approx 2.2 \times 10^4$ s, hence $t^2/2 \approx 2.3 \times 10^8$ s^2. Now we have at hand all the required data base. Substituting into the formula (4.4.17) yields

$$\begin{aligned} D(6) &= 10^{-5} + 4.4 \times 10^{-5}(-2 \times 10^{-5})\, 2.2 \times 10^4 \\ &\quad - 4.4 \times 10^{-5}(-2 \times 10^{-5} + 4.4 \times 10^{-5})\, 10^{-5} \times 2.3 \times 10^8 \\ &= 10^{-5} - 1.8 \times 10^{-5} - 0.2 \times 10^{-5} = -10^{-5} \text{ s}^{-1} \end{aligned}$$

In six hours therefore this location is to experience a convergence, and, as a result, a worsening of the weather.

Palmer has given a series of empirically deduced rules relating divergence (convergence) and weather for the Marshall Islands area (5-14°N, 160-172°E). They are usually treated as prognostic rules which are not to apply throughout the tropics unequivocally, rather, they may be used as a prototype to infer similar relations for any other tropical regions.

To circumvent the effects of computational errors in evaluating the convergence (divergence) or its forecasting the Palmer rules treat the weather element as being of the four sequential grades:

$0-5\times10^{-6}$	weak
$5.1-25\times10^{-6}$	moderate
$25.1-40\times10^{-6}$	strong
more than 40×10^{-6}	very strong

First rule. In the areas of moderate or strong divergence at 600-800 m altitude the dominating cloud type will be cumulus humilis in the amount that will not be higher than 4 balls.

Second rule. When a moderate divergence at 600-800 m altitude is paralleled by a vertical wind shear at 1-3 km altitude, the cumulus clouds are expected to spread out to form stratocumuli in increasing proportion.

Third rule. In the Northern Hemisphere, north of the strongest wind area in the trades, where a pronounced vertical wind shear is observed in lower layers of the atmosphere and the trade inversion is also low, the prevailing clouds are mostly stratocumuli. When a divergence occurs there at 600-800 m altitude, the stratocumulus field separates, producing wide gaps. However, when even a weak convergence is present, an overcast stratocumulus canopy is formed, with cumulus clouds encountered rather seldom and in small amounts.

Fourth rule. When even a light wind shear is present south of the strongest wind area in the trades at 1-3 km altitude and a weak or moderate convergence is noted at 600-800 m, then cumulus mediocris and cumulus congestus

are expected to form, in an amount not higher than 5 balls. With strong and very strong convergence the clouds increase in depth up to cumulonimbi, the number of clouds increasing insignificantly.

Fifth rule. When the asymptote of convergence in the streamline field at the 500 m level superimposes the relative minimum of wind speed in the area, then a line of cumulus congestus or cumulonimbus clouds is observed along the asymptote. This system is similar to the cold front in the middle latitudes, though any significant difference in air mass properties on either side of the system cannot be traced. When the asymptote coincides with a wind speed maximum, only separate cumulus humilis form in the area.

Sixth rule. Where at low altitudes the area of lightest wind lies aside of the convergence asymptote or being of an elongated shape crosses it making an angle near to the right one, the convergence is normally strong in the layer of 3-10 km. In the circumstances, a system of altostratus and nimbostratus forms to produce widespread rains.

4.5 Air Masses

Two types of air mass form in the tropics, continental tropical air mass (cTA) and maritime tropical air mass (mTA). Midlatitudinal air masses may penetrate in the region, yet they are rapidly transformed on their excursion. In winter of the respective hemisphere continental mid-latitude air mass (cMLA) injecting in the tropics can markedly lower its temperature.

Continental tropical air forms over dry continental areas and therefore differs in very high temperatures, low humidity, and substantial diurnal variations of all meteorologic quantities. The temperature of cTA rises to 40-42 °C in summer and to 31-33 °C in winter. The temperature lapse rate in the mass amounts to 0.60-0.65 °C/100 m. It varies with time and height only insignificantly. The intense heating of the surface air by the underlying surface seemingly must have given rise to markedly higher lapse rates, yet it fails since cTA forms in the areas of high pressure systems activity where the air mass undergoes subsidence. The subsidence makes the warming of the surface

air be followed by the air warming aloft so that the temperature lapse rates become more uniform, i.e., more steep.

In summer, the relative humidity of cTA at the surface is 16% to 18%, it increases to 21% to 23% at 3 km altitude to decrease further upwards. In winter it amounts to 24-26% at the ground, somewhat drops at 1-2 km altitude to increase higher up again to 35% at 4 km. The cTA is notorious for clear weather.

Moving oceanward cTA rapidly changes its properties, mainly increasing in humidity. The layer of high humidity though seldom grows deeper than 2.5-3 km.

The properties of maritime tropical air depend on the area where it has been formed. In the sense, it may be subdivided into equatorial air (EA) and trades air (TA). Equatorial air mass forms over the equatorial trough, not infrequently directly in the ITCZ. Characteristic of EA are high humidity traced up to high altitudes and high temperature lapse rates observed up to the tropopause. The variability of the temperature lapse rate in EA is superior to that in cTA. Weather conditions in EA vary according as the disturbance is present or absent. The disturbance area as a rule is substantially or totally cloudy and rainy. Away from disturbance, the cloudiness generally is below 8 balls with frequently clear skies.

The trades air is also characteristic of large moisture content but the humidity is distributed with height nonuniformly. Two layers may be distinguished, the lower layer having a maximum of relative humidity at 1.5-2 km altitude and the upper layer with the highest humidity at 6-7 km (see also Sec. 2.1). An intermediate layer of relatively dry air is in between. The lower sea surface air layer has a rather high lapse rate of temperature (0.9-1.0 °C/100 m). Within the troposphere it undergoes a repeated alteration, some even give rise to inversion layers.

TA is notorious in cloudy weather. The prevailing clouds are cumulus humilis, cumulus mediocris, and cumulus congestus. Cumulonimbi are also formed to produce short showers (see Secs. 2.5 and 2.6).

Drifting inward of a continent (this happens as a rule in summer) mTA undergoes transformation of its properties. Its temperature rises and the humidity somewhat drops.

The temperature of mTA at the land level is around 30 °C on the average, yet it decreases rapidly with height. The temperature lapse rate amounts to 0.8-0.9 °C/100 m. The humidity remains substantial (50-60%) up to high altitudes. With the intrusion of the mTA a continent will experience rainy unstable weather.

Midlatitude air intrudes in the tropics in winter. On its way to the tropical region it undergoes a crucial change. Maritime midlatitude air mass (mMA) arrives in the tropics having almost the same temperature as mTA (accurate to 1 °C). The continental temperate air (cMA) changes slightly slower than mMA does. So at Khartoum (17°N) an inflow of cMA in January may decrease the air temperature down to 13-15 °C. It follows by increase in cloudiness though the amount of clouds remains small due to low humidity. So in the surface air the humidity is within 45% to 50% and decreases rapidly with height. At the 3 km level it is below 17-20%.

In general the air masses in the tropics differ from each other only slightly. Most significantly differ the air masses of coastal areas. Yet even there no fronts can be found similar to those encountered in the middle latitudes. To sum up, the tropical area exhibits no fronts because of the little difference in properties between the air masses.

Review Questions

1. What is the objective to plot time-height sections?
2. What difficulties expect the analyst working on a tropical surface chart?
3. Which properties distinguish the constant-pressure-chart analysis in the tropics?
4. Which methods of streamline field analysis do you know?
5. Enumerate the special characteristics of wind fields.
6. What is a way to estimate the divergence from the streamline-isotach analysis?
7. What order of magnitude has divergence in the tropics?
8. Describe a procedure to compute divergence and vorticity for a given area A.

9. How can the sign of the vertical wind speed component be evaluated from the field of divergence at various levels?
10. If we know the initial values of divergence and vorticity, how could we determine the future values of $D\ (t)$ and $\zeta\ (t)$ for various areas of the tropical region?
11. What is the disturbance, or squall, lines; how are they formed, and how can they be traced?
12. Characterize the air masses observed in the tropics.

Chapter 5 CIRCULATION AND SYNOPTIC SYSTEMS OF THE TROPICS

5.1 The General Circulation

The major function of the tropical circulation in the atmospheric "heat engine" consists in transporting to the other areas of the globe an excessive heat which is accumulating in low latitudes due to intense insolation. The fairly permanent, on the annual basis, temperature difference between the equatorial regions and the subtropical belts is the main force driving the motion of air streams in the tropical circulation. This stable heat source also sets in motion the large-scale circulation systems that are characterized by either an outstanding steadiness (trade winds) or pronounced periodic regularity (monsoons). These systems form the main stream of the tropical atmosphere.

Within the large-scale circulations one can discern the systems of smaller scale which are called the disturbances of the main stream or, simply, disturbances. The circulation of air in the disturbances being embedded into the main stream produce the general flow pattern of the tropical atmosphere.

Solving some research or applicational problems requires that disturbances be recognized in the main stream pattern. A major distinction between these synoptic situations lies above all in their temporal and spatial scales. The main stream is considered to be the part of general motion that is characteristic of large area and that changes in time more slowly as compared with the motion of smaller objects. The disturbances are considered to consist of small-scale circulations set in motion and rapidly changing in shape and intensity.

The weather charts often give few clues to discern the disturbances and main stream. This casts a subjective shadow on main stream and disturbances evaluation. In some situa

tions the disturbances are easily traced, say typhoons, whereas in the others, when disturbances are not so evident, the distinction is hard to effect without recourse to some quantitative criterion. As such, analysts most often use the intensity of disturbance. A respective measure of the intensity, believed to supply a high degree of objectiveness, may be the value of relative vorticity. Observations indicated that in the majority of cases the vorticity of disturbances as extracted from synoptic charts is about an order of magnitude stronger than that of the main stream.

The synoptic scale disturbances of the tropics are most often of small amplitude. Thus, averaging the motions of small amplitude disturbances yields some average flow which may be regarded as a main stream. At times, however, the disturbances may be so significant as to remain discernible even in the averaged field of motion. If we allow for such disturbances, the main stream may be treated as to consist of two parts: quasibarotropic easterly flow in the low troposphere, centered almost over the equatorial trough line, and the baroclinic flow aloft with the baroclinity being augmented with height and separation poleward. In the easterly flow, the velocity reduces with height. Further to the subtropical belt in the upper troposphere they reverse to become westerlies.

There exists no exact boundary between the barotropic and baroclinic streams. Commonly, they transfer one into the other as far as 10-15° latitude from the equatorial trough line in the lower troposphere, and at 6-12 km altitude when above the trough (Fig. 5.1).

The easterly stream has the lowest speed at low levels near the equatorial trough. Farther poleward it increases and reaches its maximum values in the trades over the oceans.

In the upper troposphere the westerlies slacken poleward. They become weak easterlies or westerlies in the summer hemisphere or strong westerlies in the winter hemisphere over the surface subtropical anticyclone.

There exists a certain tendency for the flow to become meridional when moving toward the equatorial trough in the lower troposphere and when moving poleward in the upper troposphere. If this motion is added by the air descent

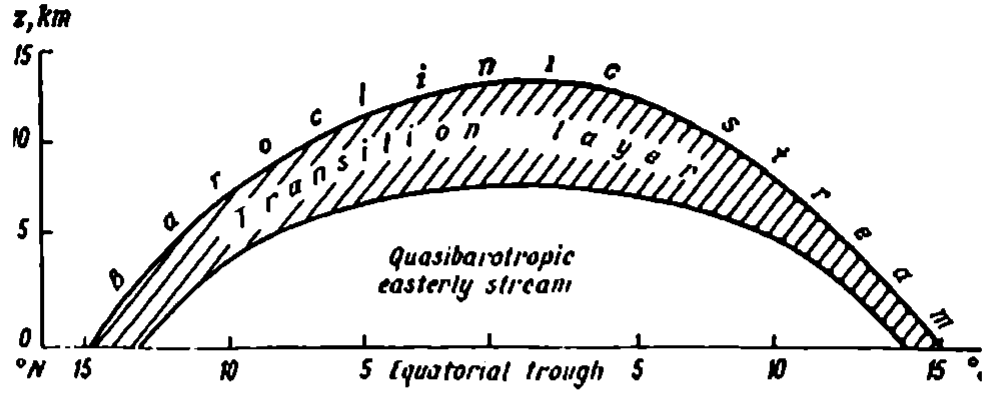

Fig. 5.1 Schematic cross-section of the basic current in the tropics

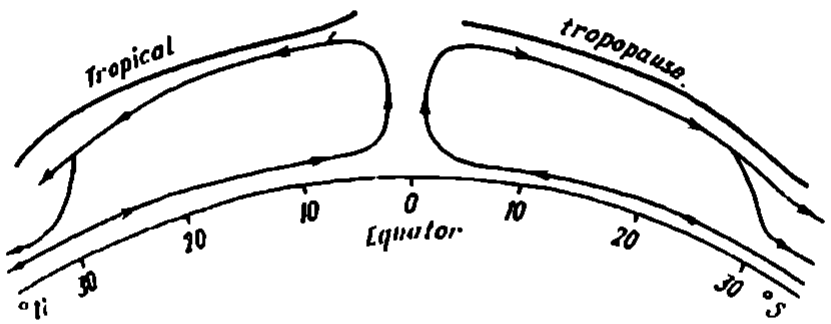

Fig. 5.2 The Hadley cells

at the latitudes of the subtropical high and the air ascent over the equatorial trough, then a large-scale circulation cell is produced, called the Hadley circulation or *Hadley cell* due to George Hadley who suggested its existence still in 1735 (Fig. 5.2).

The Hadley cell is a simplified model of circulation in the tropics. According to this model, an excess of heat near the equator is transformed into kinetic energy. A substantial amount of heat is expended on evaporation and transported with air masses as latent heat to be realized later by condensation. When the heated masses of air uplift, the water vapour they carry condenses, shaping into clouds and producing rain. Convection in the unstably stratified atmosphere also favours the transfer of energy into upper layers (see Chap. 3). The atmospheric currents existing aloft export these air masses to higher latitudes,

At 20-30° latitude the air descends in the system of the high pressure belt anticyclone. Powerful air currents flowing in the lower layers equatorward close the circulation, making it a complete cell.

This model, however, is not devoid of shortcomings.

1. It does not allow for either seasonal variation, or different conditions for the circulation at various longitudes. Observational evidence indicates that a circulation similar to the Hadley cell exists throughout the year over the Pacific and Atlantic oceans only. Elsewhere it is severely deformed. It is only in March through April and September through October, that is on the times close to the equinox, that the circulation at all longitudes assumes the symmetry of the Hadley cell.

2. The model suggests that the solely heat source is placed near the equator. In reality, a number of separate areas having a surplus heat budget are usually observed both over continents and over oceans. As the result, the circulation deviates from the model both as concerned intensity and as concerned longitudinal location of the cell itself.

3. The model ignores air motions in the middle troposphere. Meanwhile, a plentiful statistics is available testifying the intrusions of huge meridional troughs of the middle troposphere deep into the low latitudes. Air currents in the foremost parts of the troughs transport immense amounts of heat poleward.

4. Air mass exchange between the hemispheres is not taken into account. At present an ample evidence is collected on the heat transfer from one hemisphere into the other by air flows.

Though far from ideal, the Hadley circulation model describes in general the air motions pattern in the tropics and defines the main components of the tropical circulation, the equatorial trough, trades and antitrades.

5.2 The Equatorial Trough

The equatorial trough is meant to embrace the nearequatorial low pressure belt with the intrinsic convergence and uplift of air masses. The fact that air currents

(trades) converge at the equatorial trough has suggested a name for the area, the *intertropical convergence zone* (ITCZ).

The equatorial trough is the object of major importance in the tropics. It has been the focus of study by many researchers: Fal'kovich, Flohn, Khromov, Petrocyants, Riehl, and many others. Various authors named it in a variety of ways: the trade confluence, equatorial convergence zone, and monsoon trough. Not infrequently it was called the intertropical front. The last name came from the 'Norwegian school' of meteorologists who introduced the concepts of *air masses* and *fronts*. The adherents of the school believed the south and north trades also formed a front. The concept of the intertropical front was introduced by analogy with the fronts of middle latitudes without a sufficient observational background. A narrow region of bad weather is certainly present along the zone where the south and north trades meet. Yet the notion of front in the sense of the Norwegian school could hardly be applied to it, because the air masses on either side of it are essentially alike in properties (the only exclusion may be narrow strips between land and sea, which will be discussed below).

The active areas in what was called the intertropical front do undoubtedly experience considerable convergence, hence the term 'intertropical convergence zone' appears to be more suitable.

The zone of trades confluence need not be followed by a significant convergence even though low pressure is indicative for it everywhere. In view of the aforementioned, we should apply the term 'equatorial trough' to all the nearequatorial low pressure belt, and the term 'intertropical convergence zone' only to its areas of activity.

The seasonal position of the sun governs the location of atmospheric activity centers. So the subtropical anticyclones shift toward higher latitudes in summer and toward lower latitudes in winter. The equatorial trough changes its latitudinal position accordingly, the trough line tends to displace toward the summer hemisphere and over land it migrates 10-20° latitude from the equator as if it follows the sun. Thus the equatorial trough undergoes annual latitudinal variation which is different for various longitudes.

In the Atlantic and in the eastern Pacific the equatorial

trough always situates at the equator or a little to the north. The annual meandering of the trough line is in a narrow belt in this region. Its largest displacement the trough experiences over the continent of Africa and the west part of the Indian Ocean. For example, it shifts along the 40°E meridian from 10°S in January to 22°N in July. Over the West Africa, the trough situates south of the Bay of Guinea in January and over the Sahara in July.

The active areas of the trough are notably cloudy and rainy. Wind turns crossing the ITCZ while both temperature and humidity undergo a marked change in their values. Where the trough lies nearly along the borderline between ocean and continent these differences may be thought of as that between two air masses. In West Africa, for instance, air coming from the Bay of Guinea essentially differs in properties from air inflowing from the Sahara. A similar pattern is observed over India where air of the southeast monsoon markedly deviates in properties from continental air. On the other side, no difference in air mass properties is observed where the trough meanders far from such sea-land borderline anywhere over the oceans or moist tropical forests.

The trough embraces all the globe. At some portions of its meandering convergence is substantial, at others it is weak. Accordingly, the break in wind direction between the trades also undergoes longitudinal variation. At some locations the break in wind direction may serve a clear-cut indicative of the trough location, at other longitudes it can be traced only by satellite photographs.

Active centers shift along the trough. Velocities of the displacements are far from constant, the lines of the travel are complicated. Therefore, extrapolation is not recommended as a means of prediction of their routes.

The field of divergence along with the field of vertical movement over the ITCZ is notably unsymmetrical about the equatorial trough line. As unsymmetrical is the placement of cloudiness and rainfall.

Assuming an uncompressible atmosphere let us deduce the vertical component of wind making use of the continuity equations (4.4.3) and (4.4.4). After Flohn we assume that to a first approximation divergence may be sufficiently

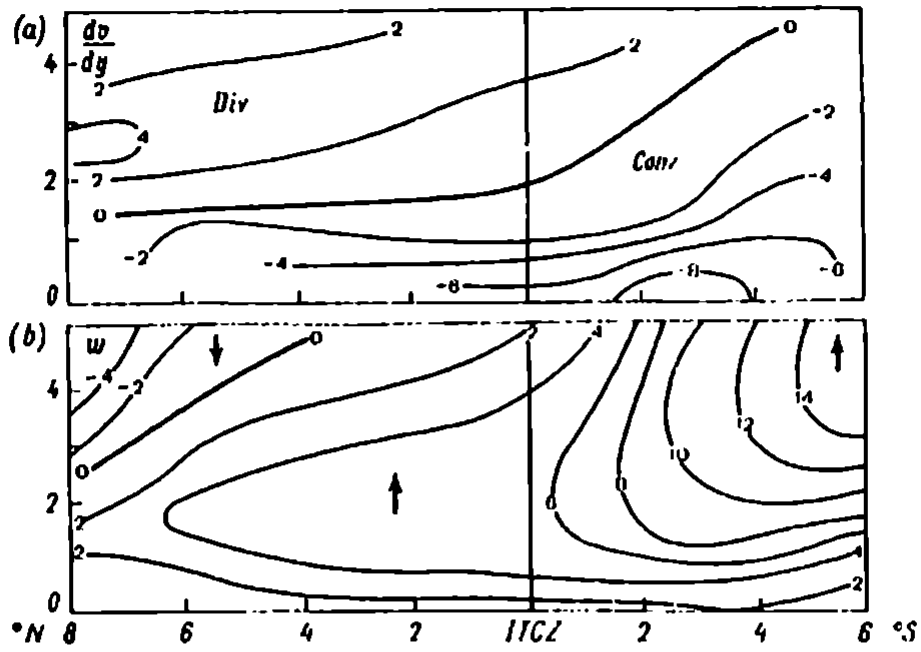

Fig. 5.3 Plotting of a vertical section across the ITCZ in the Atlantic: (*a*) distribution of $dv/dy \sim \text{div } V$ in 10^{-6} s^{-1}; and (*b*) vertical wind component, w, in mm s^{-1} (after Flohn)

defined through variation of meridional component of wind, v, along the y-coordinate pointing northward.

An example of computations of $\partial v/\partial y$ and the respective vertical movements south and north of the ITCZ is shown in Fig. 5.3. Figure 5.3*a* illustrates how north of the ITCZ surface convergence, observed at soil surface, turns into divergence everywhere from 1.3 to 1.8 km altitude. South of the ITCZ convergence is more pronounced and elevates up to 3-5 km. Vertical movements, as a consequence, have similar asymmetry (Fig. 5.3*b*). Updrafts are strongest at 4-5 km height, 500-600 km south of the surface location of the ITCZ. Taken together, these facts may be interpreted as the presence of a gradual ascent of the ITCZ southward (see also Fig. 5.5).

From the comparison of the divergence and vertical movement fields south and north of the ITCZ we may conclude that ascending motions north of the ITCZ in the NE trades overturn the trade inversion only slightly. On the

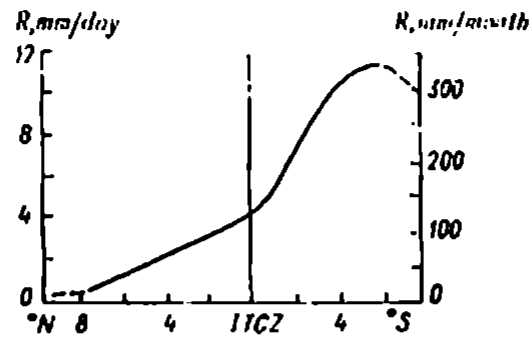

Fig. 5.4 Rainfall within an ITCZ belt (after Flohn)

contrary, south of the ITCZ, substantial updraft strongly decreases the stability in the SE trades crossing the equator south of the ITCZ.

Similar results have been obtained by Rex for the Pacific Ocean (Marshall Islands). According to the observations, the ITCZ situated at 7°N throughout the whole observational period (April-June, 1956) and the strongest updraft (3-5 mm s^{-1}) took place at 4-5°N.

The mean vertical profiles of temperature and humidity and the vertical movement distribution represented at Fig. 5.3*b* may be used to calculate a resultant rainfall in the area. The computed figures are 20-100 mm per month for the northern and 200-300 mm for the southern side of the ITCZ (Fig. 5.4).

In West Africa, cloudiness and rainfall also place unsymmetrically with respect to the surface position of the ITCZ. The weather is dry and clear north of the trough, and only an insignificant amount of cumulus humilis may be met moving about 200 km to the south of it. However, at a distance of 300-600 km south of the ITCZ a well developed convection is observed which brings about heavy showers and thunderstorms. Further south the amount and thickness of cloud cover abates and only separate short showers occur (Fig. 5.5).

The asymmetrical distribution of cloudiness and rainfall with respect to the ITCZ is noted where the surface position of the ITCZ traces several degrees latitude north of the geographical equator. The fact of the asymmetry has not been universally accepted. Most researchers of the tropical

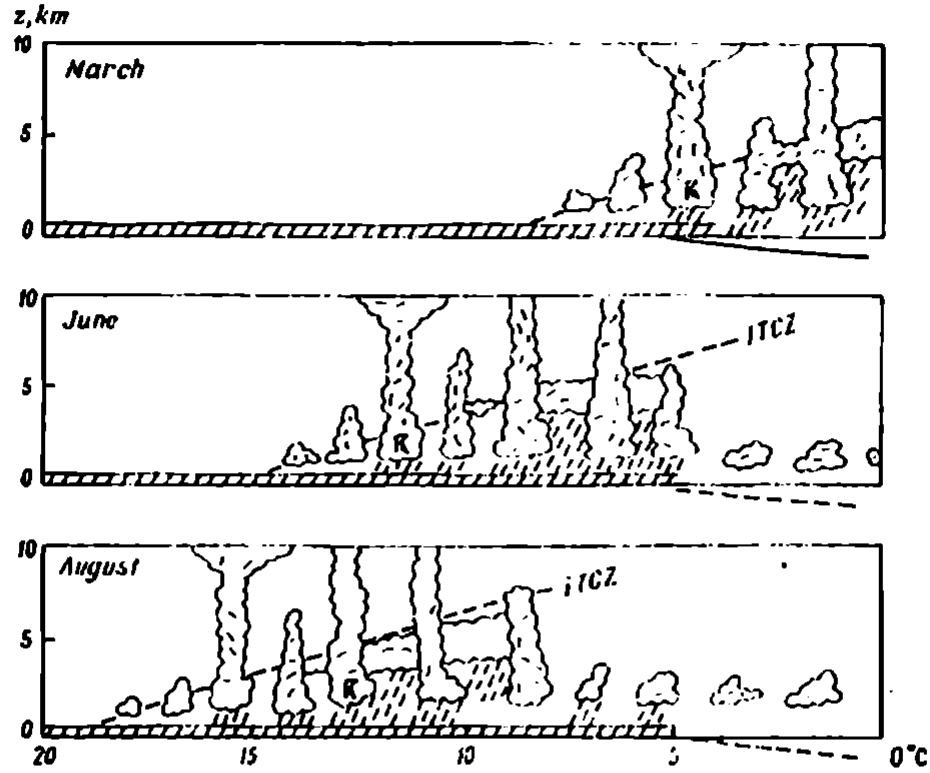

Fig. 5.5 Schematic meridional cross-section through the ITCZ in West Africa (continental massive hatched). (After Flohn)

atmosphere believe that more substantial convergence to the south of the ITCZ may be explained by the variation of the Coriolis force with latitude, the so-called β-effect, which in this case is essentially as follows. When the ITCZ situates south of the geographical equator, the south trades abruptly change the direction upon crossing the equator since at the equator the Coriolis force changes sign. Thus, south of the main position of the ITCZ forms the secondary convergence zone (Fig. 5.6).

An additional factor acting toward the asymmetry is the placement north of the ITCZ of more stably stratified air in the trades over the oceans and drier air over arid land areas.

The asymmetry is not a sole feature of cloudiness and rain distribution in the ITCZ. When the ITCZ places near

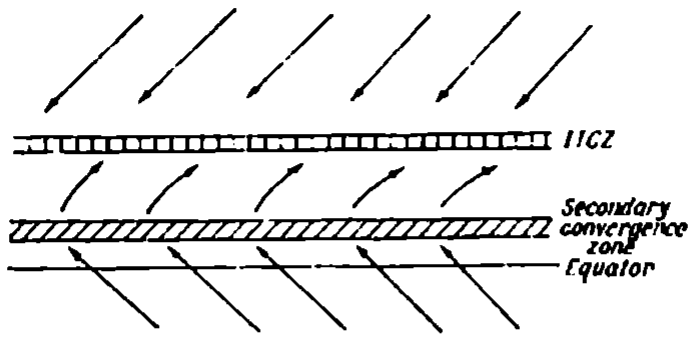

Fig. 5.6 Stream model in the formation of the secondary convergence zone

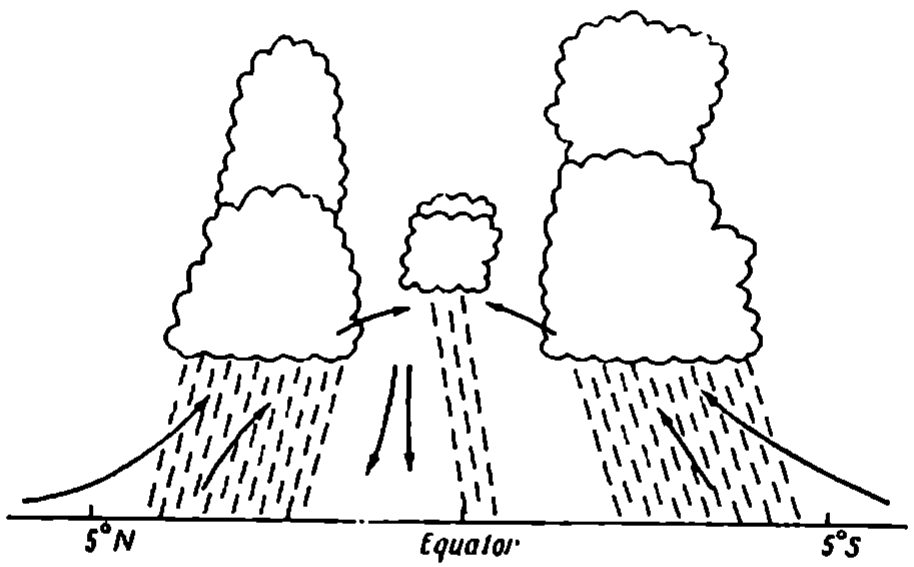

Fig. 5.7 Meridional cross-section through the ITCZ situated at the geographic equator (after Fletcher)

the equator it divides into three zones, two outer and one inner. The outer zones experience strong convergence producing thick cloud cover and substantial rain. The inner zone, called at times a center zone, has only weak convergence occurring in separate "islands", which results sometimes in westerly winds. Considerable instability of air even with weak convergence brings about clouds and slight precipitation (Fig. 5.7).

However, most of all the central zone experiences light variable winds, hence the navigator's name for the area—

the doldrums. When the central zone is predominantly swept by easterly winds downdraft movements may form over the ITCZ making it more diffuse and improving the weather.

5.3. The Trade Winds

The strong steady winds blowing in the lower troposphere between the subtropical high pressure belts and the equatorial trough have come to be known as the trade winds, or trades. Broadly speaking, they blow from ENE in the Northern Hemisphere and from ESE in the Southern Hemisphere. The trades occupy the bulk of the tropics, in two belts from 20° longitude in the winter and 30° longitude in the summer hemisphere to the equatorial trough. More than a third of the earth's surface comes under the influence of the trades any time of the year.

The trades are best developed over the eastern parts of the oceans: winds of other directions are often observed over the continents and western portions of the oceans.

Three clear-cut layers can be distinguished in the trades.

1. The layer of the lower trades, whose elevation near the subtropical highs is 500 m. It elevates even more equatorward, being up to 2500 m at the equatorial trough margin (see also Sec. 2.3). The air masses of the lower trades are commonly moist, their temperature follows that of oceanic surface, so that in general it increases equatorward.

2. The trade inversion layer which overlays the lower trades. Further into low latitudes the trade inversion gains in thickness (from several hundred meters to one kilometer) and in height (from several hundred meters to two kilometers) (Fig. 5.8.), while temperature difference between its top and bottom diminishes. The strongest inversions are observed over the eastern portions of the oceans in winter. At times several layers of inversion can be observed (see Sec. 2.1).

3. The layer of upper trades capping the inversion. The upper trades are easterlies, more weak than the lower trades. They blow at 6 km altitude in the average in the subtropical high pressure belt and about at 10 km height at the edge of the equatorial trough. Air in the upper trades is on the

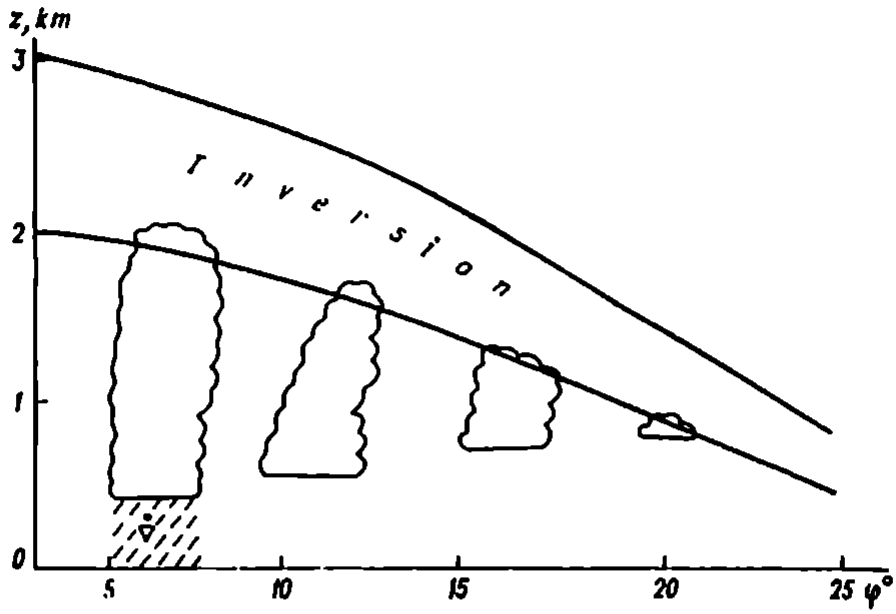

Fig. 5.8 Modelling a meridional cross-section through the trades (after Niewolt)

whole more stable and dry than air in the lower trades.

Discuss in short the sources that give birth to the trades. As we have already noted, the main driving force of air transports in the tropics is the stable temperature gradient that oxists between the hot equatorial belt and the colder regions of subtropics. At the surface this temperature gradient results in high pressure in the subtropics and low pressure at the equator. It is this gradient that produces easterly winds having a small equatorward component, that is, the trades. This viewpoint is supported by the following facts.

(a) More significant wind speeds at the surface as compared with that of winds aloft.

(b) Steadiness of the low trades.

(c) Change of speed and direction by the trades with variation in intensity by subtropical anticyclones.

The trade inversion is explained by subsidence heating of air as it sinks in the area of subtropical anticyclones, which is followed by cooling of its lower layers by the cold

water surface or cold land surface in winter. It is the reason why inversions are better developed over the eastern portions of the oceans where cold streams predominate.

5.4 Antitrades

The classical theory of the Hadley circulation call used the term 'antitrades' to denote the outflow of air from low latitudes in the upper troposphere. On the equator side of the cell these flows situate at 8-12 km height. Away from the equator, they gradually descend to be 4-6 km high at 25-30° latitude. The Coriolis force here is more strong, so that it makes them deflect to become not westerly and geostrophic.

The name 'antitrades' appears misleading for it implies that the winds should be similar in their character to the trades. However the available aerological data indicate that the continuous and regular antitrades are nonexistent. Moreover, constant pressure charts supply evidence of frequent nonexistence of the geopotential gradient that could effect in antitrades at 200 and 300 mb between the equator and about 20° latitudes. Numerous observations bring no support to the idea that poleward or eastward movements should exist at these levels in the belts of 0-20° latitude. At any case, winds of other direction are more frequent there.

The air motions at upper levels are subject to strong seasonal variations. The air streams at various longitudes are known to be markedly different, too. The air streams correspond to the old model of continuous and regular antitrades best of all over the western portions of the oceans, especially in the Southern Hemisphere in the cold half of the year. No regularity at all has been observed over the continents.

A real pattern of the air streams most frequently traceable in the upper troposphere can be visualized as follows. The subtropical jet with strong westerly winds at the 200 mb level is found at 25-30° latitude of the Southern Hemisphere all throughout the year. The corresponding jet stream in the Northern Hemisphere is observed at 30-35° latitude in winter only. In summer it gives way to the strong tropi-

cal easterly jet over Africa and Asia at around 10° latitude. The tropical jet of the Southern Hemisphere at 200 mb meanders also in summer (January) between 10° and 20° latitude over Africa, South America and Australia. From all said it is evident that the real air streams of the upper troposphere are very dissimilar to the antitrades in most part of the tropics.

But where the winds, which are naturally alike to the antitrades, are still observed, they keep their meridional component intact only to latitudes 16-20°. In higher latitudes no sign of air shifting to the poles is found in the upper troposphere.

5.5 Low-latitude Disturbances

The circulation systems as found on the tropical weather charts are notably weaker than their counterparts in middle and higher latitudes (the only exclusion are tropical cyclones). To effect weather prognoses from synoptic data the forecaster should rapidly and reliably discern these systems and track their movement and development.

In many tropical regions the seasonal and diurnal weather variations are very clear-cut in the respective time frames, i.e. recur in regular cycles, so that it would be a correct practice to compile forecasting reports basing on these regular changes. These cycles are not ideal though and at times substantial deviations are observed which could hardly be explained by some local effects. These departures expand over large areas and last considerably long. Their reign smoothes all the seasonal and diurnal oscillations. A cause for these deviations of the normal march of weather lies in appearance of tropical disturbances we have mentioned above.

The disturbances of a main stream cause circulation systems of synoptic scale. They have various shape, intensity, and length of life cycle. We shall call these disturbances the synoptic objects of the low latitudes and in the following discuss their classification.

The synoptic objects of the low latitudes may be classed according to various parameters, viz. geographical loca-

tion, shape, intensity, etc. Another approach is to divide them according to a group of the intrinsic features. On this way all the synoptic objects may be joined into two large groups: (1) those which are met in most regions, though somewhat differ from each other in intensity, shape, and some other features of lesser importance; an example may be tropical cyclones; (2) those which are observed in one or two regions, and, if in many, then markedly differ in the characteristics from each other; an example may be supplied by the disturbance lines. The last group also includes the objects that cannot always be discerned on charts, say cloud clusters.

In operational forecasting, synoptic objects can be better discerned from each other according as they are represented on weather charts, i.e. by their geometry.

Part of the synoptic objects is well discernible on weather charts or, at least under certain circumstances, these objects can be evaluated and followed in the further development. They may conveniently be divided in three large groups according to their geometry:

(1) vortices;
(2) wave disturbances;
(3) linear systems.

It should be kept in mind that the disturbances originated under the influence of the same physical processes may acquire various geometric forms, and conversely the disturbances originated by the different processes can evolve into similar geometry.

1. Vortices (closed circulations).

Cyclones. Tropical cyclones can be easily discerned on weather charts, yet it does not mean that their nature is explicitly known. In the following we shall employ the term 'tropical cyclone' in the general sense to denote any cyclonic vortex in the tropical troposphere. The tropical cyclones have already been studied for a long time. The word 'cyclone' was introduced in meteorology in study of tropical storms. First attempts to class the tropical cyclones use their intensity as a classification parameter with maximal wind speed as a measure of the intensity. In the classification that will be discussed here we shall employ not only the intensity of cyclones but also the

differences in their structure and in the physical processes that take place within the active area of the cyclones. From this viewpoint the cyclones may be divided into two classes. The first class is to include the cyclones whose intensity is largest at the earth's surface but diminishes with height (low-level cyclones); the second class is to include those cyclones of low intensity in low levels but intensifying aloft (high level, "distal" cyclones). The first have warm core, the second have it cold. Each class represents broad spectra of size and intensity.

Low-level cyclones vary in intensity very widely, from small eddies to severe hurricanes and typhoons. Their origin is at present believed to be related to the intensifying of synoptic disturbances in the equatorial trough. They might, however, form by transformation of cold-core cyclones. Latent heat of condensation evolved in convection is a major source of formation and support of warm-core cyclones over their life cycle. The cyclones travel predominantly westward with a slight shift poleward (see Chap. 6).

The high-level cyclones also vary in intensity. Some of them may originate in the middle latitudes and then drift to the tropics yet there are such that occur in the low latitude troposphere, that is, are essentially of tropical origin. At this stage they cannot be traced as vortices lower than 6-8 km. Beneath only a weak wavelike disturbance can be found.

The distal cyclones are related to vast fields of upper and mid-cloudiness. Characteristic of them is the convection that is slightly more intense than normal. Their intensifying may give rise to a vortex (closed circulation) at the surface (the intensifying is accompanied by a substantial increase in convection). At the final stage of the development the high level cyclone warms in the core, again perhaps due to convection, to become a warm-core cyclone, that is ranging to a first class.

High-level cyclones normally move slowly and erratically. Not infrequently they remain quasi-stationary for several days. In the summer hemisphere they travel often westward and seldom eastward, a reverse directional pattern is observed in the winter hemisphere. The meridional component of their movement more often points poleward and seldom equatorward.

At times the vortices are found that exhibit the features characteristic of both first and second class. The vortices move in the mid-troposphere and are governed by the distributions in the basic current. If, for example, easterlies dominate in the low levels and westerlies aloft, then in the layer where the streams change sign (in the mid-troposphere) they result in a closed vortex.

It is noteworthy that the vertical profile of the disturbance can be evaluated only by way of computation.

Motion and evolution of a tropical cyclone can be followed when it is in the surveillance area of either a network of stations or satellites. An approaching cyclone can be decided by the cloudiness, wind, and pressure tendencies. The problem of cyclone movement forecasting is, however, far from its solution because the trajectories are very sophisticated in their nature.

Anticyclones. The anticyclonic disturbances have low intensity in the tropics. Relative vorticity in the anticyclones is seldom above the Coriolis parameter in value. Similar to the cyclones, the tropical anticyclones can be divided in two classes so that the anticyclones of highest intensity at the surface and vanishing aloft belong to the first class (low-level anticyclones), and those of highest intensity aloft to the second (high-level anticyclones).

The high-level anticyclones most often appear in the summer hemisphere and are seldom found below 5-7 km altitude. They acquire the warm core in the result of two processes, air subsidence in the central part (adiabatic heating) and convection (heating due to the evolving latent heat of condensation). Accordingly, the high-level anticyclones may be further subdivided into dynamic and thermal.

Each subclass of the anticyclones may be characterized by its representative weather. With the dynamic anticyclones, the mid and high cloud decks are entirely absent. The only clouds in view are a few cumuli which owe their occurrence to suppressed convection accompanying such anticyclones. The thermal anticyclones are accompanied by strong convection and the related clouds build up of mid and upper decks, appearing as the result of transformation of cumuloformi.

Low-level anticyclones are in evidence mainly in the summer of the Northern Hemisphere in the regions where the equatorial trough departs off the equator more than 10° latitude. They are sometimes found in the western Pacific north of the equator and in the tropical North Atlantic and over West Africa.

Low-level anticyclones cannot be traced already at the 500-mb chart. They progress predominantly westward. The intrinsic convection may be classed as more than moderate.

2. **Wavelike disturbances.** Two types of wavelike disturbances in the tropics have received a most profound examination—waves in the easterlies of the Caribbean and equatorial waves over the Pacific Ocean. There is reason to believe that those are not different phenomena, rather, the manifestations of one and the same process of wavelike disturbances in the easterlies. Simply, they are observed at various latitudes in the basic stream that has essentially different characteristics there.

Easterly waves. These wavelike disturbances occur at the equatorial side of the subtropical belt of high pressure; they are weak at the surface but better developed aloft. It was not until an ample aerological information had been collected that the waves became evident. They are a phenomenon common of the middle troposphere although they offer a certain impact on the weather in the region where they emerge. They are associated with certain cloudiness, and precipitation, and certain changes in pressure and, in some degree, wind at the earth's surface. The wave proper is the disturbance of wind field (Fig. 5.9). Not infrequently these waves give birth to tropical cyclones.

First studies of easterly waves were conducted with data from the network of stations established in the Caribbean during the Second World War. These stations were mainly reporting wind observations in the area. Still prior these stations to appear in the Caribbean, there had been found a fairly definite drift of the isallobaric centers at the surface along the lines gradually sloping from east to west. Observations aloft indicated that the isallobaric centers at the surface move in phase with westward progressing wavelike oscillations in the basic eastern current. Time sections made evident that when a wave travels across a location it

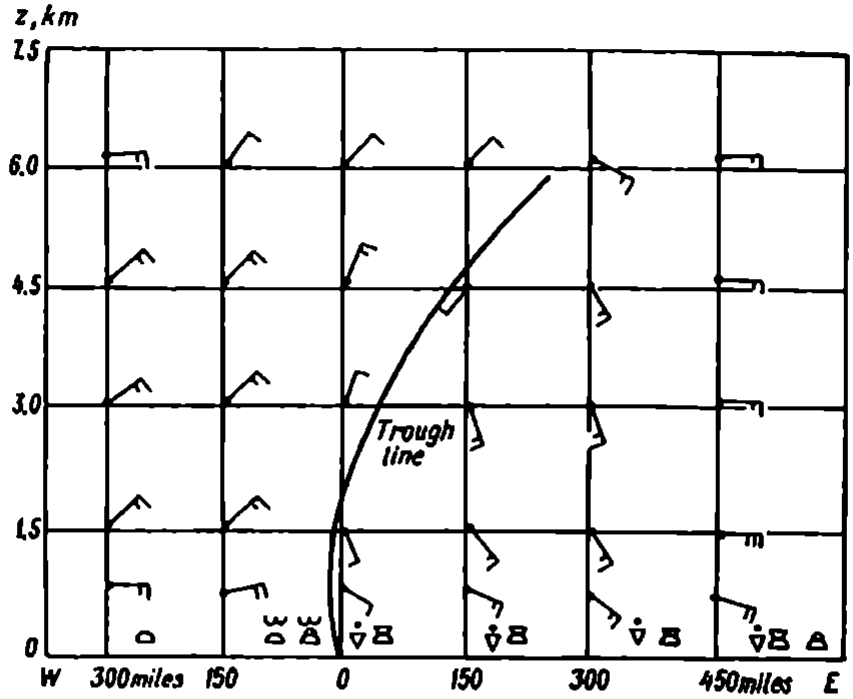

Fig. 5.9 Model of waves in the easterlies: wind and weather in vertical section

experiences two ridges and one trough. The average rate of propagation for the easterly waves is 20-25 km/hr, their mean wave length is about 15° longitude.

In the majority of situations, ahead of a wave divergence is present in the lower layers and convergence aloft so that air sinks and the associated convection is of 'suppressed' variety. To the rear of a wave, convergence is observed in lower layers and divergence aloft, the conditions that favour penetrating convection with associated heavy showers and thunderstorms. Similar weather pattern is evident when the high-level wind field is nondivergent. It is only in rare occasions that a converse distribution of divergence is observed, i.e. low-level convergence in the front and low-level divergence to the rear of a wave.

The distribution of divergence in these waves can be explained as follows. Assume that a wave is in a steady state and travels at some constant speed C. We will discuss

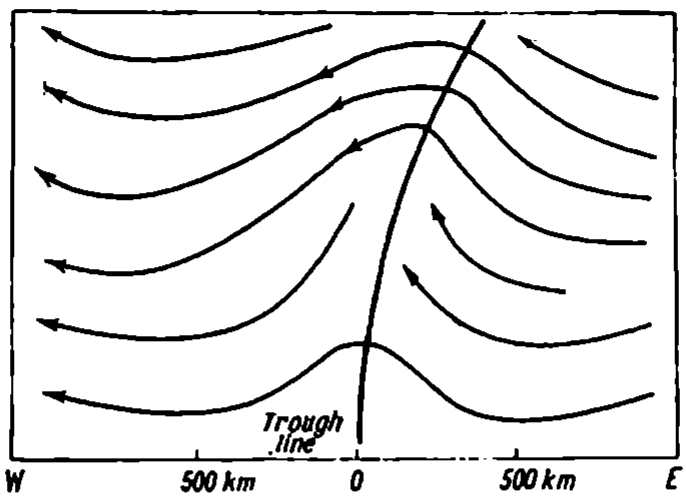

Fig. 5.10 Streamline model of a wave in the easterlies at 850 mb

a system of the 850-mb streamlines of the westerly wave with reference to a model of Fig. 5.10. Assume that the wave is sinusoidal. The meridional displacement of air particles on the right (eastern) part of the wave is directed northward, that is toward the greater values of the Coriolis parameter.

According to observations, air particles in the lower layers often move faster than the wave. With height their velocity, V, becomes slower to equal that of the wave ($V = C$) at around 6 km altitude and becomes even slower than the wave motion ($V < C$) on further ascent. This is what we shall call the normal distribution of wind, or basic current (curve V_1 in Fig. 5.11). In some circumstances a reverse distribution of basic current with height may be found (curve V_2 in Fig. 5.11). Assume that air moves faster than the wave. Then, catching up with the trough line, air inflows into an area of increasing cyclonic curvature (see Fig. 5.10) (near to the trough line the curvature is more substantial than where the air is flowing from). Recalling the expression for relative vorticity in the natural coordinates (R = radius of curvature)

$$\zeta = \frac{V}{R} - \frac{\partial V}{\partial n} \qquad (5.5.1)$$

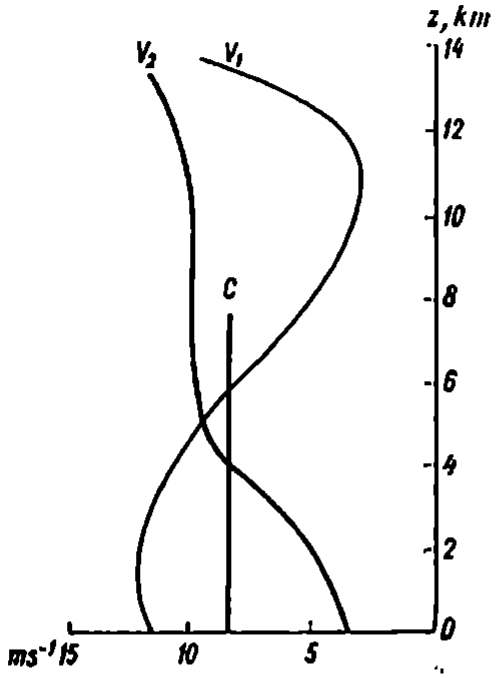

Fig. 5.11 Variation of basic current, V_1 ("normal" vertical profile for an easterly wave) and V_2 (reverse profile), relative to wave speed C

and allowing for the smallness of $\partial V/\partial n$ (see Fig. 5.10) we may safely say that the relative vorticity is mainly determined by the streamline curvature. Hence, in a basic current overtaking the trough, relative vorticity must increase downstream.

For the sake of the consideration we employ an absolute vorticity equation

$$\dot{\eta} = -\eta D \qquad (5.5.2)$$

where $\eta = (\zeta + f)$ is the absolute vorticity, positive in the Northern Hemisphere, and D is the divergence.

With reference to Fig. 5.10, when $\eta > 0$ then the equation (5.5.2) predicts $D < 0$, that is a convergence occurs upstream of the trough. A similar argument is capable of convincing that a divergence occurs to the left, i.e. downstream of the trough.

Consider now the situation that the velocity of the basic current is slower than that of the wave. Both ridges and trough overtake, as it were, the air west of them. In the process, an air column ahead of the trough approaches it and displaces obtaining a southern component (Fig. 5.12)

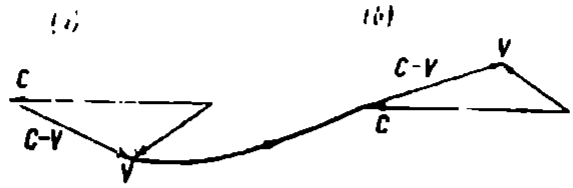

Fig. 5.12 Schematic motion of air mass in an easterly wave for $C > V$ (*a*) ahead and (*b*) to the rear of a trough

while a column in the upstream falls further back off the trough line and shifts acquiring a northern component. In approaching the trough line the air column gains its relative vorticity, but as it displaces southward where the Coriolis parameter is lower, the quantities f and ζ may balance each other. Then $\dot{\eta} \approx 0$. The air column in the rear of the trough moves northward where f for it increases but ζ decreases. Hence, there the quantities f and ζ may mutually compensate their changes as well. The absolute vorticity thus remains unchanged. The waves in the circumstances become nondivergent.

It may, however, happen so that the quantities f and ζ can no longer change in balance. If ζ changes faster than f, then with the vertical wind profile obeying a normal pattern the air ahead of wave will converge aloft and in the rear diverge.

Waves in the equatorial easterlies. In the years of atomic bomb tests the United States provided detailed observations of the upper air over a limited area around the Marshall Islands for periods ranging from weeks to months. These data have enabled Palmer to make intensive analyses of weather in the central equatorial Pacific and reveal waves similar to those in the easterlies. As they pose near the equator they were labelled equatorial waves. Although comparable in their properties to the easterly waves in the Caribbean, the equatorial waves have some individual features.

In accordance with the properties of the basic current we shall distinguish between the two types of equatorial wave: (1) wave motion in a nondivergent easterly current, and (2) wave motion in a convergent easterly current.

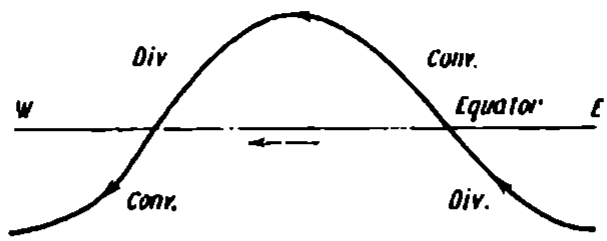

Fig. 5.13 Divergence and convergence at an equatorial wave

Waves of the first type appear in an easterly current moving at a speed of not higher than 2.5 m s^{-1} at the equator and linearly accelerating both northward and southward so that at around 15° latitude it may propagate at 10 m s^{-1}. In an initially undisturbed current the streamlines and isotachs are parallel. Wave motions in such a current propagate slower than the air of the stream, the phases of the trajectories and streamlines coinciding. In the foregoing discussion we shall conveniently call 'forepart' the part of the waves where air moves having some southward component and 'rear' the part with some northward component (by analogy to easterly waves). Accordingly, the foremost portion of the waves in the Northern Hemisphere will diverge and in the Southern Hemisphere converge; in the rear part of the waves air will converge in the Northern and diverge in the Southern Hemisphere (Fig. 5.13).

Waves of the second type occur in the easterly current whose speed at the equator is also not above 2.5 m s^{-1}, yet it increases poleward not necessarily in a linear fashion. Besides, the streamlines ran not parallel to each other and come closer together equatorward; isotachs are not parallel as well. A common pattern for the current is with a train of waves having small amplitudes, the wave of largest amplitude and shortest wave length placing farthest west. Eastward the amplitude in the train gradually decreases and wave length increases. The divergence field has a more complicated nature. The centers of divergence and convergence in the easternmost wave situate far from the equator (at 10-15° latitute) in both hemispheres. Farther west the centers come closer, so that the convergence increases and the divergence decreases in intensity. The waves travel at about the same speed as the easterly waves in the Carib-

boan, the amplitude of the former being markedly lower, in the average.

The disturbance in wind field connected with the equatorial waves is normally rather small so that it cannot be evaluated on synoptic charts.

Still another condition related to the equatorial waves is noteworthy, namely, since these waves coincide with the equator their crests and troughs can be on either side of it, consequently either ridges or troughs may represent a common circulation, say cyclonic one.

Induced waves. Wavelike disturbances in the easterly currents moving in the mid-troposphere may be induced by disturbances of the higher troposphere. One example of such influence we have already discussed when mentioning that a high-level cyclone does not often sink to the ground, in contrast to a vortex, yet its presence is marked by a cyclonic wave in the low-level easterly current. This type of waves is mostly characteristic of the summer hemisphere. Similar phenomena are often noted in the winter hemisphere, too, but here they are found below the troughs in the upper troposphere westerlies which overlie the low-level easterly current. This type of waves has been suggested to be labelled the 'polar trough'.

The induced waves in the easterlies are not unlikely to the easterly waves in their size and introduced weather. However they differ most substantially in that how erratically they travel, a contrast to the net westward advance of the easterly waves. Induced waves travel in accordance with the displacement of the upper-level cyclone or trough in the westerly current, which may slightly shift eastward, stagnate, or shift a little to the west. Surface data give no evidence to the movement of these waves.

The waves of anticyclonic type induced by the upper-level anticyclone are observed much more seldom.

Tropical waves. These waves are the wavelike disturbances that occur in the high-level currents over West Africa. They give rise to unstable weather with precipitation due to unstable stratification and convergence. The unstable stratification and convergence are believed to be induced by a trough in the upper stream which forms in a wave developing in a cold front of extratropical latitudes. These

disturbances even when close to the equator progress from west to east. In their dimensions they are comparable to small troughs or cyclones of the middle latitudes; their travel is slow. A substantial part of the equatorial West Africa comes commonly under their influence for as long as 3 days.

3. **Linear systems.** Under this category come a variety of synoptic systems whose vorticity or divergence, or both, has a tendency to concentrate along a line, or zone, whose length by far exceeds its width. Most often in these zones cyclonic vorticity is accompanied by convergence, and anticyclonic vorticity by divergence.

Lines of disturbance. These lines are often connected to squalls and other instability phenomena which travel from east to west over West Africa. Upper air data give practically no evidence to the disturbances either in wind or pressure field. On surface charts they resemble mid-latitude instability lines. To effect preventive or avoidance means in a case of dangerous weather the lines are required to be evaluated as early as practicable. So far, however, data on these systems, their evolution and travel are very sparse. Hence it is a hard task to prognose the intensity, time and location of the related squalls and thunderstorms. On the disadvantage side also is an absent rating on these systems according to life cycle, direction of travel and intensity.

Intrusion of cold fronts to the tropics. Cold fronts of higher latitudes penetrate at times the subtropical high pressure. More frequently it happens where one of the high pressure outskirts is developed stronger than the trailing anticyclone situated farther east. At the equatorial side of the high pressure belt cold fronts can be taken into eastern circulation and remain there for a long time.

A frontal zone of the type gives birth to the trains of more or less continuous clouds having as a rule a shallow depth. There can occur shower rains and even widespread rains, but in narrow lines. Wind slightly changes its direction here, and pressure undergoes a troughlike variation, though in time this behaviour is often masked by an overlapping diurnal pressure wave.

These systems cause short periods of bad weather in coastal area (exposed to wind). They cannot intrude far inland, at

least they fail to be traced over the continent because they are at once outweighed by the strong overlapping effect of convection and orography.

Atmospheric soundings performed to study the thermal structure of the systems indicated that there is no marked temperature and humidity contrast. In contrast to the easterly waves for example, they are observed in the lower troposphere so that the upper part of a front is commonly cut off by the westerlies prior than the whole system penetrates in low latitudes. In the tropics these cutoff portions, i.e. upper troughs, become obvious only at the boundary with the subtropics, particularly in northern India, South China and, to a lesser extent, in the Caribbean and North Africa. Sometimes they also can favour the formation of troughs in the equatorial streams, but this matter was already discussed.

Polar air subsides on penetrating the subtropical high and getting low obtains a sensible heat from the underlying surface so that the fronts it produces are normally very weak and said to be of residual nature. At times, however, a large mass of polar air intrudes rather far, exporting all the characteristics of a normal cold front of middle latitudes into the equatorial region. These phenomena are characteristic of the winter hemisphere.

Shear lines. When a polar front extends to the tropics the density break almost vanishes due to air subsidence and consumption of heat from the underlying surface. What remains of the front is a wind shear. The lines along which the break of horizontal wind is observed became known as shear lines. This essentially refers only to the areas of cyclonic shear, that is to what rests of the front.

The areas of anticyclonic shear are rarely met and are of no interest from the synoptic viewpoint.

Two situations around shear lines can be met. In one the line separates two streams of opposite direction (Fig. 5.14*a*), in the other two streams in the same direction but having different velocities (Fig. 5.14*b*).

Lines of the first type can often be observed in the upper troposphere between warm anticyclones in summer. Air around the lines is as a rule cooler than that in the surrounding regions. This might be caused by ascending motions.

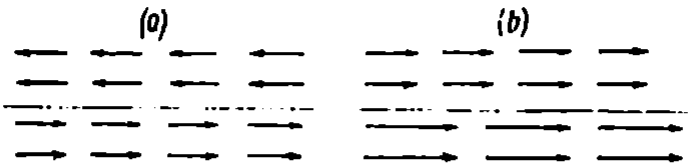

Fig. 5.14 Wind shear of first (*a*) and second (*b*) type

These motions give rise to vast decks of mid and upper cloudiness; at times they are accompanied by considerable convection. A similar pattern can emerge also in the low troposphere on the outskirts of the equatorial trough when it displaces far to the north.

The second situation is met very seldom; in the literature the phenomenon is only mentioned without any detail.

We would like to note also that from the vorticity equation (5.5.2) divergence varies inverse as the shear (5.5.1) and in direct proportion to its rate of change. For a quasi-linear flow a constant shear corresponds to $D = 0$ and does not induce weather change. When shear varies with time, even small values of shear cause considerable divergence (convergence) and, thus, change of weather.

5.6 Monsoons

Over vast oceanic areas the seasonal variations of tropical circulation display themselves only as small latitudinal shifts and narrow meandering or circulation components in intensity; the general character of the circulation remains the same throughout the year. Another pattern is found over the tropical continents and adjacent seas where circulation varies substantially and in distinct seasonal periodicity. The role played by the continents is in that they bring about more pronounced seasonal temperature variations than the oceans. Whereas the oceans absorb and accumulate heat to transfer it subsequently toward higher latitudes by currents, the continents exert their action in another way: they warm quickly at the surface and then slowly transfer heat into the adjoining air, by a mechanism well described in the books on basic

and dynamic meteorology. In the summer months an immense flux of solar energy strikes the belt of 15-25° latitude so that the surface and adjacent air warm to very high temperatures. This warming in the early summer produces over the continents between above latitudes thermal depressions which gradually take on some functions of the equatorial trough, thus forming a new region of convergence. In the circumstances, the trough at the equator changes its structure and becomes less intensive. The trades of the winter hemisphere lower their pace crossing the equator and form the secondary convergence zone (see Sec. 5.2), after which air accelerates toward the low pressure area over the continents.

In winter this latitudinal belt experiences comparably low temperatures. This raises pressure at the ground and resumes winds, analogous to the trades, though these winds cannot be as stable in both speed and direction.

Consequently, the tropical continents and the adjacent oceans evidence the semiannual change of winds. In some areas this variation takes a very distinct form. The winds whose seasonal overturn is clear-cut and the directional change exceeds a certain minimal angle are commonly called *monsoons*. From the variety of definitions a most explicit to our opinion is that uttered by S. P. Khromov: 'The monsoon is a macro-scale pattern of air flows over a considerable part of the earth's surface, which is notorious for high frequency of a single prevailing wind during a season, either winter or summer, with this direction changing to the opposite, or close to it, in coming from one season to the other'.

Figure 5.15 illustrates the regions of the globe where monsoons exert their influence. These areas are inhabited by more than a half of the globe population mainly involved with the agricultural activity. The monsoon for them is not just a seasonal weather change, rather it is a source of life and prosperity.

The classic theory of monsoons puts the thermal conditions into the forefront as being of major importance for their genesis. The most general features of monsoon circulation can more or less satisfactorily be explained in this framework. However, monsoons do not develop equally

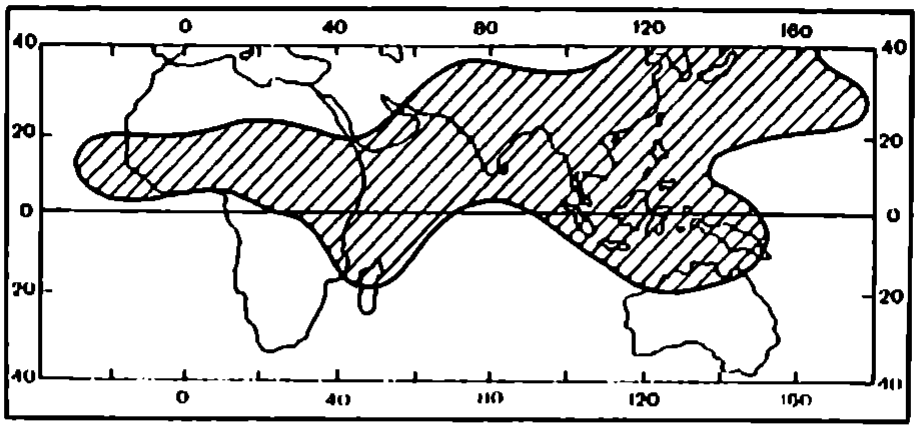

Fig. 5.15 Area of monsoon circulation (after Ramage)

overywhero. Their development is influenced by the shape of the continents, orography, and the conditions for circulation in the upper troposphere. Therefore a monsoon study presupposes the regional approach.

Let us consider the monsoons that are most pronounced, the Asiatic and the African.

Asiatic monsoon. Asia is the largest mainland on the earth. It is washed by the Pacific from the east and the southeast and by the Indian Ocean from the south. From south and southeast it is surrounded by a multitude of small and large islands. The tropical zone of Asia has the conditions for the circulation to develop with predominant winds of one direction in winter and almost opposite winds in summer. The seasonal variations of stable circulation (monsoons) are well pronounced over the huge territories from Pakistan on the west to Japan on the east (Figs. 5.15 and 5.16). The genesis and development of the Asiatic monsoon is facilitated by the tall and vast mountainous area, Tibet, stretching from west to east. Tibet serves the natural dividing screen between the tropical and polar air masses.

In the Northern Hemisphere winter, the northern part of Asian continent is the region where a vast system of high pressure forms having a large intensity and centered between 40 and 60°N; this phenomenon is known as the Siberian anticyclone. The radiational cooling appreciably lowers the

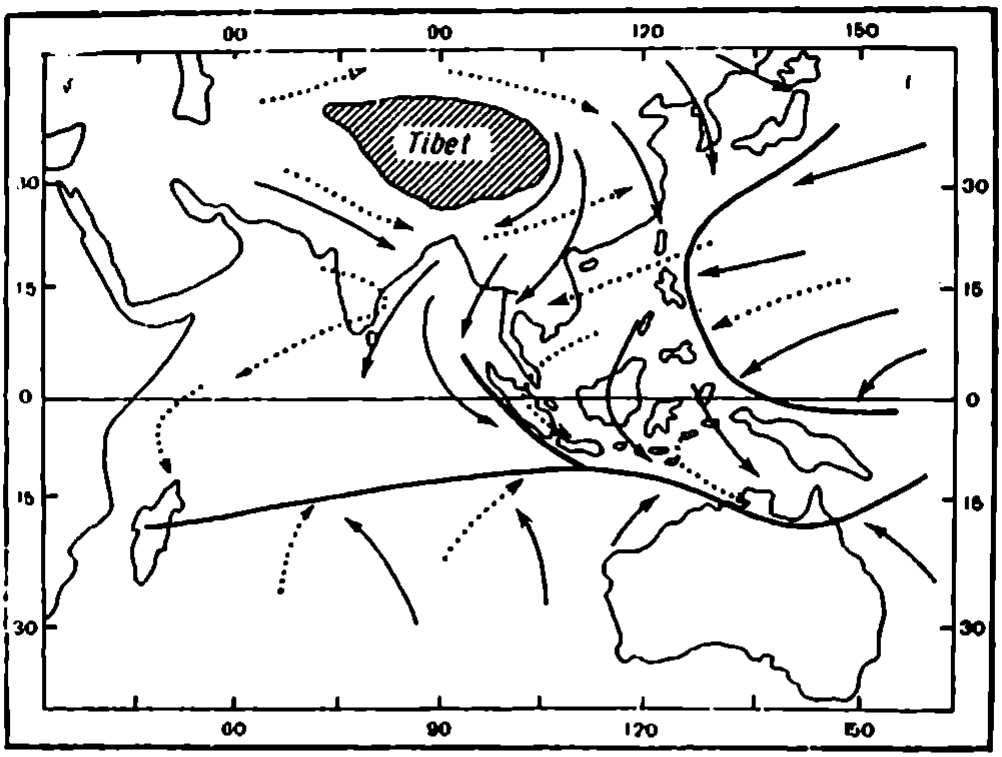

Fig. 5.16 Winter Asiatic monsoon: surface winds (*solid*), 700-mb winds (*dotted*), and the ITCZ (*heavy*)

temperature thus supporting the anticyclone during a long time. The outflow of air from the anticyclone proceeds through Korea, China, and Japan. The outflowing masses converge with the northeastern streams from the Pacific over the South China Sea at 15-20°N; this convergence often results in fronts since the continental air mass appears as a rule much cooler than the air from the Pacific. The two air streams gradually merge, progressing southwest where they form the northwestern monsoon of Malaysia. Having crossed the equator over Indonesia they turn into the westerlies advancing to the ITCZ placed at the time 10-15° latitude south of the equator over Northern Australia (Fig. 5.16). This figure clearly indicates the difference of wind at the surface and at 700 mb over the southeastern part of the continent of Asia, thus substantiating that the winter Asiatic monsoon is constrained in a shallow layer of atmo-

sphere when close to the region of its occurrence. This is another proof of its thermal origin.

The 700-mb winds are westerlies over the most part of the Asian continent. They circle the Tibet-Himalayas high plateau along its both southern and northern borders, though the main portion of the stream passes south of the mountains. At the eastern side of mountains both branches reunite into one stream which reaches Japan. Farther south where the winter monsoon merges the north Pacific trades it extends the 700-mb level. It is interesting to note that the winter Asiatic monsoon seldom extends over northern India. Here, westerlies prevail both at the surface and aloft. The natural mountainous barrier of the Tibet-Himalayas plateau seals the mid-latitude air off India. Southern India (south of 30°N) also experiences no influence of the winter monsoon, but in this area the monsoon is rather weak and transports air of extrapolar origin. Therefore in India the term 'monsoon' applies to the summer winds and especially in connection with the coupled rains.

The winter Asiatic monsoon carries cold and stable air from the Siberian anticyclone area. Travelling over the relatively warm ocean this air rapidly transforms acquiring heat and moisture from the oceanic surface. Over the South China Sea the air mass mixes with the warm stable masses coming from the Pacific. This results in an entirely new air mass exhibiting all the properties of warm maritime air and in this resembling the air of the trades. At times even inversion may be found there. Consequently, when this air reaches Indochina and Malaysia it no longer bears any traces of its origin. In its further transforming over Indonesia it assumes all the properties of equatorial air, turning on moist, warm, and unstable.

The appearance and development of the summer monsoon over Asia is a much harder task for explanation. That it is also of a thermal origin is beyond doubt, yet the course of its development in early summer indicates that the thermal depression over the continent may not be the sole cause. The depression situates over northwest India and the monsoon develops first over South China then extends over Burma and only in a month appears over India. In April and May the rains set in generally over South China and

Burma while they are retarded over India so that the temperature rises to extremely high values in May. Then late in May or early in June, roughly within a 3-week span, the monsoon "bursts", often accompanied by violent squalls and small but intense cyclones on its leading edge.

After the first burst which carries the rain roughly to the top of the peninsula, the monsoon advances more gradually toward the Himalayas and northwestern India and Pakistan. In the Indus valley the rainy season may last only a couple of months or less; here the average variability of rainfall from one year to the next is very high. Deviations of the rainfall from the normal course may be as high as 20 to 25 per cent.

The thermal depression forming in early summer is unable to explain why the monsoon is retarded over India as compared with Burma and with other continents of both hemispheres and why it subsequently advances in the spectacular manner that has given rise to the name 'burst'.

One permanent feature that might help to explain the difference between the onset of the monsoon over India and elsewhere is the channelling effect produced by the height and shape of the Himalaya mountains. In winter a considerable portion of the belt westerlies circles the southern rim of the Himalayas. Even at the altitude of 8 km the streamlines follow the contours of the mountains quite well, thus arranging in a channel, as it were. This type of circulation causes a meridional trough in high altitudes over the Bay of Bengal. In the beginning of warm season this trough favours easterly winds to occur aloft over South China and Burma, but not over India which lies west of the trough line. These upper-level easterlies play an important role in arrival of the summer monsoon. They comprise the upper return streams moving toward the equator and thus being a part of a summer circulation over the Asian continent. So far as the westerlies prevail in the high troposphere over India the monsoon will be retarded there.

In summer (end of May-early June) an entirely different picture prevails. The westerlies retreat abruptly to the north of the Tibet mountains, and a continuous north-south trough line extends from westerlies to easterlies near 75°E, just

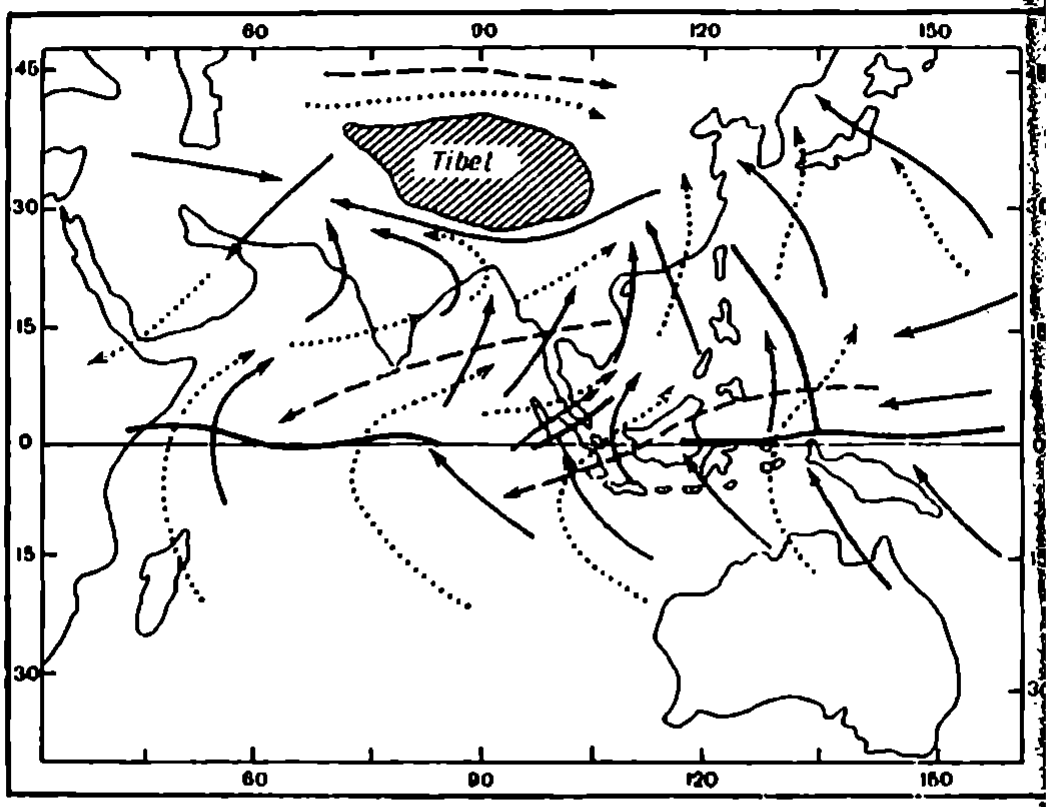

Fig. 5.17 Summer Asiatic monsoon: surface winds (*solid*), 700-mb winds (*dotted*), 500-mb winds (*dashed*), and the ITCZ (*heavy*)

west of the bulk of the mountains. Immediately the westerlies set in over northern India and give way to the summer monsoon in low levels. At this time the monsoon displays its first burst to subsequently cover India and Pakistan and all Southeast Asia (Fig. 5.17).

In the summer monsoon circulation over Asia the easterlies are strongest aloft in the easterly tropical jet. It commonly places at 12-15 km altitude with the axis at about 12° latitude. Wind speeds along the jet center line may reach 60 to 80 m s^{-1}.

The mountains and high plateaus of Central Asia favour the summer monsoon not only by deflecting the upper westerlies northward, but also by comprising an important heat source in the upper troposphere. An intense insolation of the plateau raises the temperature thus extending and

deepening the low pressure over northern India. These favourable conditions make the summer India-Burma monsoon a powerful air stream. In June and July it reaches 6 km height over India, and even 9 km over Burma. Farther east where the mountainous influence is far less the monsoon flows are found in a more shallow layer. Over Japan the monsoon depth is seldom above 2 km.

The summer Asiatic monsoon is in general less stable than the trades in both speed and direction. It often arrives in "pulses"—3 to 10 day periods of intense monsoons alternate with similar spans of weaker streams.

Ample rain comes with the summer Asiatic monsoon. In many areas of South and East Asia the largest rainfall comes for summer. The amount of monsoon precipitation is densely coupled with the properties of air masses entrained in the monsoon flows. These masses form mainly in three regions.

The first of them is in the Indian Ocean west of 100°E and south of the equator. On its way from this region to the equator the air mass covers thousands kilometers over warm oceanic surface and becomes very moist, warm and unstable (Fig. 5.17).

The second region is in the subtropical high over Australia, east of 100°E. In this area air mass is dry and stable. These properties are still evident over Indonesia, yet as the mass travels farther west it turns to more moist and less stable.

The boundary between the two air masses (zone of confluence) is often found over Malaysia being the cause of the ample rainfall. A precise position of the boundary cannot always be traced since in here both streams are already not unlikely in their properties.

The third formation area of the summer Asiatic monsoon is in the Pacific. The branch of the monsoon that is formed here flows across Japan and the northern areas of China. At the place of origin this air mass is moist, warm yet sufficiently stable. Flowing over the warm ocean it rapidly transforms and loses its stability. Its area of confluence with the mass moving from Australia lies east of the Philippines, though can extend as far as south Japan and even Korea.

All the three air masses become moist and unstable after longthy contact with the warm oceanic surface so that they acquire a considerable rain potential. This potential materializes when the air reaches a zone of convergence or is entrained in a tropical disturbance. Rain may also be caused by the influence of orography.

Here it should be emphasized that convergence and disturbances are closely related phenomena which may also come under the influence of orography. It can, for example, initiate convergence which, in turn, gives rise to disturbance. Orography can also reinforce or slacken disturbances and give birth to a new disturbance. On the other side, any disturbance always generates convergence (divergence) of air flows, at least in the lower troposphere. The conditions for convergence and disturbance formation can always be found inside a monsoon stream. Initiating in a monsoon the disturbances travel with its streams causing rains. The chain of events looks as follows: a monsoon carries moist and unstable air which gives rise to disturbances, the updrafts of the disturbances build up clouds and produce rains, coming in contact with the orography these processes intensify. The passing disturbances make the monsoon proceed in pulses. Commonly, heavy rains coupled with disturbances are followed by several days of easy flow.

Extending over vast territory, the Asiatic monsoon exhibits some regional peculiarities. Generally, the winter monsoons are stronger in the eastern territory, whereas the summer monsoons are more intensive in the west. At the southeast of the Asian continent close to the equator the summer and the winter monsoons are of about equal intensity.

African monsoon. The monsoon circulation over Africa and over Asia differ in two essential aspects. Firstly, the African monsoons are far less in area and thickness. Relatively small size of the African monsoon can be explained by the fact that the seasonal displacements of the ITCZ are not as significant in Africa—not more than 15° latitude on the west and around 30° latitude on the east—as in Asia where it amounts to 40° latitude. Secondly, polar air masses do not take part in the formation of monsoons over Africa, therefore summer and winter monsoons differ in

their properties far less in Africa than in Asia. However, the basic characteristic of monsoon, seasonal change of wind direction, exists almost in all regions of tropical Africa.

Monsoons are dissimilar in the west and east parts of Africa. In the west, monsoons of various seasons drastically differ in their properties, since they form in different air masses; in the east monsoons differ in direction only, and the air masses in which the monsoons form are almost alike in the properties.

The above regional differences are mainly caused by the shape of the African continent. On the west, the huge bulk of the continent placed north of the equator represents a pronounced contrast to the marine area of the Bay of Guinea, whereas on the east, the continent equally spans on either side of the equator so that there exists no ground for the above contrast.

The geography of Africa consists mainly of vast high plateaus and mountains; therefore to be more illustrative we shall discuss the circulations as represented at the 850-mb surface.

In the Northern Hemisphere winter when the ITCZ is situated close to the equator, the west regions of Africa come under profound influence of the northeast trades (Fig. 5.18). The NE winds prevailing up to 3 km altitude bring in dusty, cold, stable air formed over deserts. These winds bear a local name 'kharmatan'. But for a narrow south coastal line, the winter season is generally dry in the west regions of Africa.

Owing to high temperatures a heat low occurs in summer at around 20°N. Because of this low the ITCZ slowly shifts northward and in July sets at the surface at about 15°N (Fig. 5.18). As a result the SW winds intrude the continent, and it is this phenomenon that is called monsoon in the area. This monsoon carries warm and moist air formed over the Atlantic. Most part of the rain falls south of the ITCZ (see Sec. 5.2). The monsoon in the west of Africa (occasionally called the West African or Guinea monsoon) is observed in a relatively shallow layer. At 500 mb the ITCZ stays at the equator throughout the year.

In East Africa the influence of the continent is experienced

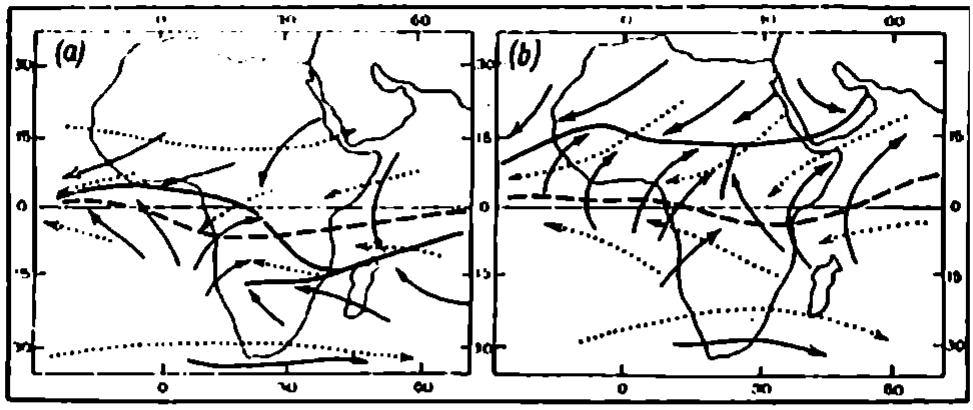

Fig. 5.18 Circulation over Africa in (*a*) January and (*b*) July; 850-mb winds (*solid arrows*), 500-mb winds (*dotted*); 850-mb ITCZ (*heavy*), and 500-mb ITCZ (*dashed*)

on either side of the equator and, as a sequence, the ITCZ shifts northward from the equator in the Northern Hemisphere summer and southward in the Southern Hemisphere summer. In January it is situated around 15°S so that most part of eastern Africa comes under the influence of the NE winds which become NW on crossing the equator. These winds mainly carry the air of continental origin, which does not produce rain over the regions of East Africa.

In July the ITCZ appears at 15°N and air from the Indian Ocean rushes into the eastern areas of Africa. This air is also appreciably dry and cannot aid precipitation (it is believed to dewater on the steep slopes of the Madagascar). Thus, both monsoons are relatively dry, and rains fall only during the intermediate season when the ITCZ traverses the area.

5.7 Interaction Between Motions of Different Scales

Different-scale motions are interrelated in the tropics in much the same manner as in mid latitudes. Through this interaction, energy is transferred between disturbances of different scales making them reinforce or decay.

Small-scale eddy friction at the earth's surface changes the curvature of wind so that favourable motions become the inflow of air to the center of a cyclone (toward the trough line) or the outflow of air from the center of anticyclone (away from the ridge), i.e. widespread fields of divergence (convergence) are created. This results in filling in cyclonic and desintograting anticyclonic disturbances. The process is essentially alike those in mid latitudes.

Observations indicate that in some occasions disturbances in the lower troposphere are overlaid by the upper tropospheric eastorly jet at 200 mb. It assists a large-scale divergence (convergence) to occur there. A. I. Fal'kovich has suggested to term the formation an 'upper boundary layer'.

As follows from GATE observations, the upper boundary layer acts in the opposite to the lower one. Considering the disturbances in the ITCZ we may state their cyclonic behaviour. At the same time an anticyclonic vortex is observed in the upper boundary layer, which favours positive divergence or "mass discharge". In the circumstances, small-scale eddy friction in the bottom layer tends to work in one sense, say to fill a cyclone, whereas in the top layer the tendency is in the other sense, say to deepen the cyclone. The net result of two layers may either conserve the disturbance, or make it gradually evolve. Certainly, the disturbance evolves under the influence of the whole large-scale divergence of the troposphere, formed by the summed action of all-scale perturbations, rather than under the two layers. Nevertheless, the formation of a large-scale divergence and its vortical profile is mainly decided by the upper and lower boundary layers.

Consider the action of large-scale movements. Let a cyclonic disturbance be influenced in a time interval by only a large-scale motion. Then, energy calculations performed by A. I. Fal'kovich on GATE data indicate that the large-scale motions lower potential energy by 1000-1300 J cm^{-2} a day in the disturbance area from sea level to 300 mb, while they enhance it by 400-500 J cm^{-2} a day in the layer 250-100 mb. In other words, the constant pressure surfaces (and, hence, pressure) in the lower troposphere must descend and in the upper troposphere ascend. It implies that the cyclonic disturbance in the lower troposphere and the

capping it anticyclonic disturbance in the upper troposphere must gain in intensity. Therefore, large-scale motions tend to increase vorticity and deepen, or reinforce, disturbances.

Also, large-scale ascending motions tend to increase the total energy content in the 0–3 km layer and decrease it in the upper layers. This brings about instability and convection (see Chap. 3). Consequently, large-scale ascending motions are responsible for creation of convective instability.

Rational cooling acts in the same sense within disturbance. In the mean, the process intensifies with height and thus amplifies convective instability of atmosphere. Its contribution into convective instability makes the flux of eddy-available energy directed from the ocean into the atmosphere.

To sum up, three processes, large-scale ascending motions, radiational cooling within disturbance, and flux of available energy from ocean to atmosphere, create favourable conditions for appearance and development of penetrating convection which compensates the action of large scale motions by transferring energy upwards.

Consider now the action of penetrating convection on large-scale motions. Recalling that tropical disturbances are mainly translated from east to west with a poleward component we assume in the considered disturbance the vertical distribution of energy, the pattern of large-scale motions, and the energy flux from the ocean do not change with time. A balance is achieved when penetrating convection and energy dissipated due to friction compensate the distortions of energy profile caused by large-scale ascending motions. An essential part in offsetting or restoring the balance plays rearrangement of stratification caused by vertical wind shear in the disturbance zone. This phenomenon arosen due to various speeds of motion in different layers of atmosphere in the disturbance zone became known as *ventilation*.

Action of ventilation may be shown as follows. Let the velocity of disturbance be C and that of air V. Let various layers in the disturbance zone move at different speeds, slower than the disturbance, $V < C$, at its pace, $V = C$, or faster, $V > C$. In the slow layers air in the disturbance is continuously renewing, i.e. ventilation due to counter

flow, and in the fast layers disturbances are ventilated by the overtaking flow. The layers of $V = C$ have no ventilation.

Assume that in travelling over ocean a balanced tropical disturbance arrives in an area where the oceanic surface is warmer. There the disturbance can abruptly deepen and a common "harmless" depression can give rise to a hurricane. The higher temperature of the water upsets the balance, raises instability, and intensifies energy flux from ocean to atmosphere, hence, reinforcing saturated adiabatic convection in the disturbance. Now the convection plays the role of an agitator of large-scale motions. First, it increases the depth of the boundary layer (low level eddies extend into higher altitudes, increasing the eddy mixing coefficient) thus reinforcing the large-scale convergence. According to Fal'kovich, not only the lower but also the upper boundary layer increases because strong convection builds up clouds to penetrate into the upper troposphere. Secondly, well-developed penetrating convection makes a significant contribution into formation of a warm core in a disturbance. For example, a cyclone with a cold core turns to the warm-core cyclone under the influence of convection: it transfers energy upwards filling in this way a minimum in the profile of static energy of moist air (see Chap. 3 and Sec. 5.5). This process proceeds the faster the stronger the convection dominates over the effects of ventilation and large-scale motions. The energy flux raises temperatures and humidity, favouring thus warm-core formation of a cyclone and rearrangement of all its structure.

5.8 Heat and Moisture Transport Mechanisms

Consider the sum of enthalpy, potential energy and latent heat, which is called the static energy:

$$E = c_p T + gz + Lq$$

where c_p is the heat capacity at constant pressure, T the absolute temperature, g the acceleration due to gravity, z the height, L the latent heat of vaporization, and q the specific humidity.

The meridional heat transfer in the tropics is effected by large-scale circulations and eddy disturbances (horizontal macro-turbulent exchange). Heat transfer aloft is effected by homogeneous vertical motions, coupled with cyclonic disturbances, and by convective streams. A substantial portion of heat comes to the atmosphere from the underlying surface as latent heat which can be made available to atmosphere through condensation and rainfall. In equatorial latitudes the sum of heat realized through condensation of water vapour and sensible heat receiving from the earth's surface exceedingly outweighs the heat deficit created by outgoing long-wave radiation.

Static energy flux (Table 5.1) is directed from the equator to mid latitudes in both hemispheres. The flux gains in amount as it departs farther from the equator. At the geographic equator the flux is markedly less than at other latitudes (except the thermal equator where it is zero) and directed southward.

Latent heat flux is essentially transfer of water vapour. Its net transport from north to south is pointed towards the thermal equator (5°N), the flux from the south substantially

Table 5.1 Mean annual heat flux across latitudinal circles (in 10^{11} W) (after Kidson, Newell, Oort, Robinson, Starr and Vincent)

Latitude circle	Static energy				
	Latent heat, Lq	Realized energy $= c_pT + gz$			Total
		eddies	circulation	subtotal	
40° N	15	28	−2	26	41
30	12	13	12	25	37
20	−1	3	23	26	25
10	−7	0	16	16	9
0	15	0	−17	−17	−2
10° S	21	−1	−34	−35	−14
20	8	−4	−34	−38	−30
30	−9	−14	−19	−33	−42
40	−20	−29	3	−26	−46

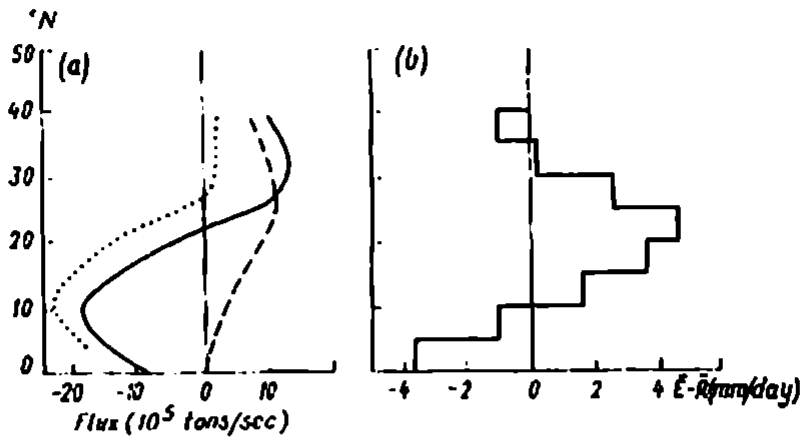

Fig. 5.19 (*a*) Latitudinal profiles of the pressure-integrated total (*full line*), mean circulation (*dotted line*), and eddy (*dashed line*) meridional fluxes of water vapour. (*b*) The zonally averaged divergence of water vapour in belts at 5° latitude expressed as evaporation minus precipitation (after van de Boogard)

exceeds that from the north. Many researchers not unfoundedly believe the south equatorial oceans are the main "suppliers" of latent heat to the atmosphere. According to H.M.E van de Bogaard, 'in low latitudes, the vapour transport is predominantly toward the thermal equator, being dominated by the mean flow in the lower trade wind branch of the Hadley cell where vapour density is greatest. The transport by eddies is almost exclusively poleward'.

Figure 5.19*a* illustrates pressure integrated vapour transport in the Northern Hemisphere. It is readily seen that the flux accomplished by eddies predominates. It is greatest at around 25°N; gradually it weakens equatorward and becomes zero very nearly at the equator. The flux due to the mean circulation reaches a minimum at 10°N, that is where the wind is strongest in the trades. At about 26°N it is close to zero and farther north reverses in direction. Here it is appreciably weaker than the eddy meridional flux.

Figure 5.19*b* depicts the zonally averaged divergence of water vapour. The positive divergence corresponds to the altitudes where evaporation exceeds precipitation. In the belt of 10–35°N the divergence is seen to be positive, that is water vapour replenishes the atmospheric content. North

and south of the belt moisture discharge falling as rain prevails over the vapour income from evaporation.

Realized energy flux ($c_pT + \Phi$) is directed northward and southward of the thermal equator. Within the tropical region this flux is larger in the Southern than in the Northern Hemisphere. It reaches greatest values at 20°S. In the Northern Hemisphere the maximum flux is also found at 20° latitude, yet it is almost 2/3 as strong as its southern counterpart.

Eddy flux of realized energy in the belt 20°N to 20°S is very weak and in equatorial region it equals zero. North and south of the latitudes the eddy flux gains substantially, reaching its maximum beyond the tropical latitudes.

Circulation flux of realized energy is directed south and north from the thermal equator. It is highest at 15°N and 25°S. Meridional heat transfer is performed by solenoid circulations of the Hadley cell type. In the ascending branch near the equatorial trough heat comes into the atmosphere, in the descending branch at the subtropical ridges the atmosphere undergoes partial loss of heat because of radiational cooling. The meridional streams connecting the ascending and descending branches, that is the trades and their opposites in the upper troposphere, flow towards low pressure. Hence, here generates the kinetic energy of horizontal streams. Under the influence of friction it dissipates in the lower layers, but conserves in the upper.

J. S. Malkus and H. Riehl proved that stable circulation of the type (with uniform ascending motions in the most part of the equatorial troposphere) is impossible. It is known, however, that the most significant heat transfer towards mid latitudes is effected at about the 200-mb level. Accordingly, in the equatorial region there has to exist a mechanism to transfer energy from lower levels to the upper troposphere. Malkus and Riehl assign the major role in this mechanism to convective streams which favour the formation of deep clouds with protected core. Having a small cross-sectional area, however, these clouds cannot perform the duties of the energy transfer mechanism. Air parcels ascending inside the clouds from bottom moist layers and having a large amount of energy are to lose this energy in the processes of mixture.

In large clouds where the air ascends over a considerably greater area the cloud core may remain unmixed so that an air parcel in this flow can preserve its energy, uplifting into the upper layers of the troposphere. Hence, large-diameter cumulonimbi (often referred to as "hot towers") may serve as "conductors" for energy transfer to the upper troposphere. The core of such clouds appears isolated, as it were, from the surroundings and conducts, in the vertical updrafts, large masses of air with high energy content picked up from the underlying surface.

In different areas of the tropical zone the conditions for convection are unequal (see Chap. 3) so that convective clouds build to various altitudes. In the average conditions, air parcels can ascend without mixing up to 200 mb and even higher in the protected-core clouds of the equatorial trough. At a distance of 20° latitude aside from the trough axis they can ascend not above 300 mb and often only to 700 mb. The clouds markedly differ in their tops elevation, being in general taller over land than over ocean. So, the upper branch of the Hadley circulation receives energy through clouds building up to various heights.

Review Questions

1. What constitutes the basic current in the tropical atmosphere?
2. What is understood under the disturbances of basic stream?
3. How would you discern a disturbance from a basic flow?
4. Describe the structure of basic stream.
5. What is the Hadley cell? Which elements compose the circulation? What are the weak points of the model?
6. Define the equatorial trough and the ITCZ.
7. Discuss seasonal displacements of the equatorial trough over the oceans and over the continents.
8. Describe the distribution of divergence, vertical motions, cloudiness and rainfall in various locations of the ITCZ.

9. Which layers are identified in the trades? Characterize each layer.
10. How do the trade winds occur?
11. What underlies the term 'antitrades'?
12. Do the winds of antitrades origin actually exist?
13. What are the principles to class synoptic objects in the tropics?
14. How can synoptic objects be discerned basing on their appearance?
15. According to what principles are cyclonic (anticyclonic) movements rated? Cyclones (anticyclones) of what class are observed in the tropics?
16. What are waves in the easterlies? What is the weather associated with them?
17. Verify the distribution of divergence and convergence in the easterly waves.
18. What are equatorial waves? In what do they differ from the waves in the easterlies?
19. What linear systems (linear synoptic objects) can be met in the tropics? How would you shortly characterize them?
20. What is monsoon? Define the phenomenon. List main causes of monsoons.
21. How does the winter Asiatic monsoon appear and develop?
22. Which air masses take part in the winter monsoon stream? How do they transform?
23. How does the summer Asiatic monsoon appear and develop?
24. Which air masses are involved in the summer monsoon stream? Where do they form and how do they transform in travel?
25. Why do heavy rains set in with summer monsoon arrival?
26. How does the West-African (Guinea) monsoon appear and develop?
27. What comprises the East-African monsoon?
28. In what do the African monsoons differ from the Asiatic?
29. What is the upper boundary layer and how can its role be defined in evolution of disturbances?

30. What influence do large-scale motions exert on disturbances?
31. Name the processes that produce effects in contrary to that of large-scale motions.
32. What is the effect of penetrating convection on large-scale motions?
33. Discuss how a cold-core cyclone transforms into that of warm core.

Chapter 6 TROPICAL CYCLONES

6.1 Formation of Tropical Cyclones

Tropical cyclones can appear at any time of the year in tropical parts of all oceans, except the southeastern Pacific and south Atlantic. Their count abruptly varies from one region to another and from year to year. Figure 6.1 plots the areas where tropical cyclones appear, i.e. the regions where the cyclonic disturbances have been registered to appear over the last eighty years.

Most often tropical cyclones form in the northern tropical Pacific. On the annual mean basis, there have been observed about 32 cyclones in the area. Their highest frequency is noted in August and September, that is in late summer (Fig. 6.2, solid curve). In the northern tropical Atlantic cyclones occur more often. On the average, the yearly count is about 10 cyclones. The highest frequency there is also noted in August and September (Fig. 6.2, dotted curve). About as many cyclones appear in the southeast tropical Pacific. Here, the maximum of occurrence falls on mid-summer,

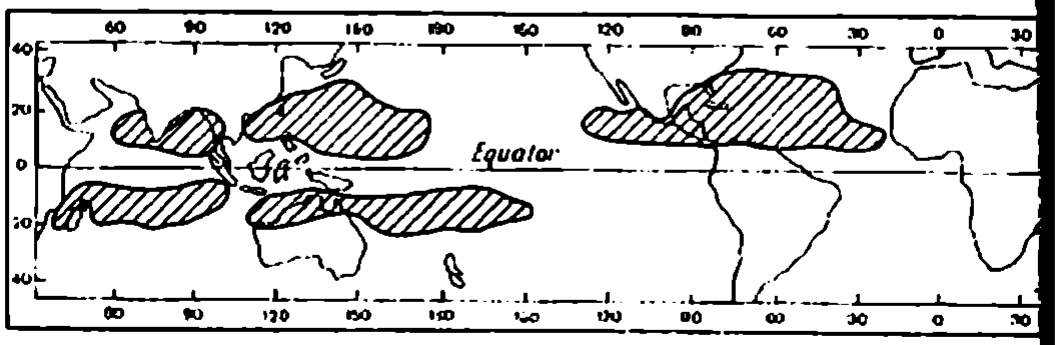

Fig. 6.1 Areas of formation of tropical cyclones (after Gray)

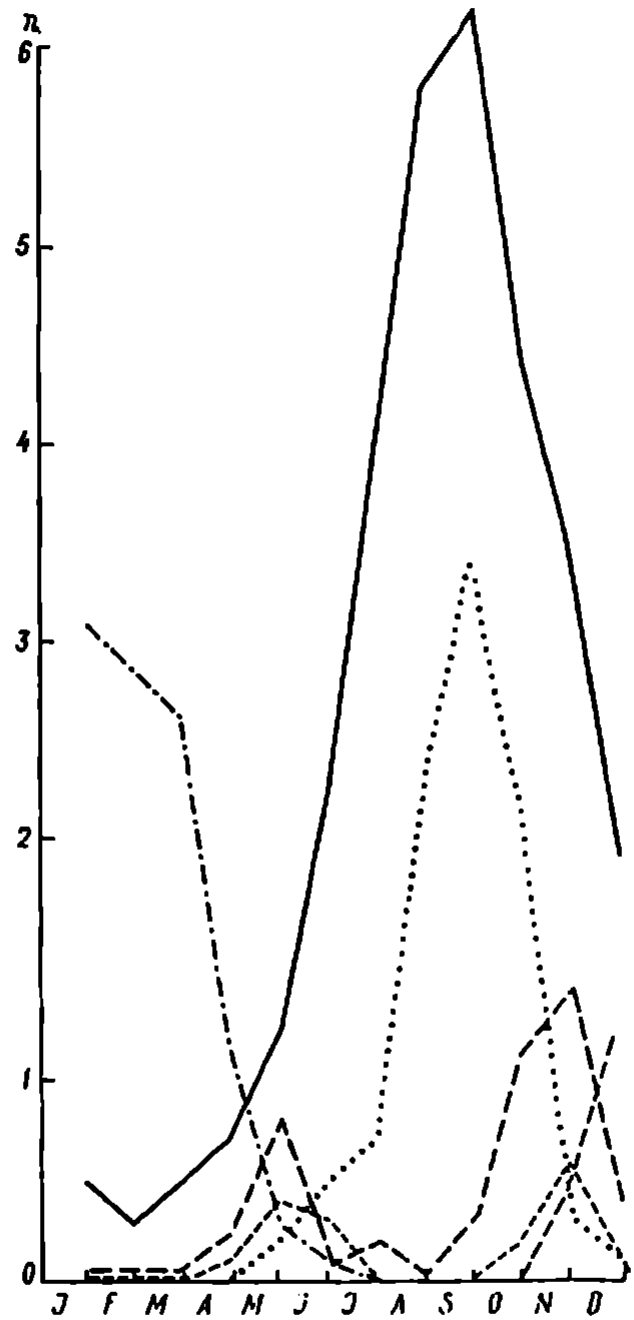

Fig. 6.2 Annual variation of frequency with which tropical cyclones occur in various regions of the tropics: the northern Pacific (*heavy solid*), the northern tropical Atlantic (*dotted*), the southeastern tropical Pacific (*dash-and-dotted*), the Arabian Sea (*dashed*), the Bay of Bengal (*dashed heavy*); n = monthly count of cyclones (after Gray)

in January (Fig. 6.2, dash-and-dotted curve). In the Indian ocean the frequency of cyclones is somewhat lower. So, over the Bay of Bengal and Arabian Sea only 2 or 3 cyclones a year are observed, on average. Here, the seasonal frequency course shows two maxima, one in May and the second in November (Fig. 6.2, dashed curves).

Most often (65 per cent of all observations) tropical cyclones appear between latitudes 10° and 20°. In the higher latitudes they form only in 13 of 100 occasions. They have never been found north of 35°N and south of 22°S. In the belts of 3-10° latitude of both hemispheres the latitudinal frequency of cyclone occurrence is 22 per cent. At 2-3° latitude only single occasions have been observed.

Severe tropical cyclones are known as hurricanes in the Atlantic and eastern Pacific, as typhoons in the western Pacific, and as cyclones or hurricanes in the other areas where they occur. There are known some local names for the storms: willy-willy in Australia, williwau in Oceania, and baguio in the Philippines.

Until 1978 the severe tropical cyclones have been labelled by feminine names. The Seventh Session of the WMO Regional Association IV (1977) adopted a recommendation on using male names, along with female, for the purpose. So, first three tropical storms swept in 1979 over the Caribbean, Gulf of Mexico, and northern tropical Atlantic received the names Ana, Bob, and Cladette, and the three cyclones passed over the northeastern Pacific the names Andreas, Blanka, and Carlos. In the Atlantic, each cyclone beside the name is supplied with the year of formation, and serial number joined into a four-digit numeral. For example, 7809 implies the ninth hurricane of 1978.

At present no universally acknowledged theory is known on appearance of tropical cyclones. There exists instead a series of empirically derived indicators which, if supported by some analytical maturity, can be used to forecast appearance or passage of a cyclonic disturbance. These indices differ from one region to another and include mainly a characteristic march of weather preceding a cyclone. So far this type of forecasting has not been supported by the logic of scientific observations.

Tropical storms are comparatively seldom phenomena,

Their appearance depends on some combination in atmospheric conditions and the state of the underlying surface. Some of the conditions are known, yet many others might still await their evaluation. Let us discuss which we know.

A tropical storm can form either of a preexisting upper-level cyclone having a cold core, or of a weakly developed area of low pressure. In either case a surface synoptic chart displays at the initial moment, what we shall call, the incipient or preexisting cyclonic disturbance, or ICD in short, as a slight trough or, at best, a small low encircled by a continuous isobar. The origin of the ICD cannot be well traced for all cases but it is very likely to be connected with wave processes in the tropics and the influence of mid latitudes (intrusion of troughs from higher latitudes).

The process of further transformation of an ICD into a tropical cyclone is decided by its position in a basic stream. Two ways are possible.

1. The incipient cyclonic disturbance is in the baroclinic part of the basic stream. A significant effect on the ICD may be exerted by the baroclinic instability defined by the horizontal temperature gradient. Thus, for example, the easterly waves are situated in the baroclinic portion of the main stream. They are stable as a rule, yet in some cases when the horizontal temperature gradients are exceedingly high, the wave fails to be stable any longer and changes to a vortex. The Coriolis force also favours the cyclonic vortex in the easterly wave observed at 18-20° latitude. This cooperative action of baroclinic instability in the area of the easterly wave and an appreciable value of the deflecting force brings about a closed cyclonic circulation.

2. The incipient cyclonic disturbance is in the quasi-barotropic portion of the basic stream, in the ITCZ. It may happen so that the ICD turns out in the area of barotropic instability, defined by the horizontal wind shear along a meridian, then a closed cyclonic vortex can form. When the ITCZ is at the equator, the closed circulation can hardly be formed by any instability, and cyclones cannot appear here. A displacement of the ITCZ 3 to 5° latitude poleward proves sufficient to produce the favourable conditions for cyclonic vortices to occur. At the latitudes it is sufficiently high to produce the required spinning effect. Hence, in

either way the non-zero Coriolis force is an essential condition of cyclogenesis.

The closed circulation is but the initial stage in formation of a cyclone. To maintain cyclonic circulation for a substantially long time the emerging cyclone should be supplied by energy. The cyclone is believed to pick up this energy from the oceanic surface. It is long noted that cyclones appear and develop over the surface with a temperature not lower than 26 °C; moreover, a well-developed cyclone contacting with a cooler surface rapidly loses its intensity. If we recall that the highest frequency of tropical cyclones falls to late summer-early autumn when the ocean surface is at its warmest everywhere, we would no longer doubt on the source of energy for cyclones. It is undoubtedly the ocean. V. V. Shuleikin indicated that a tropical cyclone may be treated as the heat engine whose heater is the oceanic surface, and heat sink—the atmosphere surrounding the cyclone. If it is so then it becomes obvious why cyclones cannot form, say in the southern Atlantic. The cold oceanic streams lower there the temperature of the waters beyond that in the other tropical oceans so that the heat engine fails to function.

An energy source available does not imply availability of a supply link. A mechanism must exist to continuously supply energy and converse it in kinetic form. The supply of energy can partly be provided by the direct contact between cyclone and water surface (see Sec. 6.3), yet it would be insufficient for a storm to develop. The major mechanism of energy transfer consists of a chain of water phase transitions. Moist air entrained in deep penetrating convection in moist liable atmosphere evolves in condensation an enormous amount of heat (see Chap. 3). The released heat of condensation converts into the kinetic energy of a cyclone. New portions of energy transported via the convection continuously make up for the energy dissipated in friction. If the supplied energy exceeds the losses, then the cyclone will develop; if the dissipated energy equals the supply, the cyclone remains unchanged; if the dissipation exceeds the supply, the cyclone will be filled.

For a long time it has been believed that the main prerequisite for a tropical cyclone to develop should consist in the presence of moist unstably stratified air and progress-

ing convection. Now it became obvious that convection alone, though an indispensible condition of a tropical cyclone development, cannot be thought a sole cause of tropical cyclogenesis.

Hence, we know that the composition of the following conditions will favour formation of tropical storms:

(a) incipient cyclonic disturbance;

(b) baroclinic instability depending on horizontal temperature gradient, or barotropic instability determined by horizontal wind shear along a meridian;

(c) the value of the Coriolis force that will suffice to produce the spinning effect;

(d) the temperature of the oceanic surface not lower than 26 °C; and

(e) convective instability of atmosphere, favourable for penetrating convection.

6.2 The Life Cycle of Storm

Tropical cyclones may deepen to various intensities. Accordingly they are termed (ratings may differ):

(1) a tropical disturbance, when the cyclonic wind is not stronger than 15 m s^{-1};

(2) a tropical depression (marked TD on charts), when the wind is 16-20 m s^{-1};

(3) a tropical storm (marked TS), when the wind is 21-32 ms^{-1};

(4) a hurricane (marked H), when the wind speed is above 32 m s^{-1}.

A cyclone may change in intensity and develop from tropical disturbance to severe storm. Only few cyclones attain a hurricane force mostly though they cannot grow beyond a tropical disturbance. The evolution of the average storm from birth to death has been divided into four stages.

1. *Formative stage.* The stage begins with the appearance of a first closed isobar. In this stage winds usually remain below hurricane force and surface pressure in the center of cyclone does not drop below 1000 mb. Strongest winds are apt to be concentrated in one quadrant only, poleward and east of the center. The cyclone moves from east to west. Deepening can be a slow process, requiring days for organi-

zation of a large area with diffuse winds. It can also be explosive, producing a well-formed cyclone within 12 hours; for this time the cyclone is encircled by a few additional isobars.

2. *Immature stage.* If intensification takes place, the lowest pressure rapidly drops below 1000 mb, and at least at one place within the cyclone winds rise to hurricane force. Two modes of further development are possible, with no regard to how the cyclone has developed in the formative stage, though often a fast development in the formative stage suggests a fast development in the immature stage. In the first, a cyclone starts quickly filling after a short period of hurricane wind in one of its parts and then it may travel long distance as a shallow depression. On the second line, a cyclone deepens sharply and the lowest pressure rapidly drops. Winds of hurricane force form a tight band around the center. The cloud and rain pattern changes from disorganized squalls to narrow organized bands spiralling inward. Only a small area is as yet involved.

3. *Mature stage.* The surface pressure at the center is no longer falling and the maximum wind speeds no longer increasing. Instead the circulation expands during the mature stage, which may last a full week. Whereas winds of hurricane force may blow within a 30-50 km radius during immaturity, this radius can increase to 300-350 km in mature storms. The symmetry is lost in the area of gales and bad weather extends much farther to the right of the direction of motion than to the left (looking downstream).

It is surprising how much the size of mature storms can vary. The radius of some storms is only 100-200 km, others can attain a radius of 1000 km.

4. *The decaying stage.* The last stage of life cycle begins when the cyclone starts filling.

Most often decaying begins when a hurricane recurves from the tropics and enters the belt of westerlies. Here its filling begins immediately, followed by slackening of the wind so that the cyclone finally dies out. This often observed sequential chain has another alternative. Having recurved to the mid latitudes a cyclone can lose its tropical characteristics, assuming a middle-latitude character of an ordinarily extratropical cyclone. It may happen so that remain-

ing in the tropics a cyclone enters over a land mass. Here, it fills in, however, after a lot of destructions. It is only seldom that tropical cyclones fill in over the oceans.

6.3 Structure of Tropical Cyclones

An approximate structure of tropical cyclone has been known to meteorologists already for long, however, the reliable data on the tropical storms and satellite pictures of the recent times have substantially improved our knowledge about the meteorological quantities within a tropical cyclone. Starting with 1955 suitably equipped airplanes began the reconnaissance flights within tropical cyclones supplying data on their structure.

Surface pressure. Pressure in the center of ordinary tropical cyclones amounts to 950-960 mb. Occasionally this pressure has dropped to 890 mb, and the lowest recorded drop was 877 mb. Tropical cyclones have notably large pressure gradients, 14-17 mb/100 km. In some cyclones the gradients run as high as 60 mb/100 km. Asymmetry in the gradient distribution (Fig. 6.3) is explained by the overlapping of the cyclonic pressure field over that of the basic stream.

A barograph trace makes a sharp dip when a tropical cyclone approaches, then as it passes over, as sharply rises (Fig. 6.4).

Wind. In the cyclones of the Northern Hemisphere winds blow counterclockwise, in the Southern Hemisphere they are in the clockwise direction. No one knows how high wind speeds can rise in tropical storms. At surface stations the anemometer is usually blown away at speeds which exceed 50 m s^{-1}. A few anemometers, specially constructed for hurricane measurements, have recorded speeds up to 90 m s^{-1} and then also failed. Indications are that over the sea the wind speed may attain 110 m s^{-1} in a very small area.

At low levels winds spiral inward to the center of a cyclone. The highest wind belt can be distanced in a wide range of radii from the center of a cyclone (10-150 km and at times even farther). In a typical cyclone the belt is between 20 and 50 km radii. Within the belt wind speeds markedly diminish toward the center where weak winds of various directions are observed. Away from the center, beyond the high-

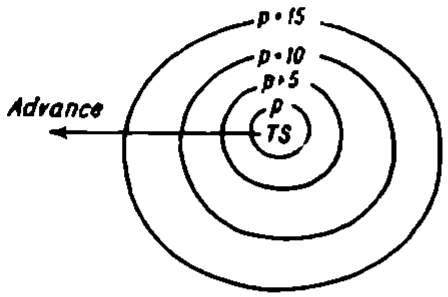

Fig. 6.3 Asymmetry of pressure in a tropical cyclone

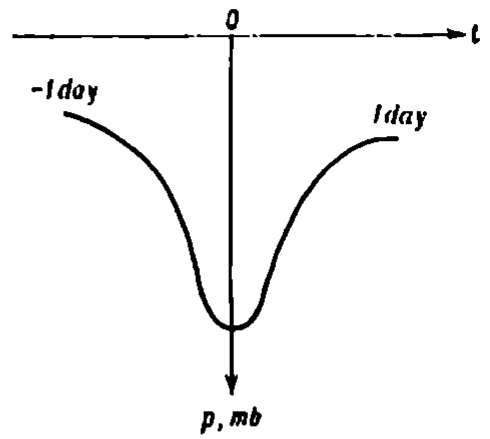

Fig. 6.4 Barograph trace upon passage of a tropical cyclone

est winds belt, winds slowly and unevenly fade. The distance of the 25 m s^{-1} isotach varies from 75 km to several thousand kilometers.

Aloft, wind speeds in cyclone abate, first, up to 6 km height they vary slowly and then, above this level, much faster. With increasing height cyclonic circulation gradually converts into anticyclonic one forming an outward spiral of streamlines. The radius of the anticyclonic vortex aloft (13-16 km) amounts to several thousand kilometers.

Similar to the gradients the wind is also asymmetrically distributed. Highest winds are concentrated in the right quadrant of the storm (looking downstream).

E. S. Jordan has computed a mean picture of the circulation pattern at different heights, based on about 130 wind reports reaching at least 10 km. As data within 2° latitude from the storm centers were very scarce, the zone of strongest surface pressure fall, wind, and precipitation remained unexplored aloft. He plotted the fields of tangential wind component at different heights over the tropical cyclone (Fig. 6.5). The center circles represent the unexplored areas. A plus sign signifies counterclockwise rotation, a minus sign clockwise. It is seen that the wind is asymmetrically distributed in the horizontal and that the positive tangential component decreases with height. A zero line separating counterclockwise- and clockwise-rotating winds (zero iso-

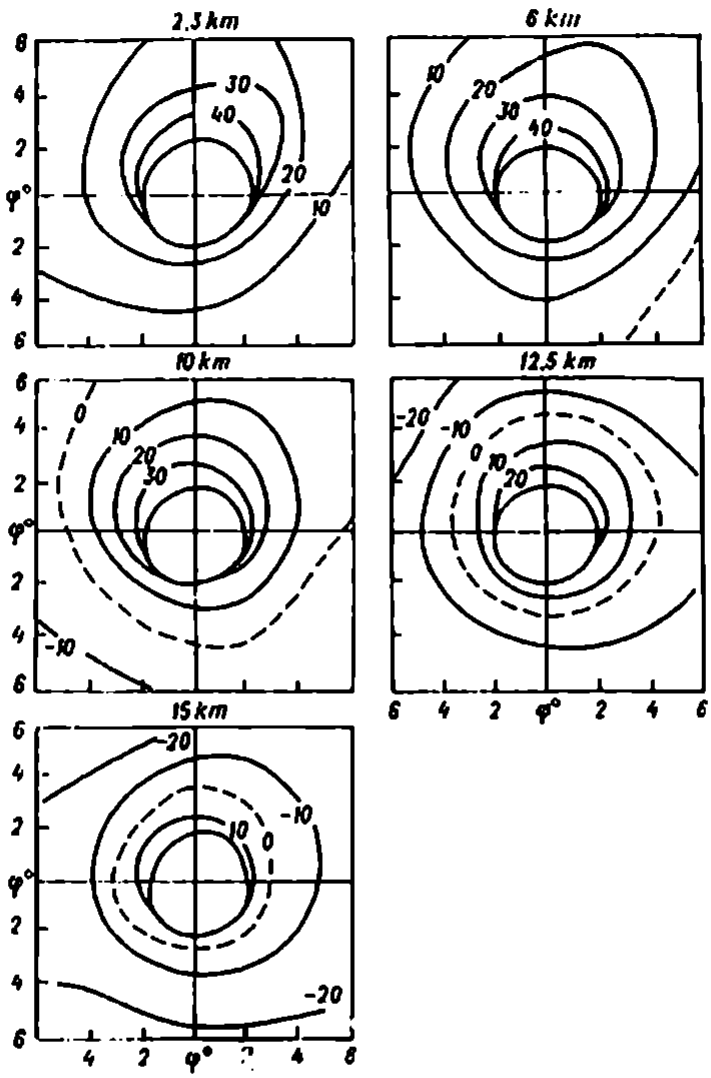

Fig. 6.5 Tangential velocity (knots) (after E. S. Jordan)

tach) appears in the outer portion of the circulation. Still higher this zero line is contracting toward the center. Inside, the strength of the cyclonic circulation continues to weaken upward steadily. Outside, speeds in the ring of air rotating anticyclonically gradually increase with height.

The field of the radial component could be ascertained with some certainty only at the lowest and highest levels (Fig. 6.6). Through the deep layer from 3 to 10 km radial speeds are small and vacillate between inflow and outflow.

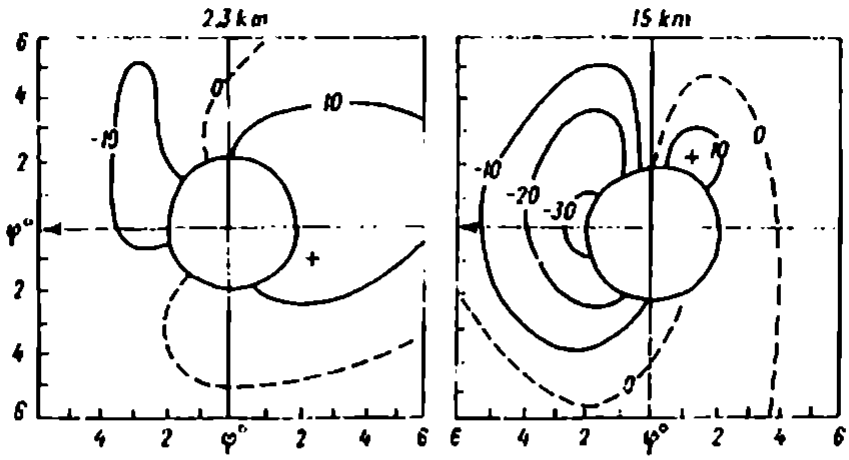

Fig. 6.6 Radial velocity (knots) (after E. S. Jordan)

Radial speeds might be very small in this layor and could hardly be measured, yet thoy are highly probable to play an important part in the development of tropical cyclones. At low levels the radial component is inward, above 10 km height it is outward. This distribution makes fair the conclusion made by Riehl that 'all major inflow is confined to the low troposphere, all outflow to the high troposphere'. Figure 6.6 demonstrates that the net inflow at 2.3 km height is highly insignificant. The major inflow might be confined in the lowest kilometer of the atmosphere. At 15 km height pronounced outflow is centered along the direction of motion.

Temperature. As would be recalled, the tropical cyclones attaining hurricane force have a warm core. Within the storms, temperature gradients at the surface are very small. According to Riehl, potential temperature of the surface air increases along the inward trajectories. In other words, the surface air gains in heat content during its travel toward lower pressure, acquiring both latent and sensible heat.

A source for the heat and moisture increment is obvious. The ocean is greatly agitated, and large amounts of water are thrown into the air in the form of spray. It is hard to say where the ocean ends and where the atmosphere begins! As the air moves toward lower pressure and begins to expand adiabatically, the temperature difference between ocean and

air suddenly increases. Since the surface of contact between air and water increases to many times the horizontal area of the storm, rapid transfer of sensible and latent heat from ocean to air is made possible. In the outskirts the turmoil is less and the process of heat transfer is not operative. Yet the temperature gradients at the surface are very small.

Between 3 and 13 km levels temperature in the center of a storm is exceedingly higher than in the surrounding areas. In some recordings the temperature in the warm core was 5-15 °C above the temperature at 150 km distance. Greatest temperature gradients have been observed at the outside boundary of the warm core.

Cloud system of tropical storms. Although thick cloudiness develops over tropical cyclones, in the center of the cloud system generally there is a cloudless spot known as *the eye of the storm* (Fig. 6.7). However, the eye is not totally devoid of clouds. Surveillance flights often find there different decks of cloudiness. Comparing to the surrounding areas, though, this cloudiness is much inferior.

The eye area is encircled by a cloud wall of high vertical extent (often they are 15 km tall). Generally this wall consists of cumulonimbus clouds merged into bands which spiral toward the center of the storm and converge at the wall. It is at this boundary that the clouds are deepest and accompanied by strongest squalls. The cloud bands in a well-developed cyclone can be 300-400 km long, in the average, and in some cases even 900 km long. The shortest band can be about 50 km. A cyclone may have several of them. In some cases the count was seven.

Rainfall. Rainfall reports during a cyclone passage are rather nonuniform. The scattering is due to great difficulties encountered in measuring rainfall in stormy weather. The wind drives the rain horizontally and picks up water already fallen to the ground, filling the rain gauge on the ground with driven rain and surface basins water. When measuring on ships, rainfall is admixed by a large portion of sea splash. Since most records stem from tropical islands, usually mountainous, reports of rainfall amount and distribution vary widely.

The average rainfall in passing one tropical storm amounts to fairly common 500 mm. Yet it can be as extreme as

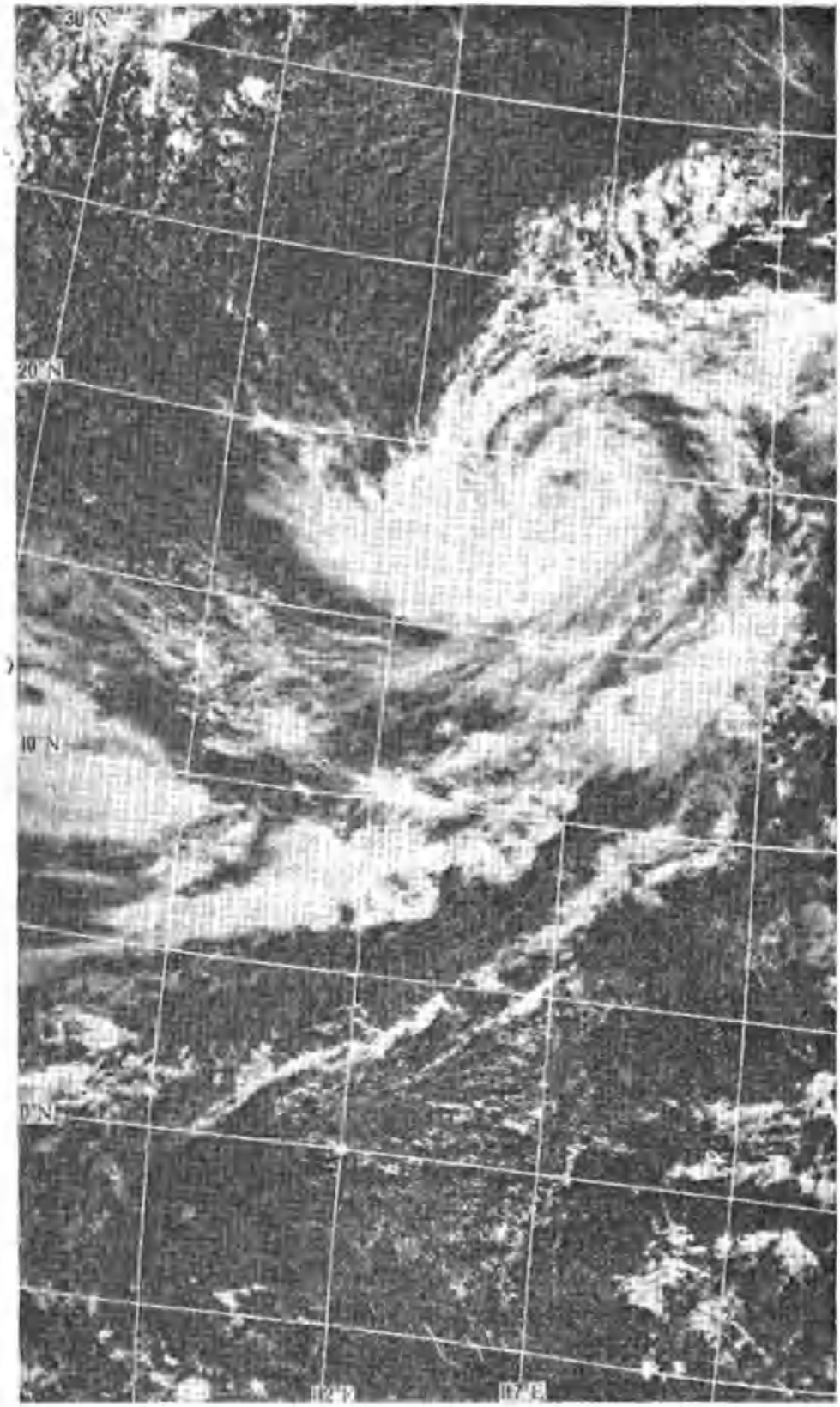

Fig. 6.7 Satellite image of the tropical cyclone observed on August 26, 1978 in the South China Sea

2500 mm, three to four times the average annual precipitation at most cities of the temperate zone.

Riehl has suggested a method to compute the rainfall in a tropical storm as solution of continuity problem for moisture. The rainfall (minus the evaporation) within a circle of specified radius must equal the difference between inward and outward transport of moisture across this circle. Since the outflow takes place in the high troposphere, where the moisture content of the air is less than 10 per cent that in the subcloud layer, we can neglect it for an order of magnitude computation. The inflow of moisture across the circle of radius r is equal to the circumference of the circle $2\pi r$ multiplied by the mean specific humidity $\bar{q}$ of the inflow and the mass flux $v_r \rho p/g$ across the circle. This product must be equal to πr^2, the area within the circle, multiplied by R, the rainfall per unit area and time. Thus

$$R = \frac{2v_r}{r} \bar{q} \frac{\Delta p}{g}$$

Calculation with this formula gives results close to observations. It must be noted, however, that this formula assumes a symmetrically distributed rainfall about the center of a cyclone, actually by far nonsymmetrical. To the right from the direction of motion the precipitation area is larger and the rainfall more intense than to the left where the precipitation area abruptly fades already at a distance of 60-70 km from the center.

As tropical storms recurve toward higher latitudes, the precipitation pattern can change abruptly and unpredictably.

Characteristics of the eye. The eye of the hurricane is one of the oddest phenomena in meteorology, striking by the features of its development and behaviour. Precipitation ceases abruptly at the boundary of well-developed eyes; the sky partly clears; and the wind subsides appreciably, at times to a dead calm. Observers have described conditions in the eye as oppressive due to a psychological reaction of an eyewitness on the rapid transition from hurricane winds and torrential rain to a relative calm.

Although it is usually described as circular, the eye sometimes becomes elongated; sometimes it is diffuse with a

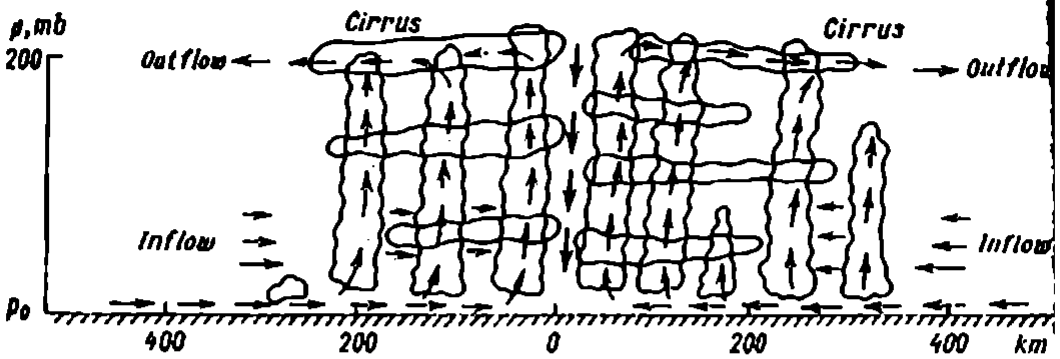

Fig. 6.8 Schematic vertical cross-section through a tropical cyclone

double structured appearance. An eye does not remain in steady state but is constantly undergoing transformation.

Inside the eye, the surface temperature of the air does not differ from that of the outside. With rising height the temperature inside the eye first increases and then markedly exceeds that of the surroundings. The highest temperature difference (16 to 18°C) is usually observed at 2-6 km altitudes. Maximal horizontal gradients are noted at the boundary of the eye. High temperature inside the eye can be traced to descending motions of air in the core of a storm (Fig. 6.8).

Generally the pressure field in the eye is distributed uniformly. On a barograph trace the eye appears as a generally flat area with only small deviations. Sometimes the barometer drops a little from the edges to the center of the eye.

The size of the eye depends on a number of factors. Since the air moves curvilinearly in a cyclone it undergoes action of centrifugal force. The force rises to the center with increasing curvature of the motion. Finally, at some distance from the center, call it a critical distance, the centrifugal force increases so much as to prevent any further advance of air parcels inward. We can estimate this distance from the gradient wind equation

$$r_{cr} = -\frac{V^2}{Vf + \frac{1}{\rho}\frac{\partial p}{\partial r} + F}$$

where V is the wind speed in the cyclone, r is the radius of curvature, and F is the force of friction.

Calculations with this formula give too large values for r_{cr}. This may be explained by the fact that some parcels of the air acquiring large velocities become capable of passing the margin where the centrifugal force must be balanced by the sum of the Coriolis force, pressure gradient and friction force. Beyond the boundary the parcel still continues to work against the centrifugal force so that it diminishes and drops out entirely at some distance from the center.

In mature storms the diameter of the eye averages 20-25 km, less in immature storms. It may attain 60-70 km in large hurricanes and typhoons. In some cases the average diameter of the eye reached even 300 km. A substantial increase in the diameter of eye commonly indicates that the cyclone loses its intensity. However it is not always possible to measure the size of the eye in a dying storm as its edges become very diffuse and the shape fairly uncertain.

In immature storms the eye may be absent. So in the tropical hurricanes having a pressure in the center above 994 mb the eye fails to be evaluated.

Energy aspects. According to several order-of-magnitude calculations the energy release rate in a cyclone averages to 5×10^{19} J a day. On the atomic bomb scale it amounts to half a million of explosions of 10^{14} J each.

As D. V. Nalivkin noted, 'an atomic test at the Bikini uplifted in the air 10 thousand tons of water, yet 250 times as large rain downpoured Puerto-Rico only in several hurricane hours'. The kinetic energy of such a medium scale tropical storm is equivalent to 1000 atomic explosions.

6.4 Relation Between Lowest Pressure and Highest Wind in Storms

The wind speed at any point of a tropical storm is defined by the pressure gradient and the distance of the point from the center of the cyclone. With pressure gradients equal, wind is the stronger the farther is the point from the center of a cyclone. A cyclone has finite dimensions: pressure gradient inside the cyclone first increases with the distance from the center, attains a maximum and then decreases. Therefore every tropical storm exhibits the so-called ring of maximal wind speed (see Sec. 6.3). If the ring is suf-

ficiently narrow it is also termed the circle of highest wind. The speed of the highest wind depends beside the pressure gradient on the radius of the circle.

Precise evaluation of pressure gradient inside the tropical storm cannot always be done. Approximately it can be estimated as the difference between the pressure outside, p_1, and in the center, p_0, of the cyclone. If we assume that the outside pressure is constant, as it is customarily done in numerous studies, and equal to some value close to standard pressure, say $p_1 = 1010$ mb, then the gradient will depend solely on pressure in the center of cyclone. With the dimensions of the cyclone unchanged, the lower is the lowest pressure in the cyclone the greater is the pressure gradient, and hence, the stronger is the highest wind.

An earliest objective of meteorology is to relate the lowest pressure and highest wind in the tropical storm. K. Takahashi of Japan suggested in 1939 that this relationship should be sought in the following form

$$V_m = K (p_1 - p_0)^a \qquad (6.4.1)$$

where V_m is the maximum wind speed, p_1 is the pressure at the outside, p_0 is the pressure in the center of a cyclone, and K and a are some empirically derived constants.

In 1950s, a more accurate form of the above relation was suggested by way of converting K into a variable $K = K_1 - \varphi/5$, where φ is the latitude. The resulted expression is

$$V_m = (K_1 - \varphi/5) (p_1 - p_0)^a \qquad (6.4.2)$$

The search for the constants by different investigators has produced results which are far from unanimous. A series of corrections having done in the early 60s and having allowed for reconnaissance flights data on tropical cyclones, the formula (6.4.2) acquired finally the appropriate constants so that now it is written as

$$V_m = (20 - \varphi/5) (1010 - p_0)^{1/2} \qquad (6.4.3)$$

or

$$V_m = (19 - \varphi/5) (364 - h_{700}/8.54)^{1/2} \qquad (6.4.4)$$

Here h_{700} is the lowest height of the 700-mb surface over the center of cyclone. In (6.4.3) pressure at the outside is as-

sumed equal to 1010 mb, and in (6.4.4) the height of the 700-mb surface at the outer side of the cyclone is assumed 364 dam. Both formulas yield wind speed in knots.

To compute the highest speed of wind in the tropical cyclones at the northwest Pacific at 15-18° latitudes G. D. Atkinson and C. R. Holliday derived another type-(6.4.1) expression

$$V_m = 6.7\,(1010 - p_0)^{0.644} \tag{6.4.5}$$

They emphasize that the formula (6.4.5) yields the averaged maximum speed (over 1 minute intervals) rather than the instantaneous speed (wind gust). When the cyclone shifts to 20° latitude and higher poleward the recommendation is to increase the speed by 10 knots. Another recommendation is to assume the outside pressure equal to 1020 rather than 1010 mb in the Atlantic.

With some assumptions the relationship of wind and pressure fields in a tropical storm may be approached theoretically. We start with the gradient wind approximation

$$\frac{1}{\rho}\frac{\partial p}{\partial r} = \frac{V^2}{r} + fV$$

In the free atmosphere where the motion is supposed to be along the isobars, and at $r \leqslant r_0$, that is within the core of an isolated vortex where the fluid rotates as a solid body, the tangential speed varies linearly with r so that $V = \omega r$, where ω is the angular speed of air in the cyclone. Hence, we may write

$$\frac{1}{\rho}\frac{\partial p}{\partial r} = \frac{\omega^2 r^2}{r} + f\omega r \tag{6.4.6}$$

Upon integration first from r to r_0 and from p to p' and then from r_1 to r_0 and from p_1 to p' (the partition is because at $r > r_0$ $V = cr^{-n}$) and after some rearrangement we get an expression for the pressure at the center of a tropical cyclone, p_0, where $r = 0$:

$$p_0 = p_1 - \frac{\rho\omega^2 r_0^{2(n+1)}}{2nr_0^{2n}}\left[1 - \left(\frac{r_0}{r_1}\right)^{2n}\right] - \frac{\rho f\omega r_0^{n+1}}{(n-1)\,r_0^{n+1}}$$

$$\times\left[1 - \left(\frac{r_0}{r_1}\right)^{n-1}\right] - \frac{\rho\omega}{2}(f+\omega)\,r_0^2 \tag{6.4.7}$$

Denoting $k = r_0/r_1$ and recalling that $V_m = \omega r_0$ we have after some rearrangement

$$V_m^2 + fr_0DV_m - A\frac{2(p_1 - p_0)}{\rho} = 0 \qquad (6.4.8)$$

where

$$A = \frac{1}{n}(1 - k^{2n}) + 1, \quad D = \frac{n(n + 1 - 2k^{n-1})}{(n-1)(n+1-k^{2n})}$$

Solving (6.4.8) for V_m yields

$$V_m = -\Omega_z r_0 D\left[1 - \sqrt{1 + \frac{(p_1 - p_0)}{\rho A \Omega_z^2 r_0^2 D^2}}\right] \qquad (6.4.9)$$

The sign of the radical is chosen so that as $\Omega_z = \Omega \sin \varphi = f/2 \to 0$, V_m should be positive.

The order-of-magnitude estimation for the terms in (6.4.9) indicates that the unity under the radical may be neglected in comparison with the other addend. Consequently, (6.4.9) turns to

$$V_m = -\Omega_z r_0 D + \sqrt{\frac{2}{A}\frac{p_1 - p_0}{\rho}} \qquad (6.4.10)$$

The variable n in (6.4.7) according to available data may vary from 0.5 to 1.0. We discuss the simplest case with $n = 1$. Along the above lines we get

$$V_m = -\frac{r_0\Omega_z(1 - 2\ln k)}{2 - k^2} \times \left[1 - \sqrt{1 + \frac{p_1 - p_0}{\rho}\frac{2(2 - k^2)}{r_0^2\Omega_z^2(1 - 2\ln k)}}\right] \qquad (6.4.11)$$

Since the second term under the radical is exceedingly larger than unity (it may range anywhere between 10 and 200) we may write approximately

$$V_m = -\frac{r_0\Omega_z(1 - 2\ln k)}{2(1 - k^2/2)} + \sqrt{\frac{p_1 - p_0}{\rho}\frac{1}{1 - k^2/2}} \qquad (6.4.12)$$

Analysis of observations employed to check the derived relations has indicated that with 60 per cent of data the quantity $k^2/2$ is below 0.14. So it would be safe to assume that not infrequently a reliable approximation will be supplied by the simplified formula

$$V_m = -\frac{r_0\Omega_z(1 - 2\ln k)}{2} + \sqrt{\frac{p_1 - p_0}{\rho}} \qquad (6.4.13)$$

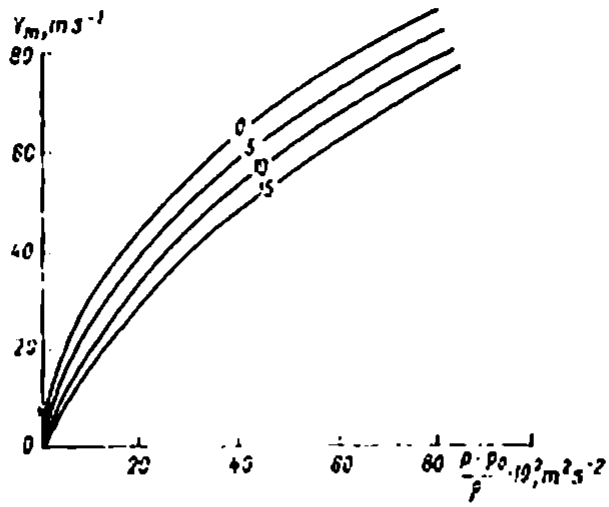

Fig. 6.9 Nomograph to define the highest wind V_m as a function of pressure difference $(p_1 - p_0)$, between pressure at the outskirts, p_1, and in the center, p_0, of a tropical cyclone, and term M

which as $\Omega_z \to 0$ assumes a still more simple form of

$$V_m = \sqrt{\frac{p_1 - p_0}{\rho}} \qquad (6.4.14)$$

Instead of computing along the lines of the expression (6.4.13) one may estimate V_m by the nomograph of Fig. 6.9. The nomograph makes more illustrative the fact that the relative contribution of the first term $M = \Omega_z r_0 (1 - 2 \ln k)/2$ reduces as the term $(p_1 - p_0)/\rho$ increases. Account of M reduces V_m not more than by 15 m s^{-1}.

Most difficult is the derivation of r_0. Basing on measurements, we may assume that r_0 approximately corresponds to the radius of the dense cloud circle so as to derive it from satellite photographs. In storms of various maturity (over different regions) r_0 varies between 25 and 150 km. According to some estimates, the vorticity, on the 900-mb surface, changes sign at a distance of 350-500 miles (650-920 km) from the center. These values may, perhaps, be thought of as estimates for r_1. At radii around 180 miles (330 km) positive vorticity remains markedly strong (about 1.5×10^{-5} to 2.5×10^{-5} s^{-1}) and this area to a certain approximation may be considered as the core of vortex, r_e. Considering a

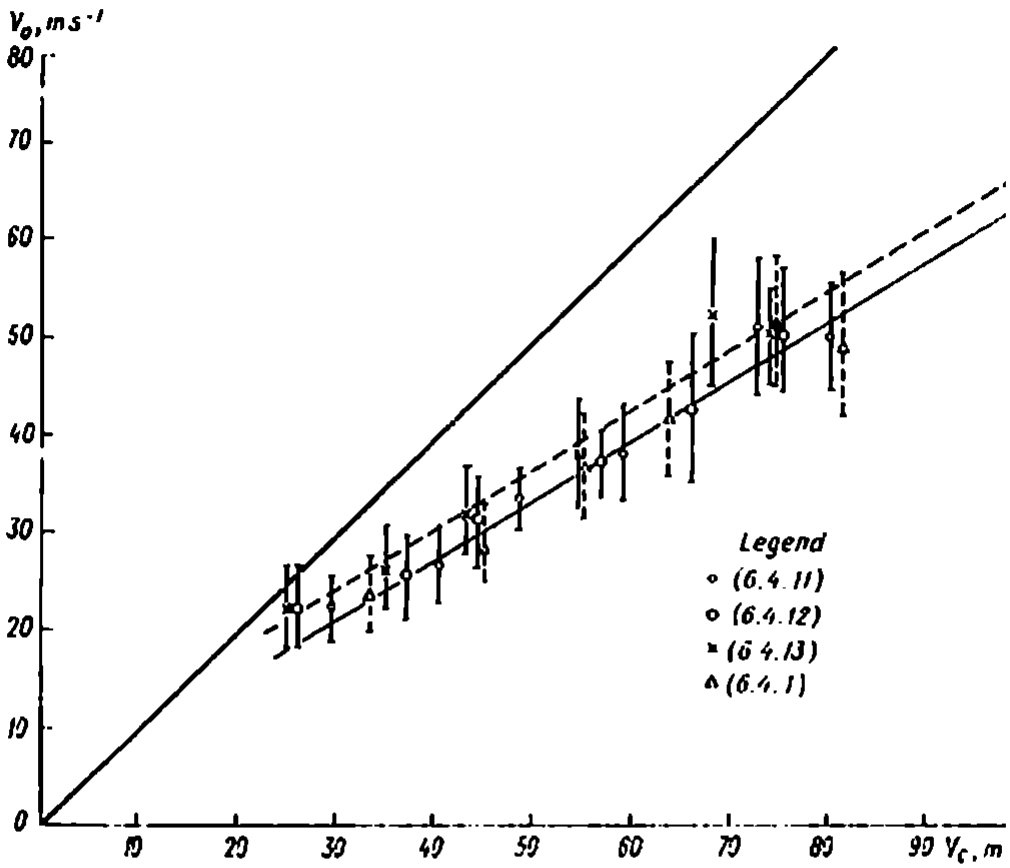

Fig. 6.10 Observed, V_o, and calculated, V_c, maximum wind speeds; line of unity ratio (*heavy*), thin full line is drawn through "circles"; dashed line through "crosses" and "triangles"

slight effect of the term M, the uncertainty in defining the values of r_0 and r_1 has only a little influence on the results of computations. This is especially so because r_0 and r_1 come into the computational expression as a logarithmic ratio so that the uncertainty in r_0 is compensated, as it were. Numerical estimates indicate that in the latitude belt of 15-40° with $r_1 = 400$-600 km a possible two-fold exaggeration in r_0 brings about the respective underestimation in V_m by 15-3.0 m s^{-1}.

The observed and computed maximal winds are plotted in Fig. 6.10. It is seen that calculations with (6.4.11) and (6.4.12) yield practically coinciding results, so they are fitted with a single (dashed) line, while the calculation with

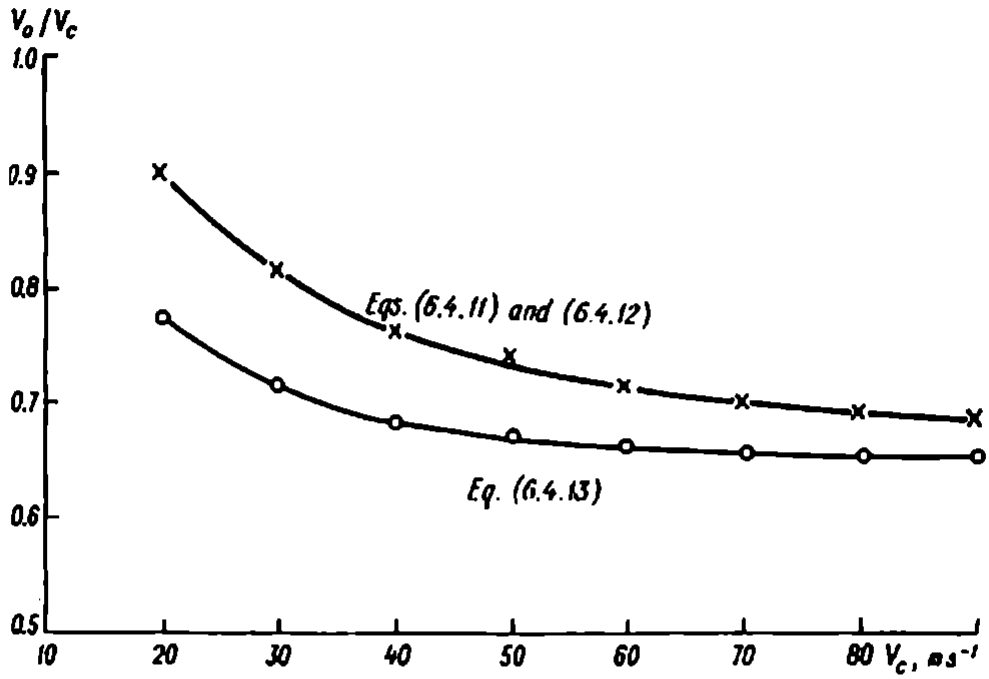

Fig. 6.11 Ratio V_0/V_c as a function of V_c

the simplified expression (6.4.13) are RMS fitted by the solid line. The deviation of the maximum speeds computed with the complete, or approximate, expression, V_{m1}, from those computed with the simplified expression, V_{m2}, can with sufficient accuracy be described (measuring in m s^{-1}) as

$$V_{m1} = V_{m2} - 3.0$$

Figure 6.11 depicts the relative variation of the observed and computed wind speeds with respect to the computed speed. For the complete and approximate expressions it ranges from 0.650 to 0.775, for the simplified formula from 0.7 to 0.9. If the computed wind is considered as a wind at the top of the boundary layer, and the observed wind as a wind at the earth surface, then both the above estimates and the character of the dependence of V_0/V_c agree with the estimates obtained by L. Golodko and V. Radikovich with a model of the planetary boundary layer. In the Takahashi model, the computed and observed winds also exhibit a systematical deviation. At about the same deviation of the mean as in Fig. 6.10 the ratio V_0/V_c amounts to 0.77.

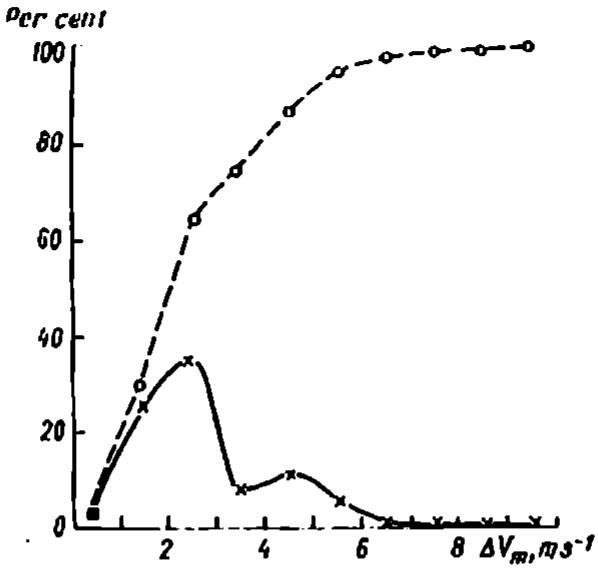

Fig. 6.12 Probability density (solid and crossed line) and cumulative (dashed-and-circled) distribution functions of ΔV_m frequency

Computations have been performed for $n = 0.5$ as well. Figure 6.12 illustrates the plots of probability density and cumulative distribution functions for the frequency of the difference $\Delta V_m = V_{m1} - V_{m0.5}$ computed between the highest speed at $n = 1$, V_{m1}, and that at $n = 0.5$, $V_{m0.5}$. It is readily seen that the maximum frequency falls to 2-3 m s^{-1} and the probability that ΔV_m will fall within 3 m s^{-1} is 65%, i.e. with this probability the quantity ΔV_m will be within the accuracy margin when wind speed is measured in stormy conditions. However, in view of the uncertainty in selecting n, the consideration for $n = 1$ may not be discarded as out of place.

Analysis of computational results gives evidence that ΔV_m depends on $\Omega_z r_0$ only slightly and is mainly determined by $(p_1 - p_0)/\rho$ and k (ΔV_m increases proportionally as the former and inversely as the latter). Since ΔV_m is always negative it assumes the character of systematic error. The most probable value for the error is 2.5 m s^{-1}, therefore for practical purpose the values of maximum wind speed deduced by (6.4.11) should be reduced by 2.5 m s^{-1}.

The model discussed enables us to estimate with a sufficient reliability the maximal wind (at the top of the planetary

boundary layer) in the tropical storms. Its major advantage over the empirical relationships consists in its wider range of application which makes it more perspective.

6.5 Forecasting the Movement of Tropical Cyclones

It has long been noted that in many areas the tropical cyclones first move from east to west with some, at times significant, component directed poleward. Having arrived at the latitudes where westerly currents prevail the storms turn to the east. Not all the tropical storms reach the areas of the westerlies. Many of them, having moved inland of a continent become filled and it occurs earlier than they are catched by the westerlies.

In various areas of the tropics cyclones move exhibiting some local features which are well known and allowed for when attempting a forecast. For example, the typhoons that are formed near the Philippines often recurve from their model path, from east to west, toward the north and northeast. Occasionally, they cross the East China Sea and strike Japan and Soviet Far East and even penetrate farther north to the Sea of Okhotsk and the Kamchatka. When they travel along the model route, under their influence come South China and the Indochina. In the early summer (June) and in autumn (October) the typhoons traverse south of Japan, and in the period from July to September they often recurve into higher latitudes.

Other areas also evidence deviations of the main (westward) travel of cyclones, but these deviations are developed far weaker. Everywhere, though, a tendency is observed to deviate from the main course.

Cyclones mainly move on curvilinear tracks. Roughly the curvature may be divided into hyperbolic and parabolic. However, all attempts to fit the tracks of the storms with these curves have fallen flat. The reason is in that a cyclone track may experience an unexpected change and become essentially abnormal; such tracks can exhibit even loops.

The average velocity of a tropical cyclone amounts to about 20 km per hour. However, as soon as a cyclone passes

the inflection point (recurvature) on its path it accelerates to 30-40 km per hour.

At present the travel of tropical storms can rather easily be tracked by satellites and radars. However, tracking does not imply forecasting of their further movement. Numerous attempts have been made at the development of a reliable prognosis of tropical storm path. Each next year has these methods more accurate and versatile, yet so far they suffer from a wealth of unsolved problems.

The development of storm movement prognosis may be traced as far back as 1898 when a common extrapolation was first applied for this purpose. By 1919 the researchers concluded that the cyclones tend to travel in a steering current around more substantial pressure systems. In 1924 the accumulated data on tropical storms were resolved into the charted hurricane tracks on a monthly basis. These historic charts facilitate cyclone path forecasting from the climatic angle.

In 1935 a technique was worked out to evaluate a steering current (field of translation) by wind data aloft in two points symmetrically chosen on both sides of the storm center. This technique initiated a series of attempts based on the steering layer concept.

Riehl was the first who attempted at an objective forecasting of storm movement still in 1950. Subsequently his method has been somewhat modernized. At present tropical cyclone forecasting is performed on high-speed computers involving both synoptic and climatic data, though climatic prognosis also exists.

Developing a method of hurricane prognosis each investigator first of all has tried to elucidate the causes that control hurricane movements.

Driving forces of tropical cyclones

E. S. Jordan experimentally proved in 1952 that the hurricane moves in the direction and with the speed of the steering current which is defined as the pressure-weighted mean flow from the surface to 300 mb in the band 2-4° latitude from the center of the cyclone. J.E. Miller in 1958 found that cyclones move as the mean current in the layer from 0 to 12.5 km altitude in the band 2-4° latitude from the center.

Two forces are believed to be the main causes controlling the movement of a cyclone. According to C. Rossby one of them is due to the change of the Coriolis parameter on the southern and northern slopes of cyclones. This force is directed poleward and is strongest in large intensely developing cyclones. The second force appears because the stream produced by a vortex superimposed on a steering current is nonlinear. This force makes a cyclone move along trahoidal path shapes, common for many tropical storms.

Numerous experiments with dynamic multilevel models having been built for the last 15 years indicated the cyclones travel as influenced by the integral flow of the whole bulk of the troposphere and that the steering current changes itself upon interaction with the winds of vortex so that the resulted path of the cyclone is controlled also by interaction between vortex and steering circulations rather than by the steering current alone. For the forecasts in the range 12-36 hours the component of the steering layer may be deemed as being 4 to 10 times stronger than the component resulted from the interaction between vortices.

Subjective forecasting

First prognoses of tropical hurricane movement were based on account of clouds and sea swells movement ahead of the storm. When the horizon of aerological data widened and synoptic and constant-pressure charts appeared, in an effort to improve forecasts of hurricane motion many schemes have been advanced. For instance, a hypothesis has been suggested that cyclones move passing around a closest larger in size anticyclone. Other hypotheses were that cyclones move along tongues of warm air, in the middle and upper troposphere, or in the direction of steering current (wind at some level or layer). In different countries different forecasting techniques were suggested. Unfortunately, the qualitative techniques have not always yielded reliable results. This fact prompted meteorologists to search for new objective methods of storm movement forecasting.

Simple objective forecasting techniques

The simplest objective forecasting can be performed by just extrapolating a cyclone path. With the set of precise

6-hr data for the previous 24 hours a formal extrapolation of cyclone path may not be inferior to the most skilled forecasting techniques. The highest precision has been gained in extrapolatively forecasting cyclone paths in the westward direction in low latitudes. The formal extrapolating should not be applied when a cyclone exercises loops and humps on its travel.

The past tracks of tropical storms have been charted to form a base of climatological prognoses. It is essentially an assumption that a cyclone will move in the same manner (in the same direction and with the same speed) as the cyclone that was observed in the very place and month earlier. Since in some areas cyclones tend to move along a modal path the climatological forecasting often produces good results. This way of prognosis has an obvious advantage over extrapolation—the forecaster need not know a precise previous position of the storm. Practically, forecasters often employ various mixed combinations of extrapolation and climatological technique.

Sophisticated objective forecasting techniques

In 1950, Riehl and coworkers advanced a method of forecasting which uses historic data in setting up a diurnal forecast regression equation. The equation was to yield the projected meridional and zonal components of tropical cyclone motion basing on the respective wind components at 500 mb. The wind components were measured in the points of the grid extended 7.5° longitude both to the west and to the east, 5° to the south and 5-10° latitude to the north from the center of a cyclone. Subsequently this method has undergone numerous improvements. The latest and most sophisticated modification indexed NC-73 was suggested in 1973. The method is a combination of formerly known techniques and differs in a large amount of data required.

In 1963 in Honkong the so-called control point technique was first verified. It is based on a good correlation between wind direction in some points aloft over a cyclone and the movement of its center. The method has been verified for six years to yield positive results.

An especial emphasis in the development of this method has been placed on careful drawing the tracks of studied

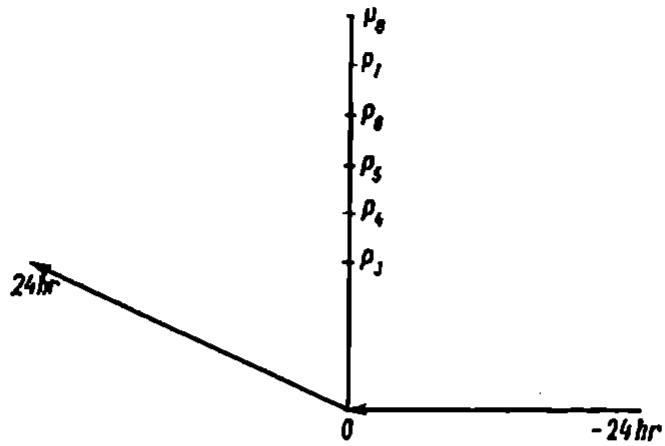

Fig. 6.13 Illustration of reference points arrangement

storms. From the latest point of a track a perpendicular was set to the right, looking downstream; in six points on this perpendicular, spaced at 1° latitude from 3° to 8° (see Fig. 6.13), the deviations of wind direction were measured from the 24-hr direction of the cyclone. For typhoons, the smallest deviation was found at 5° point, P_5, of the 500-mb surface. For less intense cyclones, as the most attractive is recognized point P_4 at the same surface. These points were labelled the control points. This procedure was performed on 230 cyclonic movements with storms of various intensity, including mature and immature typhoons.

With this technique, to effect prognosis of a cyclone it is sufficed to reliably determine the direction of wind in the control point. This direction indicates where the cyclone is intended to move in the next 24 hours.

The speed of a cyclone was computed as a half sum of the mean speed of cyclones having passed in this area in this month (climatic speed) and the speed of a studied cyclone for the last 12-24 hours.

The reference point method is fairly simple and does not require data from over the center of a storm.

In 1968, R. J. Renard suggested another advanced method of prognosis based on the steering current concept. It uses charts of mean flow compiled by numerical methods. During 12-24 hours prior to time zero the cyclone movement is monitored in an attempt to evaluate deviation from the mean

stream. This deviation, if found, is introduced in the forecast as a correction.

Verification of tropical storm forecasts indicate that the mean error of diurnal forecast varies between 160 and 170 km in low latitudes, rising to 300 km in higher latitudes. It is found that various methods markedly differ in skill when forecasting in the identical synoptic situations. In low latitudes best results have been obtained with statistical prognosis, in higher latitudes with climatic prognosis. Forecasting with dynamic models so far has been far from ideal even though some results have been fairly promising.

6.6 Analysis and Prediction of Storm Intensity on Satellite Data

Surveillance of tropical storms by meteorological satellites provides valuable information about their movement and intensity. From satellite photographs meteorologists evaluate the stage of maturity of a cyclone and its intensity—all from the clues that give the cloud system of cyclones. We shall follow the cloud systems of various life cycle stages using data compiled by L.S. Minina.

In the formative (disturbance) stage of cyclones development, satellite pictures exhibit disorderly scattered cumuloformi, stratus and cirrus clouds. Gradually the amount of clouds increases along with their depth, and cloud bands form. However, at this stage the bands exhibit disruptions, humps, deflections and other nonuniformities. The whole cloud system has an irregular shape and is unsymmetrically placed with respect to the center of forming cyclone.

At the stage of cyclonic vortex, represented on the chart by one or two closed isobars, the cloud field on satellite photographs looks as an enlarged comma turned eastward with its convex part. The cloudiness becomes more dense, the amount of gaps decreases.

When cyclonic vortex attains the maturity of intense tropical storm, satellite pictures portray a more wide, thick and ordered cloud field. A bright, clear-cut band of convec-

tive clouds appears. Most often this cloud band looks as a turn of the helix. A central cloud system begins forming; this system is overlaid by a cirrus dock which may cover the eye of storm already formed by this moment.

If a mature cyclone builds up into a hurricane the cloud system becomes even more dense and extended. Cloud bands concentrate around the center of the cyclonic circulation. Spiralling outward from the center field, these bands can be 100-200 km wide and up to 900 km long. They are oriented in accordance with the direction of wind in the cyclone. Clusters of cumuloformi are evident on the edge of the cloud field. At this stage, most pronounced are cirrus clouds and their structure is more distinct. Separate bands of cirrus clouds indicate spreading of the air in upper layers above the storm. Black spot of the eye is, as a rule, clearly distinctive on the background of the white cloudiness.

Early stages of filling a cyclone can be evaluated on satellite photographs by an oval shape of the cloud system and its diffuse edges. In the process of further disintegration the cloud system breaks into separate spots. Cirrus cloudiness disperses. So far as the cyclone remains sufficiently intense the eye is evident. When the eye acquires double structure, its walls become diffuse, or the eye disappears at all, the cyclone can be deemed as filled.

From the characteristic pattern of cloud systems in various stages of life cycle of cyclones in the Pacific a technique designed to forecast their evolution has been developed. An image from a satellite photograph is compared with the set of easily discernible cloud patterns describing various stages of cyclone development and decay. The procedure envisages five sequential stages of comparison.

Stage one. Evolution of a cyclone is estimated from the moment of previous observation. The procedure does not specify any time interval between observations, yet the collected experience indicates that material changes in cyclonic image may be evaluated in 12-16 hours. Therefore the evolution is estimated by comparing the latest picture with one of the previous shots made at least 12 hours ago. The results of the comparison undergo coding. Developing disturbance is coded by the letter *D*, weakening one by *W*, and that remaining in steady state by *S*. To make a decision

on the current changes of a cyclone the following sets of signs are employed.

Signs of developing disturbance (cyclone)

1. The eye is well seen:

(a) the eye becomes more distinct, enlarged, and the clouds around the center gain in density;

(b) the most dense clouds contract to the center of cyclone.

2. The eye is out of sight, the center of cyclone is covered by dense cloud canopy:

(a) the center dense cloud cover (DC) has changed in shape from an irregular outline to a polygon, or from a polygonal to an oval or round shape;

(b) the DC does not change in shape, but is enlarged in area.

3. An overcast cloud canopy is observed consisting of quasi-circular bands:

(a) the bands around the center part of cyclone widened;

(b) the bands remain in their previous width yet change their curvature becoming closer to a circular shape.

Signs of weakening disturbance (cyclone)

1. The eye is well seen:

(a) the eye becomes less distinctive, the clouds in the eye wall become less dense;

(b) the dense clouds spread farther from the center.

2. The eye is out of sight, the center of the storm is covered by a dense cloud canopy:

(a) the DC outlines appear more diffuse and are changing to irregular shape;

(b) the area of the DC contracted.

3. An overcast cloud canopy is observed consisting of quasi-circular bands:

(a) the bands around the center part of the storm narrowed;

(b) the cloud bands assumed an irregular (noncircular) shape.

Signs of stable disturbance (cyclone)

When satellite pictures do not reveal any material changes then the disturbance is concluded to remain in its previous state.

Stage two. From the structure of the cloudiness portrayed on a satellite image it is decided what state the cyclone assumes at a given moment. The cloudiness appearance, however, not always gives the clues on the intensity of the cyclone in general, since the intensity depends also on the wind speed (see Stage three).

Evaluation of a state of cyclone is the most complicated operation involving certain subjective shadow.

The code employed in the model envisages the following conventional notation to denote the states of a cyclone. A shortly formed and only slightly discernible disturbance is assigned the number $T = 1$, a large mature hurricane is assigned the other extreme value $T = 8$, intermediate states are coded by the numbers from 3 to 7. In some situations fractional numbers ($T = 1.5$ or $T = 2.5$, etc.) are used. Evaluation of T requires certain experience and necessitates continuous tracking of the cyclone.

At a first evaluation of a cyclone the value of T is found as the sum

$$T = C + B$$

where C is the number characterizing the cloudiness in the central area of a cyclone; B is the number characterizing the cloud bands.

To facilitate assessment of the number C the diagram of Fig. 6.14 is recommended, which considers the presence or absence of a dense cloud cover in the central part of a disturbance (DCC), its size and shape, size and shape of the eye, and the structure of cirrus and convective cloudiness at the center of disturbance. Working with the diagram, the analyst should take into account the following.

1. The DCC is a dense overcast cloudiness, well developed in the vertical and covering the central area of the disturbance, or encircling the eye of the storm. A shape of DCC gives clues to estimate the state of the disturbance when the eye is either out of sight at all, or hardly distinctive. In deepening storms the shape of DCC changes from irregular to oval or from oval to round (Fig. 6.15).

2. To estimate the state of a disturbance when the eye of the storm is out of sight, or is seen yet not discernible enough, it will be of value to know the size of DCC in degrees

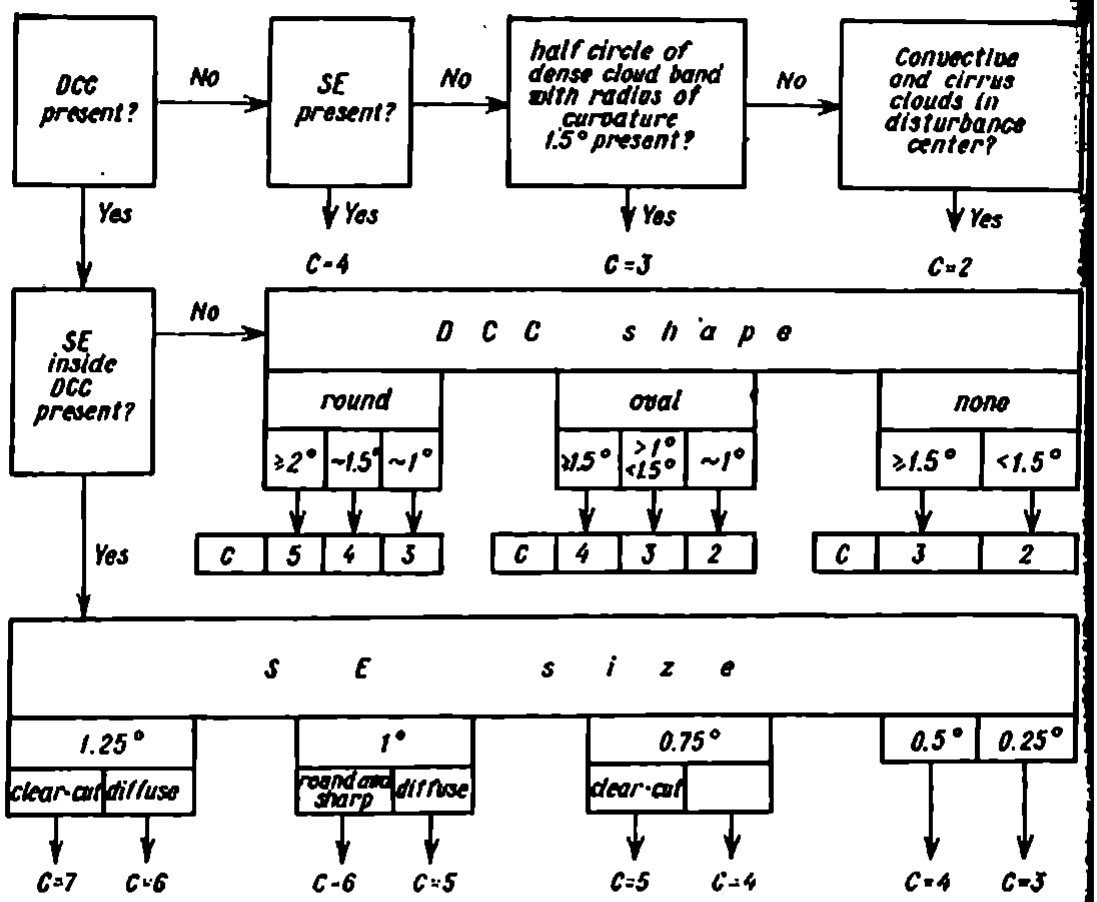

Fig. 6.14 Defining C-number which characterizes the cloudiness in the center of cyclone; *DCC*—dense cloud cover in the central area; *ES*—the eye of storm

latitude. The dimensions of other cloud characteristics are also determined in latitudinal degrees.

3. The boundary of DCC has clear-cut edges when the storm is deepening. Closer to maturity the boundary generally changes from destructive to more continuous. As soon as the development ceases, the boundary becomes diffuse and poorly discernible.

4. If DCC is absent then the size of eye is estimated by a circular gap in the cloudiness defined with the cloud bands around this free ring (Fig. 6.16).

5. Development of a disturbance can be traced through changes in the cloud pattern either as a combination of

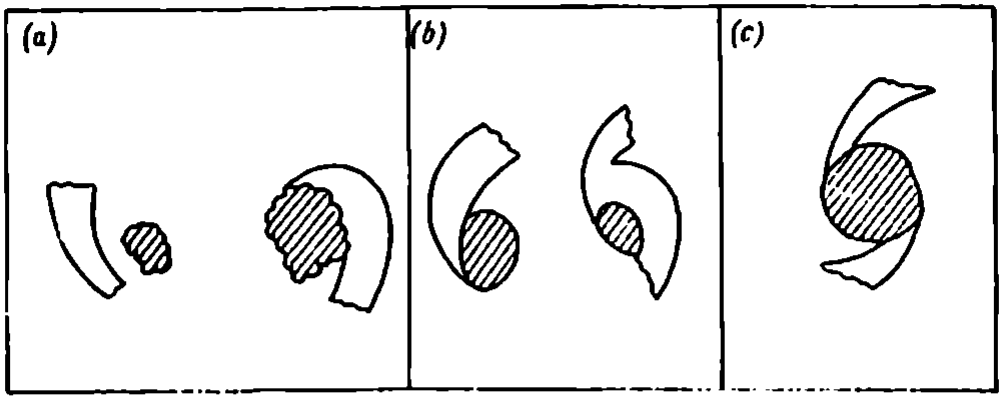

Fig. 6.15 Shape of continuous cloud canopy in the central area of a cyclone (*DCC*); (*a*) irregular, (*b*) oval, and (*c*) round

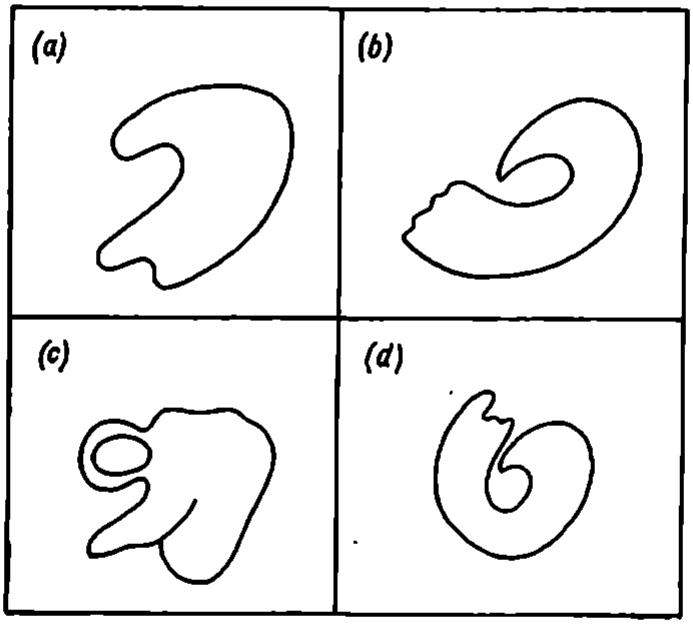

Fig. 6.16 State of disturbance prior to (*a* and *b*) and during (*c* and *d*) the formation of the eye

convective cloud bands (inflow of air inside the cyclone) or as a field of cirrus clouds (outflow of air from the cyclone) and presence of a DCC. In the circumstances two cases are possible.

Case 1. A curvilinear band of convective clouds is seen around the central part of disturbance covered by an over-

cast cloud canopy. If the canopy consists of a cirrus clouds massive $\geqslant 3°$ in diameter, then it implies that the current aloft is weak or anticyclonic one and conditions are present for the cyclone to deepen. If the cirrus clouds over the central part arrange in an elongated pattern, thus indicating a streamlined flow in one direction, it signifies that no conditions exist for the cyclone to develop.

Case 2. When a photograph displays a convective cloudiness arranged in bands and implying a well-developed inflow, the elongation of cirrus cloudiness clustered in streets at the center may be discarded. Appearance of dense cloud cover near the center of the storm and increasing in size to about 1° latitude or more indicates favourable conditions for development of the cyclone.

Having obtained the number C, the analyst may proceed to evaluating the number B.

The index B is related to the amount of dense continuous cloudiness represented on a satellite picture as a band gradually curving around the central area of the disturbance within a radius of 4° latitude from the center.

$B = 0$ when only a few clouds of quasi-circular shape are present around the center of disturbance, or the clouds are absent at all.

$B = 0.5$ when a cloud band 0.5 to 1° wide goes round the central area of disturbance yet fails to complete the circle by a large arc (Fig. 6.17*a*).

$B = 1$ when the band of clouds having a width about 0.5° almost totally encircles the center area, or when the cloud band 1.5° wide borders a larger portion of the circle around the center area (Fig. 6.17*b*).

$B = 1.5$ when the cloud band about 1° wide completely encircles the disturbance center, or when the band of clouds 1.5° wide almost encircles the center area (Fig. 6.17*c*).

$B = 2$ when a band of clouds of any width turns a few times around the center of disturbance (Fig. 6.17*d*).

A sum $C + B$ yields a primary value of T. In subsequent continuous monitoring the disturbance, or storm, the variable T changes in accordance with varying state of the disturbance, that is, with the results of Stage one. In the model, T is to vary in the process of reinforcement or decaying a disturbance by 0.5 or 1 full unit a day, yet it cannot go beyond

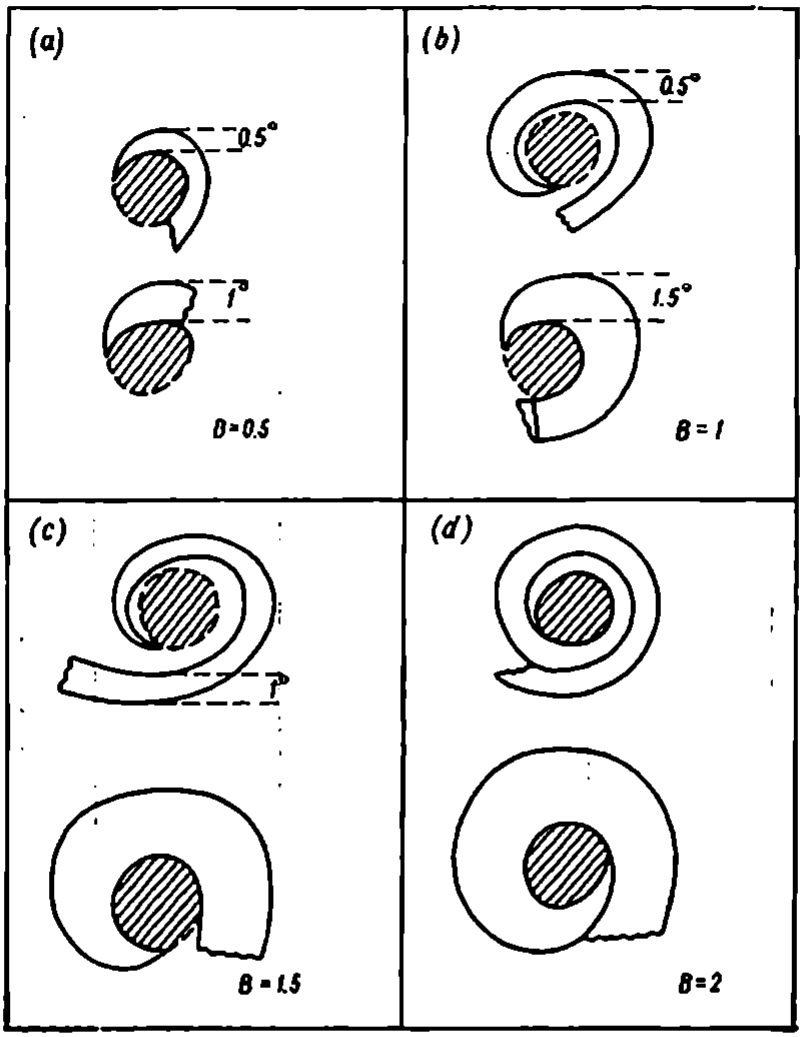

Fig. 6.17 Schematic cloud bands at the center of a cyclone

8. When a disturbance is developing, a primary T is incremented by 0.5 or 1 (depending on how fast the evolution is progressing); when a disturbance loses its intensity, T is subtracted by 0.5 or 1, respectively. The resulted T characterizes the state of cyclone over the current observational period.

Similar operations are repeated at any next observational time until the cyclone fills up or recurves into extratropical latitudes. A weak point of this stage is in that the analyst has to make a decision judging the evolution of a cyclone

subjectively. However, if data are available about the strongest wind or lowest pressure in the cyclone, then this subjective decision may be appropriately corrected (see below).

Stage three. At this stage the analyst determines a current intensity of disturbance (cyclone) and describes it by a conventional number I. The variable I is found according to the values of strongest wind in the cyclone, V_{max}, and lowest pressure at sea level in the center of cyclone, p_{min}, (Table 6.1) or the value of T if the two former variables cannot be determined. Accordingly there may be two situations.

Table 6.1 Relation of current intensity, I, strongest wind, V_{max}, and lowest pressure at sea level, p_{min}, in tropical storms of northern Pacific

I	V_{max}, m s^{-1}	p_{min}, mb	I	V_{max}, m s^{-1}	p_{min}, mb
1.5	12	1004	5	42	964
2	15	1001	5.5	48	954
2.5	18	997	6	55	942
3	22	992	6.5	62	928
3.5	26	987	7	70	914
4	31	982	7.5	79	900
4.5	36	973	8	90	885

In one of them V_{max} and p_{min} are unknown. The model is designed so that when the cyclone is in steady state (S) or is developing (D) the cloud field pattern well correlates with V_{max} and values of T and I are identical. Therefore, if Stage one results in D or S code, I is found as T and for this value of I the corresponding V_{max} and p_{min} are looked up in Table 6.1.

In filling cyclones wind speed markedly decreases in about 24 hours since the cloud characteristics have degenerated indicating thus that the disturbance is reducing. Hence, a change in T will be 0.5 ahead of the corresponding change in I. For example, if $T = 6$ and the cyclone is filling the current intensity will be $I = 6.5$.

On the other side, when V_{max} and p_{min} (or at least one of them) are known, the number I is looked up in Table 6.1

and the found value is used to correct the respective value of T to make all the further estimations of the state of cyclone with this corrected value of T.

Stage four. At this stage the trend of cyclonic evolution is evaluated. Satellite images portray some or other signs of deepening or filling of storm. The objective is to evaluate from satellite photographs and the set of signs of Table 6.2 the current behaviour of cyclone: intensifying or weakening of the inflow in the lower and the outflow in the upper layers, and ascending motions in the storm. When these processes intensify, the cyclone deepens, when they weaken the cyclone fills. The evolution of a cyclone can be decided by the integral pattern of the cloud cover. When all the cloud cover appears as a comma on a photograph, this implies that the cyclone is deepening. If the cloudiness appears as a circle, or a shape close to it, the cyclone is recognized as filling. To estimate the evolution of a disturbance more accurately the analyst should employ all the set of signs.

When the current evolution of a cyclone does not differ from the evolution 24, or 12, hours back, the results of Stage four may not be taken into account. When no such correspondence is in sight, the coding letters D, S and W, i.e. the results of Stage one, receive a plus or minus sign.

A plus sign is added when for the latest 24 hours the cyclone has weakened or remained unchanged and the latest shot delivers signs of its deepening. This sign is also added when the average development rate of the cyclone for the latest 48 hours has exceeded the pace of the model, that is the number I has changed, say increased, by more than 2 units.

A minus sign is added when the diurnal evolution indicates a steady state or deepening, and the latest photograph indicates the current weakening, or when the average weakening rate for the latest 48 hours has exceeded the rate of the model, that is when the number I has changed, say decreased, for the latest 48 hours more than by 2 units.

Stage five. The final stage endeavours a prognosis of evolution of cyclone for the next 24 hours. As the result of the four previous stages the forecaster has at hand a conditional characteristic of the cyclone, including indices D, S, and W, the number I, and, at times, additional signs for the indices. For example the code $D5.5$ indicates that for the

Table 6.2 Characteristic signs of evolutionary trend in tropical cyclones

Process	Signs indicating	
	reinforcement	weakening
Inflow at low levels	1. Bands of convective clouds spiral inward penetrating the central cloud massive at large angles	1. Bands of convective clouds have diffuse edges, or are undiscernible
	2. The outlines of dense and continuous clouds are clear-cut and contrastive	2. Bands are discernible, they uniformly encircle the central part of disturbance
Outflow at upper levels	1. Cirrus clouds make the disturbance image look obscure away from the center, at least from three sides	1. Cirrus clouds have greyish shade and show a small anticyclonic curvature
	2. Cirrus clouds seen as anticyclonically curved bands	2. Cirrus clouds exhibit clear-cut edges at one side of disturbance and diffuse edges on the opposite side
Ascending motions	1. Dense clouds in the central part of disturbance look bright and reveal sharp boundary, at least in one quadrant	1. Small amount of cirrus clouds is seen at the very center of disturbance
		2. Dispersed or cell-like remnants of formerly dense cloudiness are evident around the center

last 24 hours the cyclone has deepened, but the latest shot reveals the signs of its filling; the current intensity of the storm amounted to 5.5 conditional units.

The objective of the forecast is to predict intensity of a cyclone in 24 hours. The forecast is based on the data of

Table 6.3 Modelled variation of intensity in tropical cyclone for 24 hours

Code	*I* number														
	Current intensity														
–	1	1.5	2	2.5	3	3.5	4	4.5	5	5.5	6	6.5	7	7.5	8
	24-hr projected intensity														
D	1.5	2	3	3.5	4	4.5	5	5.5	6	6	6.5	6.5	7	7.5	8
S	1	1.5	2	2.5	3	3.5	4	4.5	5	5.5	6	6	6.5	7	7.5
W	1	1	1	1.5	2	2.5	3	3.5	4	4.5	5	5.5	6	6.5	7

the modelled development of cyclones presented in Tables 6.3 and 6.4. Table 6.3 relates the current intensity with the expected intensity in 24 hours, and Table 6.4 displays corrections to the expected intensity for those codes having a plus or minus sign.

In accordance with Table 6.3 the expected intensity in the discussed example must be 6 units. However the minus

Table 6.4 Corrections to forecasted intensity

Code	$+D$	$+S$	$+W$	$-D$	$-S$	$-W$
Correction	+0.5	+0.5	+1.0	−1.0	−0.5	−0.5

sign bounds to introduce a correction of −1.0 from Table 6.4. Therefore the expected intensity will be 5 units.

Prognosing evolution of tropical cyclones on the above lines the forecaster may take into account the signs of especially intense hurricanes which are sometimes called superstorms. The storms whose intensity is given by the number I equal to 7 or 8 usually form from the disturbances that also display great intensity ($I = 6$). The characteristic features of such hurricanes are

(a) widening of DCC or bands and increasing their number;

(b) a band of wide uniform structure which completely encircles DCC of round shape, with the eye of regular shape and clear-cut outlines in the center;

(c) appearance of the eye, when inside of one wall of clouds another wall may be seen of smaller size and in lower levels.

6.7 Impact of Tropical Storms

Damaging impact of tropical storms is due to winds of hurricane force, hurricane waves, and floodings caused by heavy showers. Majority of storms inflict heavy losses either because of strong wind or because of storm waves. However, in mountainous areas damaging effects can be produced by powerful surface runoffs smashing everything on their run down.

Kinetic energy head of wind rises as square of the wind speed. Also it depends on the shape of the obstacle counteracting the stream pressure.

Intensity of storm waves depends on wind speed, pressure gradient, topography of sea bottom, and profile of coast line. When a cyclone is rushing inland it piles the waters up into huge tides that sweep the seaboard. A well-developed storm can uplift water walls 1.5 to 8 m high, and in narrow bays even higher. These huge water walls accompanied by intense sea swells and strong winds represent the most devastating forces of storm.

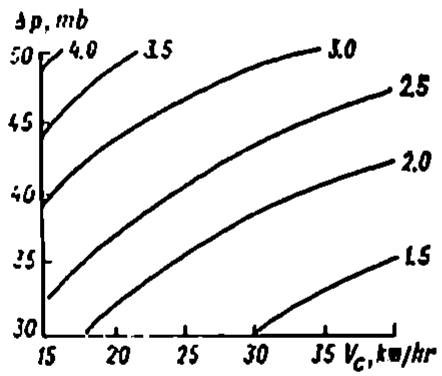

Fig. 6.18 Height of waves (meters) computed as a function of model intensity of a cyclone (pressure deficiency at the center $\Delta p = 1013 - p_0$) and its travel velocity V_c along the SW to NE path within the framework of the numerical model of storms for the Bay of Bengal (after Das, Singh, and Balasubramaniam)

Height of storm waves unleashed by a tropical cyclone may be computed with mathematical models based on the shallow water equations. Some shorelines have the diagrams calculated to predict swells for tropical cyclones in the area. Figure 6.18 illustrates such a diagram for the Bay of Bengal. It is seen that the highest waves should be expected with the slowest cyclone of lowest pressure in the center.

Passage of any tropical storm may entail casualties and

losses in spite of warning systems introduced in many countries and activated means of protection. Table 6.5 lists the most damaging storms of 1974-77. Of the 27 storms recorded, casualties have not been reported only for 4 storms, and 5 storms have not inflicted life losses; in 12 cases the count of people suffered exceeds 100, while in half of the storms more than 100 people have been killed. Material losses have not been reported for only 3 storms and only in one case the loss is reported to have been small; in all the other cases material losses have run into significant sums of money.

According to data published in the United States, material losses caused by hurricanes increase from one year to the next. In some cases, reportedly, a hurricane caused a direct loss exceeding a thousand million dollars. However, indirect losses due to production break down may add to this figure substantially.

The United States develop methods of artificial hurricane damping so that to abate the speeds of wind. The expected results have been estimated to diminish the wind in hurricanes by about 15 per cent. This would effect in reduction of the hurricane strength by at least 30 per cent. For the country it would entail a 100 million dollars diminished loss as referred to an average hurricane. If it proves successful, similar economy might unburden losses in the other parts of the globe.

High-skill short-range forecasts of motion and evolution of tropical storms are another means preserving economy from heavy losses. Timely issued warning about a narrowing storm may activate avoidance measures thus protecting the population and possibly damping inavoidable losses. Accurate forecasts of storms are also of primary importance for the areas depending on the amount of rainfall. In many arid areas tropical cyclones relieve the drought and fill water basins and reservoirs. An average tropical cyclone can downpour 250-500 mm of rain. In mountainous areas the rainfall is 2-3 times higher. Correct prognoses on an advancing tropical cyclone may be used to advantage in arid areas so as to retain the poured water.

Meteorologists see but another important side of tropical cyclones: the influence exerted on the processes of the general circulation. We have already mentioned the important part

Table 6.5 Intensity of and losses (from published data; "—" implies

Country	Date	Name	Intensity		
			lowest pressure, mb	highest wind, m s⁻¹	rainfall, mm
		1974			
Madagascar	January	Esmeralde	—	—	—
Tanzania	April	Norina	—	—	—
Japan	July	Jilda			
Japan	September	Polly	—	—	—
Japan	September	Shirley			
Australia	December	Trixi	—	77	—
		1975			
Madagascar	January	Camille	—	56	—
Madagascar	January	Fernanda	963.5	56	—
Mauritius	February	Jervese	951.0	57	—
New Caledonia	March	Alison	942	53	—
Japan	August	Phyllis			
Japan	September	Rita	—	—	—
Japan	October	Kira			
USA	September	Heloise	—	—	300
India	October	—	—	45	—
Australia	December	Joan	—	—	—
		1976			
India	September	—	—	40	—
Japan	September	Fran	—	—	1138
Mexico	October	Liza	—	—	—
India	November	—	—	40	—
		1977			
Madagascar	January	Emilia	—	50	—
Madagascar	January	Harvey	—	50	—
Japan	July	Vera	—	70	—
Japan	August	Bimy	—	—	662
Japan	September	Babe	907.3	—	—
Japan	September	Emma	—	—	—
India	November	—	941.0	—	—

due to tropical storms of 1974-77
no information available)

Casualties			Material losses
killed	wounded	homeless	
8	—	—	$ 13 000
—	—	—	$ 140 000
163	208	—	28 263 mln. yens
50	—	—	280 mln. dollars
2	—	1 700	—
0	—	134	—
6	—	—	$ 150 mln.
—	—	—	55 mln. French francs
108	—	—	88 bill. yens
a few people	—	170	$ 150 mln.
85	—	—	750 mln. rupees
—	—	—	25 mln. dollars
40	—	—	2 240 mln. rupees
167	455	—	250 bill. yens
000	200 000	—	700 mln. pesos
150	—	—	—
31	—	30 000	$ 73 mln.
5	—	6 750	—
a few people	—	—	$ 24 mln.
0	—	—	$ 24 mln.
1	139	—	$ 84 mln.
9	—	—	$ 8 mln.
10 000	—	—	—

played by the tropical atmosphere in the global circulation system. Tropical cyclones represent an important part of this circulation. Numerical models for climatic outlooks require realistic description of all processes in the tropical atmosphere, including interactions between different scale systems, which may bring about disturbances in a basic stream, such as tropical cyclones. The tropical storms, in turn, exert their influence on the basic current to change its character and thus to extend their effect on the atmospheric circulation at least on the regional scale.

Tropical cyclone give rise to intense penetrating convection cells producing cumulus and cumulonimbus clouds, which are hot tower energy suppliers to the upper atmosphere. The energy exported aloft drifts with outgoing currents toward higher latitudes giving birth to new disturbances and, hence, transforming processes of the general circulation. In short, tropical cyclones being the local circulation systems can play an essential part in the formation and evolution of the global atmospheric circulation.

Review Questions

1. List the areas where tropical cyclones appear. Where do they occur most often?
2. Which time of the year is marked by the highest frequency of tropical storms?
3. What should be the conditions for a tropical cyclone to form?
4. Describe the process of forming a tropical cyclone.
5. The oceans play an essential part in forming a tropical cyclone. Why?
6. What is the effect of convection in appearance and evolution of tropical cyclone?
7. Which stages passes a tropical cyclone in its evolution? Characterize each stage.
8. How can the tropical cyclones be differentiated from the viewpoint of their intensity?
9. How is the surface pressure distributed in a tropical cyclone?
10. What is the wind profile in a tropical cyclone? Where can the belt of highest winds be found?

11. What are the horizontal and vertical profiles of the tangential and radial components of wind in a tropical cyclone?
12. What is the temperature distribution?
13. Characterize the cloudiness in a tropical cyclone.
14. What is an average rainfall brought by a tropical cyclone? Why is this rainfall difficult to measure?
15. What approach can be used to determine the rainfall in a tropical cyclone?
16. What is the eye of a storm? How can its size be estimated? What is the weather in an eye?
17. Characterize in general the relation of highest wind and lowest pressure in a tropical cyclone?
18. In which direction and at what speed the tropical cyclones travel most frequently?
19. List main ways to forecast travel of tropical cyclones.
20. What is in essence the reference point method?
21. Describe the satellite image of cloud system at various stages of development of a cyclone.
22. How can the evolution of a tropical cyclone be estimated from satellite photographs?
23. The satellite image of a cyclone can reveal its intensity. How?
24. How can the trend of the current evolution of cyclone be determined?
25. Forecast the evolution of a cyclone if at time zero its conditional characteristic is $+S4.5$.
26. What are the main dangers of tropical storms?

BIBLIOGRAPHY

In English

Haltiner, G. *Numerical Weather Prediction*. Wiley and Sons, 1971.
Holton, J. R. *An Introduction to Dynamic Meteorology*. Academic Press, 1972.
Palmen, E. and Newton, C. W. *Atmospheric Circulation Systems*. Academic Press, 1969.
Ramage, C. S. *Monsoon Meteorology*. Academic Press, 1971.
Riehl, H. *Tropical Meteorology*. McGraw-Hill Publishing Co., 1954.
Riel, H. Climate and Weather of Tropics. Academic Press, 1979.

In Russian

Abramov, R. V. Basic factors of diurnal variation in the surface layer over the equatorial oceans. *Meteorologiya i Hydrologiya*, 1977, 2.
Belevich, R. R. Spatial distribution of temporal pressure variation in the atmosphere of equatorial Atlantic. *Meteorologiya i Hydrologiya*, 1975, 1.
Borovikov, A. M. and Nevzorov, A. N. Aircraft observations of cloudiness during GATE'72 mission. *Meteorologiya i Hydrologiya*, 1974, 11.
Burlutsky, R. F. On the structure of tropical atmosphere in formation of typhoons. *Meteorologiya i Hydrologiya*, 1964, 3.
—Causes of burst and invasion boundaries of the summer Indian monsoon. *Meteorologiya i Hydrologiya*, 1974, 9.
—Bel'skaya, N. N., and Selezneva, V. S. The summer monsoon in the Arabian Sea. *Meteorologiya i Hydrologiya*, 1973, 2.
Vitvitskii, G. N. *Atmospheric Circulation in the Tropics*. Gidrometeoizdat Publishers, Leningrad, 1971.
Gedeonov, A. D. On the latest African droughts. *Meteorologiya i Hydrologiya*, 1975, 5.
Gruza, G. V. and Gres'ko, P. D. *Statistical Forecasting of Tropical Cyclone Paths in the Atlantic*. Gidrometeoizdat Publishers, Leningrad, 1977.
Dobryshman, E. M. Wind and pressure fields in the equatorial region. *Meteorologiya i Hydrologiya*, 1964, 5.
—On the waves in the equatorial belt. *Meteorologiya i Hydrologiya*, 1977, 1.
—and Fal'kovich, A. I. On some models of stationary motion in the equatorial atmosphere. *Meteorologiya i Hydrologiya*, 1967, 7.

Ingel, L. Kh. On the theory of tropospheric circulation in the equatorial latitudes. *Meteorologiya i Hydrologiya*, 1977, 6.

Kats, S. A. The formation and vertical structure of the summer ITCZ in the Indian Ocean. *Trudy Hydrometeotsentra*, USSR, 1972, 107.

Kopycheva, V. S. and Svetlova, T. P. The structure of rainfall field in the tropical Atlantic. *Meteorologiya i Hydrologiya*, 1976, 10.

Koshel'kov, Yu. P. Differences in the circulations of the northern and southern hemispheres. *Meteorologiya i Hydrologiya*, 1974, 7.

Krivelevich, L. M. and Romnov, Yu. A. Some features of atmospheric circulation over the equatorial oceans. *Meteorologiya i Hydrologiya*, 1977, 5.

Lebedeva, N. V. and Zaval'skaya, N. A. The conditions in the convection of the ITCZ over the eastern Atlantic. *Meteorologiya i Hydrologiya*, 1974, 5.

Litvinenko, L. I. Zonal circulation in the equatorial latitudes. *Meteorologiya i Hydrologiya*, 1966, 3.

—On the air mass transfer between the southern and northern hemispheres. *Meteorologiya i Hydrologiya*, 1965, 6.

Mamedov, E. S. and Pavlov, N. I. *Typhoons*. Hydrometeoizdat Publishers, Leningrad, 1974.

Marchenko, A. S. On defining the highest wind speeds in tornados and tropical storms. *Meteorologiya i Hydrologiya*, 1981, 5.

Minina, L. S. *Practice of Nefanalysis*. Hydrometeoizdat, Leningrad, 1970.

—and Chan Din Ba. On the size of cloud systems in typhoons. *Meteorologiya i Hydrologiya*, 1974, 12.

Morozova, I. V. Conditions of cloudiness in the tropical part of the northern Atlantic. *Meteorologiya i Hydrologiya*, 1975, 1.

Nguen Cuan-Zui and Yudin, M. I. On the theory of inertial waves in the low latitudinal atmosphere. *IAN USSR, Fizika Atmosphery i Okeana*, 1972, VIII, 10.

Petros'yants, M. A. and Fal'kovich, A. I. On the diurnal variation of weather elements in the GATE region. *Meteorologiya i Hydrologiya*, 1977, 7.

—Snitkovskii, A. I. and Fal'kovich, A. I. On the circulation of air in the ITCZ. *Meteorolygiya i Hydrologiya*, 1977, 5.

Ponomarenko, S. I. The conditions for convective cloud cells and precipitation in the trades and equatorial areas of the Atlantic. *Meteorologiya i Hydrologiya*, 1975, 6.

—and Glasovo, O. P. Location and evolution of the ITCZ in the Atlantic and Indian Ocean on June 4-July 12 and August 1-9 of 1971. *Trudy Hydrometeotsentra*, USSR, 1972, 109.

—The thermodynamic conditions for the formation of convective clouds and showers in the Indian Ocean. *Meteorologiya i Hydrologiya*, 1976, 6.

Romnov, Yu. A. Divergence and vorticity charts of the resultant wind over the Indian Ocean. *Trudy IOAN*, 1965, vol. 78.

Romanova, N. A. and Romanov, Yu. A. On the pressure gradients in the equatorial latitudes. *IAN USSR, Fizika Atmosphery i Okeana*, 1965, 11.

—Some features of wind field at the equator as a function of pressure distribution. *Meteorologiya i Hydrologiya*, 1974, 6.

Semenov, E. K. Some elements of the ITCZ as viewed by satellites. *Meteorologiya i Hydrologiya*, 1975, 2.
—On the aerocllmatology of the equatorial westerlies in the lower troposphere. *Meteorologiya i Hydrologiya*, 1974, 2.
—On the structure and migration of the equatorial westerlies in the eastern hemisphere. *Meteorologiya i Hydrologiya*, 1974, 9.
—Cloud clusters of the ITCZ in the Indian Ocean. *Meteorologiya i Hydrologiya*, 1977, 6.
—Tropical cyclones in the southern hemisphere. *Trudy Hydrometeotsentra*, USSR, 1967, 13.
Sitnikov, I. G. Numerical analysis and forecasting of tropical storms and their motion. *Meteorologiya i Hydrologiya*, 1964, 10.
—Scaling analysis of the dynamic equations for the tropical atmosphere. *Trudy Hydrometeotsentra*, USSR, 1077, 197.
—Numerical modelling of tropical cyclones and forecasting of their paths. In: *Tropical Oceans and Related Global Processes*. Hydrometeoizdat Publishers, Leningrad, 1973.
—and Agrenich, E. A. On the theory of tropical cyclone motions in a baroclinic atmosphere. *Trudy Hydrometeotsentra*, USSR, 1974, 145.
Tarakanov, G. G. On the motion of tropical cyclones in the central Atlantic. *Trudy Hydrometeotsentra*, USSR, 1975, 141.
GATE'72. *Works of the Geophysical Mission on the National GARP Program*. Edited by M. A. Petrosyants, D. L. Laikhtman, V. N. Ivanov, and V. S. Samoilenko. Hydrometeoizdat Publishers, Leningrad, 1074.
GATE'74. *Collected works of the expedition with the GARP experiment*. Vol. 1. Atmosphere. Edited by M. A. Petrosyants, A. M. Borovikov, V. N. Ivanov, V. S. Samoilenko, A. I. Snitkovskii, and E. M. Feigel'son. Hydrometeoizdat, Leningrad, 1976.
Fal'kovich, A. I. *Dynamics and Energetics of the Intertropical Convergence Zone*. Hydrometeoizdat, Leningrad, 1979.
—and Sharonova, V. A. Scaling factors of weather elements from GATE'72 mission. *Meteorologiya i Hydrologiya*, 1974, 11.
Khromov, S. P. On the character of the ITCZ. *Izvestiya VGO*, 1960, vol. 93, 2.
—The types of surface wind distributions at the equator. *Izvestiya VGO*, 1961, vol. 93, 2.
—The nature of rainfall over the tropical oceans. In: *Quasi-biannual Cycle and Circulation in the Atmosphere and Ocean*. Hydrometeoizdat, Leningrad, 1971.
—Kats, A. L. and Burlutsky, R. F. The structure of the ITCZ in the Atlantic. In: *Quasi-biannual Cycle and Circulation in the Atmosphere and Ocean*. Hydrometeoizdat, Leningrad, 1971.

INDEX

A

Accretion, 65
Adjustment of wind-pressure fields, 49
Air mass, 98, 101, 102, 108, 109, 117
  continental
    mid-latitude, 104
    tropical, 102
  maritime
    equatorial, 103, 136
    mid-latitude, 104
    trades, 103
    tropical, 103
  polar, 140
  stably stratified, 114, 136
Anticyclone, 122
  dynamic, 122
  high-level, 122, 129
  low-level, 122
  Siberian, 134, 136
  subtropic, 107, 117
  thermal, 122
Antitrades, 118
Asymptotes, 89, 102
ATKINSON, 169

B

Barbados Island, 25
Basic current, 106, 119, 122, 126, 127, 154
Bay of Bengal, 137, 192
β-effect, 114
BJERKNES, 87
Brightness
  cloud on photographs, 10
  IR images, 9
Buoyancy
  force, 79
  formula, 71
Burma, 137

C

Capture coefficient, 64
Caribbean, 123, 154
Channelling effect of Himalaya mountains, 137
Circulation
  general, 106-109
  models of, 44, 50, 109, 118
  monsoon, 133, 134, 137, 141
  seasonal variation of, 110
  systems of, 106
Climatic pressure map, 53
Cloud, 18, 55-60, 110, 111, 115
  banks of, 56-59, 61, 73
  chimney, 56
  cirrus, 19, 57, 58, 181, 186
  clusters of, 18, 20, 73
  cumulonimbus, 20, 56, 57, 59, 62, 71, 74, 78, 80, 83, 89, 97, 102, 149
  cumulus, 55, 71, 78, 101, 122, 181
  diurnal march of, 55
  fields of, 18, 73
  of vertical development, 57, 58
  stratocumulus, 101
  stratus, 58, 181
  tower, 57, 149
Cloud bands, 163, 181, 182, 183, 184, 186, 190
Cloud condensation nuclei (CCN), 63

Cloud droplets, 62
  critical conditions for, 65
  growth of, 64
  non-supercooled, 62
Coalescence efficiency, 64
Col, 80
Cold front, 130
Collection efficiency, 64
Condensation, 63, 73, 108, 146, 156
Control point technique, 178-179
Convection, 12, 56, 57, 73, 74, 98, 121, 122, 132, 144, 145, 156
  adiabatic model of, 75, 74
  cumulus (cell), 70, 74, 76
  deep (penetrating), 70, 74, 76, 124, 144, 145, 156
  entrainment jet model of, 77-83
  level of (free), 75, 77
  mechanism of, 70
  parameters of, 75-77
  suppressed, 71, 124
  thermal, 63
Convectively unstable layer, 74, 75
Convergence, 112-114, 124, 125-127
  field of, 143
  lines of, 89
  points of, 88
  region of, 133, 140
  secondary, 114, 133
  wind, 12, 59, 60, 63, 69, 73
Coriolis parameter, 12, 44, 47, 48, 54, 122
Cyclone, 143
  cloud system of, 158, 181, 182
  cold core, 121, 145
  dimensions of, 158
  genesis of, 157-159
  highest wind in, 121, 157, 158, 188
  high-level, 121, 129
  impact of, 192-196
  in monsoon's leading edge, 137
  life cycle of, 157-159
  low-level, 121
  pressure in, 157, 158, 167-175, 188
  rainfall of, 163-165
  tropical, 11, 16, 33, 45, 61, 120, 122, 152-196
    formation of, 152-157
  warm core, 121, 145
  wind in, 45, 157-161

D

Density of weather station network, 13-16
Depression (low), 73
  equatorial, 22, 31
  thermal, 133, 136, 137
  tropical, 157
Discontinuities of wind, 89
Disturbance, 84, 91, 106, 107, 143
  anticyclonic, 143
  cyclonic, 143, 146, 152, 154
  dimensions, 84-85
  eddy, 145
  intensity, 84-85, 106-107
  lines of, 97-99
  scale of, 73
  structure of, 84-85
  synoptic scale, 107
  tropical, 119-132, 145, 157
  wavelike, 123-130
Divergence, 111, 112, 124, 129, 132
  air stream, 12, 84
  field of, 111, 112, 128, 143
  large scale, 143
  points of, 88
  streamlines of, 88-89
  velocity, 90-102
  water vapour, 147
Djakarta, 34, 35, 37
Drought, 11
Dynamic balancing, 49-55

E

Energy
  dissipation of, 144, 156
  eddy flux, 148
  flux ascending, 148
  flux from ocean, 144, 156
  instability, 77
  kinetic, 108, 148, 156, 167
  potential, 145

realized, 148
static, 145, 146
tropical cyclone, 156, 167
Enthalpy, 145
Entrainment, 78
Equation
continuity, 92
diagnostic, 52
divergence, 95
gradient wind, 166, 169
hydrostatic, 12, 71
momentum, 12
horizontal, 47, 48
vertical, 12
prognostic, 48
vorticity, 94, 132
absolute, 126
Equator, 108, 110, 113, 127, 128
geographical, 24, 38, 113, 146
meteorological, 22
kinematic, 48
heat, 22, 146
Equatorial region of westerlies, 43
Euler-backward scheme, 49
Eye of storm, 163, 165-167, 181, 182, 183, 191, 192

F

Fanning Island, 25, 67
FLETCHER, 43
FLOHN, 43
Force
centrifugal, 45, 167
Coriolis, 114, 156, 157, 167
horizontal pressure gradient, 45, 167
Forecasting,
intensity of storms, 181-192
movement of cyclones, 175-180
numerical, 47
objective, 176, 177
weather, 84
Frequency of weather observations, 16
Friction layer, 12

G

GARP, 10
GATE, 11, 15, 18, 27, 42, 46, 48, 58, 61, 143
Gradient
geopotential, 47, 49
pressure, 31, 45, 46, 47, 53, 159, 167
temperature
horizontal, 157, 166
vertical, see temperature lapse rate

H

HADLEY, 108
Hadley (circulation) cell, 108, 118, 147, 148
Hawaiian Islands, 62
Heat, 108, 132
latent, 74, 108, 121, 145, 146
sensible, 145-147
Himalaya mountains, 137
HOLLIDAY, 169
HOVERMALE, 49
Humidity (water content in atmosphere), 12, 66, 75, 78, 103, 104
vertical profile of, 20, 27-29, 77
Hurricanes, 121, 154, 157, 167, 181, 183
Hydrostatic approximation, 12

I

India, 136
Incipient cyclonic disturbance, 155-157
Instability
baroclinic, 155, 157
barotrophic, 155, 157
conditional
of the first kind (ordinary), 73
of the second kind (CISK), 74
convective, 74, 144
Intertropical convergence zone (ITCZ), 42, 58-61, 71, 85,

103, 110-116, 135, 141, 142-143, 155
Intrusion of cold fronts, 130
Isobars, 85
Isogons, 87
Isolines, 85
Isallobars, 85
Isotachs (isovels), 87

J

Java Island, 35
JORDAN, 161, 176

K

Kharmatan, 141
Khartoum, 26

L

LAIKHTMAN, 53
Langmuir chain, 65
Linear systems, 130-132

M

Main stream, see basic current
Malaysia, 136, 139
MALKUS, 148
MARCHUK, 49
Marshall Islands, 137
Meteosatellites, 18
MIYAKODA, 49
Monsoon, 107, 111, 132-142
  African, 38, 140-142
  Asiatic, 38, 134-140
    summer, 130
    winter, 136
  bursts of, 137
  of Malaysia, 135
  pulses of, 139
  summer India-Burma, 139
Movement (tracks) of
  cyclones, 122, 175-179
  isallobaric centers, 123
MOYER, 49

N

NITTA, 49

O

Ordinary conditional instability, 73

P

PALMER, 67, 89, 127
Parcel
  method, 71
  saturated, 72
Philippine Islands, 11, 175
Point
  dew, 75
    deficit of, 75
  maximum curvature, 90
  neutral, 89
  saddle, 89
  singular, 88
Pressure, 31-37
  dynamic, 47
  field of, 129, 130
  inside the eye, 166
  Laplacian of, 95-97
  nonperiodical, 33
  periodical, 33-35
Pressure chart
  average flow, 179
  climatic, 53
  cyclone track, 176, 178
  surface, 85, 119, 120, 130, 177
  upper-air, 49, 84, 86-90, 118, 177
Pressure oscillations, see wave
Pressure relation with cloudiness, 36
Pressure tendency, 33

Q

Quasi-geostrophic approximation, 45

R

Radar stations, 19
Radiant energy budget, 22, 146

Rainfall, 60-68, 111-112, 138, 139
  amount of, 113
  in trades, 68
  mechanism of formation, 62-65
  seasonal march of, 67
  shower, 57, 60, 61, 130
  variation of, 66, 68, 137
  widespread (continuous), 61, 130
Rain of warm clouds, 61
  continuous, 61, 62, 102
  monsoon, 139
  season of, 137
  shower, 58, 61, 62, 66, 104
Ridge, 124, 126
RIEHL, 9, 148
Rossby number, 95

S

SAMOILENKO, 60
SOLNTSEVA, 60
SANDSTRÖM, 87
Satellite photographs, 18, 57, 86, 159, 180, 182, 183
Secondary separation layer, 28
Showers, 76, 77, 113, 124
Sigma system of coordinates, 50
Singular points of convergence and divergence, 88
Soundings
  radar, 19, 20
  satellite, 19, 21
Squall, 97, 130, 137, 163
  lines, 97
Static energy, 145
  flux of, 146
Stations
  aerological, 13, 15, 127
  automatic, 16
  meteorologic, 13, 14, 85, 159
  radar, 19
Steadiness
  of low trades, 117
  of wind, 30
Steering current, 176, 177
Storm waves, 192
Stream
  baroclinic, 107
  jet, 87
  subtropical, 118
  tropical easterly, 119
  upper-level easterly, 137
Streamline
  analysis, 86-88
  field, 86, 89
Subtropical high[(pressure belt), 9, 31, 39, 116, 123, 130
Synoptic analysis, 84
  surface chart of, 85
  upper-air chart of, 86
Synoptic objects, 85, 86, 119-132

T

Temperature
  annual variation of, 21-26
  diurnal, 29-30
  field of, 22, 78
  ocean surface, 157
  range, 22-30
  seasonal variation of, 22, 132
  vertical profile of, 20, 28-30
Temperature lapse rate, 27, 29, 70, 78, 103-104
  dry adiabatic, 70
  geometric (environmental), 72
  moist adiabatic, 70
Termals, 72
Thunderstorms, 75, 77, 113, 124, 130
Tibet-Himalayas, 130
Trade inversion, 27, 77, 85, 116, 118
Trade winds, 106, 110, 114, 116-118, 133, 147
  lower, 116, 117
  upper, 116, 117
Tropic
  of Cancer, 9
  of Capricorn, 9
Tropical region, defined, 9
Tropical storms, 157, 181, 183
Trough, 85, 124, 130
  equatorial, 31, 40, 68, 86, 107, 109-116, 121, 132, 133
  meridional, 109, 137
  upper-air, 131, 137
Typhoon, 107, 121, 154, 167, 175

U

Upwelling, 24

V

VAN DE BOGAARD, 147
Ventilation, 144
Vertical cross section
  radar, 21
  space, 84
  time, 84, 108, 123
Vertical motions, 62, 73, 92, 145
  ascending (updrafts), 72, 73, 93, 108, 144, 145, 189, 191,
  descending (downdrafts), 73, 74, 94, 107, 166
  field of, 111, 112
Vortex, 120-123
  anticyclonic, 48, 124
  cyclonic, 120, 125, 156, 181
Vorticity
  absolute, 47, 48, 125, 126
  field, 90-102
  relative, 47, 92, 99, 107

W

Wake Island, 34, 37
Water vapour transfer, 146-147
Wave
  easterly, 123-127, 155
  equatorial, 123, 127
  induced, 129
  in streamline field, 80
  pressure, 33-37, 130
    diurnal, 33, 36
    semidiurnal, 33-35, 85
  speed of, 124-125
  tropical, 129
Weather elements, variation of, 13
Weather forecasting, 44
Weather observations
  accuracy of, 18
  errors in, 14
  frequency of, 16
  system of, 13-21
Wind
  actual, 45
  cyclostrophic, 45
  field, 38, 40, 88-90, 130-131
  geostrophic, 45, 47
  in trade wind region, 38
  relation to pressure, 44-55, 86, 169-172
  shear, 131
    lines, 85
    vertical, 144
  steadiness, 39
  vertical profile of, 40-43
Wind-pressure relationship, 44
WOODCOCK, 65
World Meteorological Centers, 16

TO THE READER

Mir Publishers would be grateful for your comments on the content, translation and design of this book. We would also be pleased to receive any other suggestions you may wish to make.

Our address is:

Mir Publishers
2 Pervy Rizhsky Pereulok,
I-110, GSP, Moscow, 129820
USSR

Printed in the Union of Soviet Socialist Republics